Publicly Accessible Penn Dissertations

1-1-2016

Microfluidic Approaches to Thrombosis and Hemostasis: Towards a Patient-Specific Test of Antiplatelet Therapeutics and the Assessment of Coagulopathy in Hemophilic and Trauma Patients

Ruizhi Li
University of Pennsylvania, ruizhili@seas.upenn.edu

Microfluidic Approaches to Thrombosis and Hemostasis: Towards a Patient-Specific Test of Antiplatelet Therapeutics and the Assessment of Coagulopathy in Hemophilic and Trauma Patients

Abstract

Current in vitro or ex vivo models of hemostasis and thrombosis fail to recapitulate the hemodynamic conditions and biorheologic phenomena found throughout the vasculature. Microfluidic technology enables physiologic hemodynamics for the study of platelet deposition and coagulation using minimum volumes of human whole blood. This dissertation describes the application of microfluidic assays, the manipulation of surface-patterned procoagulant and sub-endothelial proteins, anti-coagulation, and flow conditions to investigate platelet function and coagulation under flow. First, we demonstrate a novel method to assess the in vivo or in vitro therapeutic efficacy of anti-platelet therapies on platelet aggregates adhering to collagen type I surfaces. We phenotyped individual healthy donor platelet function responses to in vivo or in vitro aspirin, a common antiplatelet therapy over collagen type I surfaces at venous shear rates. Utilizing the same flow assay, we also characterized mechanism-based resistance to aspirin conferred by non-steroidal anti-inflammatory drugs. Furthermore, we have also developed a new model to assess the intrinsic pathway of coagulation under flow on collagen type I surfaces and investigated the role of the intrinsic pathway in recombinant coagulation factor VIIa (rFVIIa) therapeutic efficacy. We then extended this mechanistic investigation of rFVIIa to flow assays where clotting is initiated by collagen and immobilized lipidated tissue factor to evaluate the role of the intrinsic tenase in conjunction with exogenous rFVIIa when surface-triggered extrinsic pathway is present. Finally, we continued to assess coagulopathic patients by first mimicking resuscitation-driven hemodilution, hyperfibrinolysis, and plasmin-inhibitor therapy under flow. We then evaluated downregulation of platelet function in whole blood from trauma patients during the acute phase of trauma-induced coagulopathy. The development of microfluidics, microfabrication, and its applications in hemostasis and thrombosis is essential in advancing our knowledge of clinical and pathological disorders such as myocardial infracts, hemophilia, and deep vein thrombosis. Beyond this work, microfluidic platforms in hemostasis and thrombosis can potentially be used as drug screening platforms for antiplatelet or clotting factor therapies, or a point of care diagnostic test for bleeding and pin-pointing the therapeutic index of novel biopharmaceutics.

Degree Type
Dissertation

Degree Name
Doctor of Philosophy (PhD)

Graduate Group
Chemical and Biomolecular Engineering

First Advisor
Scott L. Diamond

Keywords
Fibrin, Hemophilia, Hemostasis, Microfluidics, Platelets, Thrombosis

Subject Categories
Biomedical | Chemical Engineering

MICROFLUIDIC APPROACHES TO THROMBOSIS AND HEMOSTASIS: TOWARDS A PATIENT-SPECIFIC TEST OF ANTIPLATELET THERAPEUTICS AND THE ASSESSMENT OF COAGULOPATHY IN HEMOPHILIC AND TRAUMA PATIENTS

Ruizhi Li

A DISSERTATION

in

Chemical and Biomolecular Engineering

Presented to the Faculties of the University of Pennsylvania
in
Partial Fulfillment of the Requirements for the
Degree of Doctor of Philosophy

2016

Supervisor of Dissertation

_____

Scott L. Diamond

Professor, Chemical and Biomolecular Engineering

Graduate Group Chairperson

_____

John C. Crocker, Professor, Chemical and Biomolecular Engineering

Dissertation Committee

Lawrence F. Brass, Professor, Department of Medicine

Talid R. Sinno, Professor, Department of Chemical and Biomolecular Engineering

Matthew J. Lazzara, Assistant Professor, Department of Chemical and Biomolecular Engineering

MICROFLUIDIC APPROACHES TO THROMBOSIS AND HEMOSTASIS: TOWARDS A PATIENT-SPECIFIC TEST OF ANTIPLATELET THERAPEUTICS AND THE ASSESSMENT OF COAGULOPATHY IN HEMOPHILIC AND TRAUMA PATIENTS

ACKNOWLEDGEMENTS

First and foremost I would like to thank my thesis advisor, Dr. Scott L. Diamond, without

your guidance and mentorship this dissertation would not have been possible. The research

experience, problem-solving abilities, project management skills, and written and oral

communication skills I learned during my degree will forever shape by my professional

career as an engineer and scientist. They are a testament to the exceptional learning

opportunities afforded to me while in Scott's lab and his ability to bring the best out of his

PhD students. I would also like to extend thanks to the other members of my thesis

committee, Dr. Lawrence Brass, Dr. Matthew Lazzara, and Dr. Talid Sinno. Your

suggestions and thoughtful insights during my proposal and along the progression of my

dissertation helped me think critically about my work. Furthermore, I would like to

acknowledge all of my collaborators around Penn, without your resources and support this

work could not have been possible either. Special thanks to Professor Tilo Grosser, Dr.

Xuanwen Li, Dr. Adam Cuker, Dr. Patrick Forgarty, Karen Panckeri, Dr. Thomas Diacovo,

Dr. Carrie Sims, and Ryan Walters, all of whom have provided me with opportunities I

could have never imagined. Additionally, I want to express my gratitude towards the past

and current members of the Diamond lab: Xinren Yu, Brad Herbig, Shu Zhu, John Welsh,

Dr. Ryan Muthard, Dr. Viraj Kamat, Dr. Melissa Myint, Dr. Thomas Colace, Dr. Andrew

Dolan, Dr. Roman Woronov, and Huiyan Jing. I am especially grateful to Tom and Ryan for

being ever so helpful with my work and bringing me under their tutelage. I would also like to

thank the many friends outside of lab, those that stayed in Sansom (Neil, Keith, etc.), those I

met at Pottruck (Jeff, Paul, Andrea, etc.), members of GCC (Brian, Chris, Minna, Shirley

etc.). I'm also thankful for Katlin, whose happiness, exuberance, kindness, and compassion has brightened me ever since the day we met. I can always count on you to support me, to listen, and to be there for me through the best of times and worst of times. I would also like to thank my Lord and savior for loving me, protecting me, and blessing me all five years in Philadelphia. Finally and most importantly, I would like to thank my parents, whose love and support has always been there through the countless hours, days, and years. The love and dedication you have shown me in both my personal and professional life is unfathomable. The lessons the two of you have taught me have made me into the man I am today. Without my parents, I could have never accomplished so much and would have never learned the values of love, hard work, responsibility, respect, and perseverance in this lifetime. Your unwavering support and faith in me have gotten me this far and will undoubtedly carry me even further into the future. For this I dedicate the entirety of this PhD dissertation to my parents.

ABSTRACT

MICROFLUIDIC APPROACHES TO THROMBOSIS AND HEMOSTASIS: A
GLOBAL INVESTIGATION OF ANTIPLATELET THERAPEUTICS AND THE
ASSESSMENT OF BLEEDING AND COAGULOPATHY IN HEMOPHILIC AND
TRAUMA PATIENTS

Ruizhi (Richard) Li

Scott L. Diamond

Current in vitro or ex vivo models of hemostasis and thrombosis fail to recapitulate the

hemodynamic conditions and biorheologic phenomena found throughout the vasculature.

Microfluidic technology enables physiologic hemodynamics for the study of platelet

deposition and coagulation using minimum volumes of human whole blood. This

dissertation describes the application of microfluidic assays, the manipulation of surface-

patterned procoagulant and sub-endothelial proteins, anti-coagulation, and flow conditions

to investigate platelet function and coagulation under flow. First, we demonstrate a novel

method to assess the in vivo or in vitro therapeutic efficacy of anti-platelet therapies on

platelet aggregates adhering to collagen type I surfaces. We phenotyped individual healthy

donor platelet function responses to in vivo or in vitro aspirin, a common antiplatelet

therapy over collagen type I surfaces at venous shear rates. Utilizing the same flow assay, we

also characterized mechanism-based resistance to aspirin conferred by non-steroidal anti-

inflammatory drugs. Furthermore, we have also developed a new model to assess the

intrinsic pathway of coagulation under flow on collagen type I surfaces and investigated the

role of the intrinsic pathway in recombinant coagulation factor VIIa (rFVIIa) therapeutic

efficacy. We then extended this mechanistic investigation of rFVIIa to flow assays where

clotting is initiated by collagen and immobilized lipidated tissue factor to evaluate the role of

the intrinsic tenase in conjunction with exogenous rFVIIa when surface-triggered extrinsic

pathway is present. Finally, we continued to assess coagulopathic patients by first mimicking resuscitation-driven hemodilution, hyperfibrinolysis, and plasmin-inhibitor therapy under flow. We then evaluated downregulation of platelet function in whole blood from trauma patients during the acute phase of trauma-induced coagulopathy. The development of microfluidics, microfabrication, and its applications in hemostasis and thrombosis is essential in advancing our knowledge of clinical and pathological disorders such as myocardial infracts, hemophilia, and deep vein thrombosis. Beyond this work, microfluidic platforms in hemostasis and thrombosis can potentially be used as drug screening platforms for antiplatelet or clotting factor therapies, or a point of care diagnostic test for bleeding and pin-pointing the therapeutic index of novel biopharmaceutics.

TABLE OF CONTENTS

LIST OF TABLES

LIST OF ILLUSTRATIONS

LIST OF EQUATIONS

1 INTRODUCTION TO PLATELETS, BLOOD COAGULATION, AND MICROFLUIDICS

1.1 Hemostasis and the Role of Platelets

Human blood is primarily comprised of plasma proteins, platelets, red blood cells, and white blood cells. In human whole blood, platelets are the primary anucleate cells that are responsible for hemostasis, more commonly described as the physiologic balance between bleeding and excessive blood clotting (thrombosis). Healthy whole blood on average contains 150,000 – 400,000 platelets per microliter[1]. These anucleate cells stay in a quiescent state circulating the blood vasculature patrolling the human body for vessel wall damage and exposure of the subendothelium. Once damage occurs to the vessel wall, tissue factor (TF) is exposed and the coagulation cascade (to be described in detail later) is triggered. This cascade produces a potent serine protease thrombin (IIa) which activates platelets[2]. The final downstream product of the cascade is fibrin, which is a fibrous biopolymer network that stabilizes and seals a blood clot[3].

Platelets are able to remain in a quiescent state as they are inhibited by chemical mediators from the endothelium, prostacyclin (PGI_2) and nitric oxide (NO_2)[4]. Additionally, platelets have numerous receptors and respond to activating stimuli such as collagen, von Willebrand Factor (vWF), epinephrine, and histamine[4]. In the presence of these agonists, platelet become activated through a series of transmembrane receptors on their surface. This then results in an increase in intracellular calcium that cause changes in platelet morphology and the platelet cytoskeleton[5]. In addition to platelet shape change, platelet activation also

1

results in the secretion of additional agonists from platelet alpha and dense granules. These granules are packaged prior to platelet release by megakaryocytes during megakaryopoiesis[6]. Secretion of these agonists [Adenosine Diphosphate (ADP), Thromboxane A_2 (TXA_2)] results in both autocrine and paracrine signaling which are biochemical signaling processes important for the recruitment of additional platelets to the site of injury and the stabilization of previously deposited platelets during blood clotting.

1.2   Thrombosis

Once the delicate balance of blood clotting is perturbed, excessive clot growth or thrombosis then occurs. Thrombosis is the cessation of blood flow through a vessel due to an occlusive blood clot. Two clinically-relevant types of thrombosis are clots that emanate from the venous circulation or clots that emanate from the arterial circulation of the vasculature. The most prevalent venous thrombosis is deep vein thrombosis (DVT). Deep vein thrombosis usually occurs due to continuous immobilization, surgery, or heart failure[7]. Medical treatment for DVT consists of anticoagulant drugs such as heparin or vitamin K antagonists[7]. Arterial thrombosis is pathologically different from venous thrombosis and occurs within arterioles[8]. A prime example of arterial thrombosis is myocardial infarction (MI), otherwise commonly known as a heart attack. This sudden occlusive event prevents blood flow to the heart. The major causes of MI are usually genetic risk factors, atherosclerotic plaque build-up and rupture, or a combination of high blood pressure, cholesterol and obesity[8]. Common treatment for arterial thrombosis includes antiplatelet therapies, drug-eluting stents, and bypass surgery. A major concern with venous and arterial thrombosis is the risk of thromboembolism. Thromboembolism is a scenario

where an occlusive clot dislodges from the injury site and eventually travels downstream and becomes lodged in another vascular bed. Thromboembolism is a major concern with patients who have DVT or have experienced acute MI. Thrombus dislodgement followed by adherence either in the lungs or brain could put an individual at risk for pulmonary embolism or stroke. The investigation of the biophysical and biochemical characteristics of venous and arterial thrombi is on-going and much additional research is still needed[9].

1.3   Hemostatic clot growth under flow: platelet adhesion biology & receptor interactions

Hemostastic clot growth under physiologic flow environments occurs in three stages, initial platelet adherence to subendothelial proteins, growth of the clot through autocrine and paracrine signaling, and stabilization of the platelet aggregate (**Figure 1-1**). Platelets initially adhere to either collagen or vWF at the site of injury. This initial adhesion is mediated through platelet receptors $\alpha_2\beta_1$ and glycoprotein VI (GPVI) for collagen and glycoprotein IB (GPIB) for vWF respectively[10]. Beyond this initial monolayer of platelets adhered to collagen and vWF, local platelet secretion of agonists ADP and TXA_2 help activate more platelets and recruits those additional platelets to the site of injury[11]. Furthermore, platelet calcium levels Ca^{2+} rise due to its release from intracellular stores. Rising Ca^{2+} levels results in platelet integrin $\alpha_{IIb}\beta_3$ activation. Platelet integrin $\alpha_{IIb}\beta_3$ is a major integrin involved in platelet aggregation, it undergoes a conformational change which then facilitates its binding to fibrinogen, a major plasma protein in blood and vWF[12]. The high copy number of platelet $\alpha_{IIb}\beta_3$ and multiple binding sites on fibrinogen and vWF for $\alpha_{IIb}\beta_3$ then ensure platelet aggregation, extension of the hemostatic blood clot and the cessation of

bleeding. This is further supported by platelet mechanosensing as increases in platelet activation and changes in the local flow environment results in single platelet and platelet aggregate contraction that secures the clot against the vessel wall and stops bleeding[13,14].
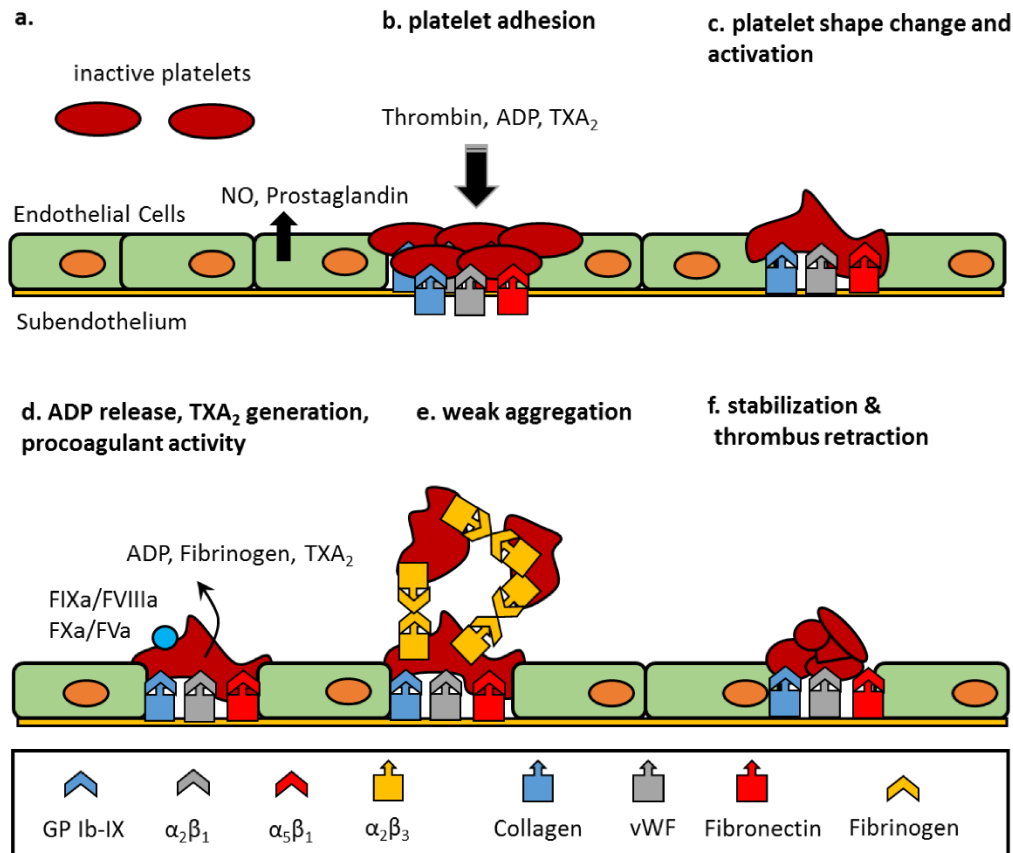
Figure 1-1 Hemostatic Plug Formation, Aggregation, and Contraction

(**a**) Circulating platelets are kept quiescent by PGI_2 and NO released from endothelial cells. (**b & c**) At sites of vessel injury, platelets adhere to proteins of the exposed subendothelium through interactions with collagen, vWF through their receptors integrin $\alpha_2\beta_1$ and GPIb respectively. Agonists, ADP and thrombin then cause platelet shape change. (**d**) Activated platelets release ADP and fibrinogen from their intracellular granules. ADP and TXA_2 recruits additional platelets to the site of injury through autocrine and paracrine signaling. (**e**) Platelet

$\alpha_{IIb}\beta_3$ becomes engaged and activated platelets bind fibrinogen or vWF resulting in platelet aggregation. (**f**) Clot contraction then leads to a stable thrombus under flow.

A final important role of platelets during blood clotting is the ability of their phospholipid membrane surfaces to support coagulation. The surface of activated platelets becomes negatively charged due to phosphatidylserine (PS) and phosphatidycholine (PC) exposure as these phospholipids are transferred from the inner leaflet of the platelet membrane to the outer leaflet of the platelet membrane[15]. This negatively charged surface then provides a surface for the adherence of plasma proteins which then can support the coagulation cascade[16].

1.4   Coagulation

Blood coagulation is a series of biochemical, enzymatic pathways that is governed by zymogens, serine proteases, and enzymes. This serious of reactions results in generation of a master enzyme, thrombin and the formation of a biopolymer network, fibrin, which then stabilizes the clot. The coagulation cascade is divided into two pathways, the contact (intrinsic) pathway and the tissue factor (extrinsic) pathway. These two pathways converge to the formation of clotting factor Xa (FXa). The subsequent steps following FXa generation are known as the "common pathway". This leads to the formation of thrombin. Thrombin then acts on fibrinogen to convert fibrinogen into fibrin monomer which then polymerize into fibrin. Fibrin fibers stabilize the loose platelet aggregate. These pathways occur in the presence of serine protease inhibitors that limit the activity of active proteases. The coagulation cascade is schematically depicted in.
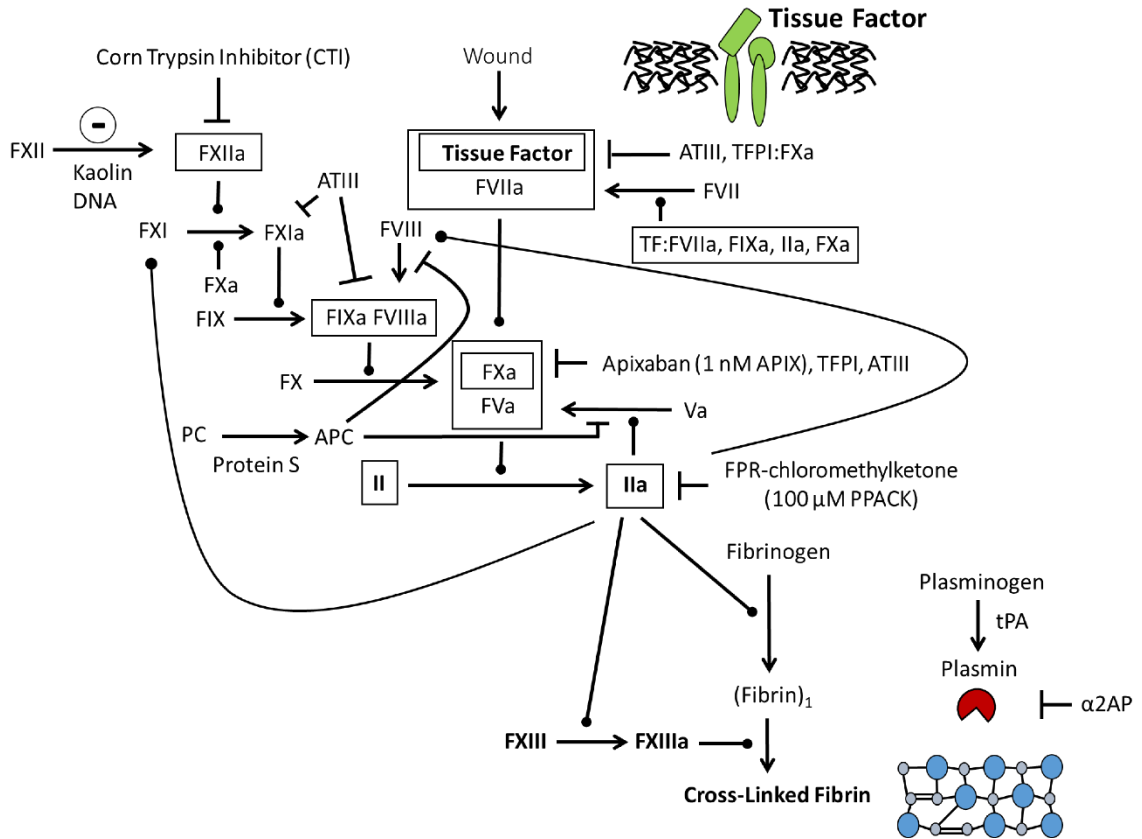
Figure 1-2 Schematic Depiction of the Coagulation Cascade

The coagulation cascade involves a series of sequential plasma reactions that lead to the generation of thrombin. The cascade is triggered either by exposure of TF at the site of injury (extrinsic pathway) or by exposure to negatively charged surfaces and activation of FXII (intrinsic pathway). Both pathways lead to thrombin formation and then fibrin production.

In in vivo scenarios, the extrinsic pathway is the predominant trigger of the coagulation cascade. This involves the exposure of TF at the site of vascular injury. TF is commonly expressed by smooth muscle cells and fibroblasts. TF exposure to flowing blood in vivo then allows binding of activated soluble clotting factor seven (FVIIa). FVII is a member of the vitamin K-dependent clotting factors, the others are FIX, FIX, and proteins

C and S[18]. Most coagulation factors have gamma-carboxyglutamic acid residues in the N-terminal region (Gla-domain) of their protein structure which then enables them to bind calcium and assemble on the phospholipid surfaces of platelets. Once the TF/FVIIa complex forms it can activate FIX via limited proteolysis. However, TF/FVIIa complex can directly activate FX and this is a heavily favored pathway in vivo. Once FIX is activated, it can also activate FX as long as FVIIIa is present. Factor VIIIa is the cofactor for FIXa and the assembly of these two active factors together to promote FXa generation is known as the 'intrinsic tenase' complex'. As all serine proteases and clotting cofactors in the coagulation cascade exist as zymogens in the plasma component of whole blood, it is surprising how such potent biocatalytic reactions can be triggered via the ensemble of these inert precursors. However, previous studies have shown that sub-nanomolar concentrations of FVIIa does exist in circulation while active forms of other clotting factors are even more miniscule in comparison. Exposure of TF to this small but nevertheless potent amount of FVIIa then sets up autocatalytic feedback where VII bound to TF is activated. Furthermore, other clotting enzymes can also activate FVII which thus makes the coagulation cascade a network of self-amplifying, feedforward, and feedback reactions.

In a traditional sense, the other arm of the coagulation cascade is the 'intrinsic' pathway. Its name is derived from the 'intrinsic' ability of blood to clot when placed in a glass tube. Specifically speaking, blood derived from the human blood tends to clot in vitro when in direct contact with negatively charged surfaces. Non-physiologic surfaces for contact activation of blood include glass, clay, and kaolin, while physiologic substrates for contact activation include DNA, RNA, and histones. The contact pathway has been viewed

previously as non-physiologic as severe deficiencies in the most upstream source of this pathway(FXII) causes no severe bleeding defect[19]. In fact, studies have shown inadequate levels of FXII may actually result in increased risk of thrombosis[20]. However, recent in vivo models have shown that mice deficient in FXII have a tendency to form unstable thrombi, thus suggesting that this previously overlooked part of the coagulation cascade may have an important physiologic role. The intrinsic pathway is activated once zymogen FXII comes into contact with negatively charged surfaces. The heavy chain of FXII is the portion that binds to negatively charged surfaces which then leads to increases in local enzyme concentration, autoactivation, and activation of FXI. Then FIX is activated by dimerized FXIa.

Nevertheless both the intrinsic and extrinsic pathway converge to FXa generation. Factor Xa along with its cofactor FVa converts prothrombin into thrombin. Factor Xa assembly with FVa in the presence of calcium on a phospholipid surface results in a 300,000 fold increase in thrombin generation as compared to FXa alone. Thrombin is central to the formation of the haemostatic blood clot as it controls its own generation and inhibition by acting on numerous substrates such as fibrinogen, FV, FVIII, FIX, platelet receptors, protein S, and protein C. One major role of thrombin is its cleavage of fibrinogen, a heavily abundant protein in both plasma and platelet granules. Thrombin cleavage of fibrinopeptide A and B of fibrinogen results in a self-association and restructuring of fibrin monomers[21]. The progressive lengthening of initial fibrin monomers into dimers and beyond occurs initially through half overlap of fibrin monomers which then forms long, thin fibrin strands.

Factor XIIIa can then crosslink these loose fibrin strands and confers degradation by plasmin.

1.5 Anticoagulation for in vitro and ex vivo research

1.5.1 Citrate or Ethylenediaminetetraacetic acid (EDTA)

Citrate or EDTA are potent calcium chelators that can completely inhibit thrombin production and platelet adhesion under flow. Thus these reagents are ideally used for pure biorheological studies of platelet/red blood cell interaction under flow. The addition of exogenous Ca^{2+} for recalcification can recover extracellular calcium levels, however EDTA tends to destroy $\alpha_{IIb}\beta_3$ function and citrate also significantly impairs $\alpha_{IIb}\beta_3$ after recalcification[22]. Basic scientific and clinical studies of TF or contact pathway triggered coagulation predominantly uses citrate as an anticoagulant. However, it is important to note that FXIIa can be generated in the absence of calcium.

1.5.2 Corn Trypsin Inhibitor (CTI)

CTI is an intrinsic pathway inhibitor which when used in the 20-120 μg/ml range can inhibit the activity of βFXIIa, the soluble cleavage product formed from surface-bound αFXIIa. As CTI does not inhibit αFXIIa, it can provide approximately 30-60 min of inhibition of the contact pathway without interfering with the cation levels required for extrinsic pathway medicated coagulation. Thus high exogenous concentrations of CTI are commonly used to test TF-initiated coagulation under flow given that blood can be tested in vitro immediately following phlebotomy. Furthermore, recent studies have shown that a low level of CTI (4 μg/ml) can partially delay the contact pathway allowing study of FXIIa and its subsequent reactions ex vivo provided that blood is perfused ex vivo within 5-15 minutes

of phlebotomy[23,24]. Other reagents have also been used to control in vitro contact activation. Monoclonal function-blocking antibodies have been used against FXIIa and FXIa[25]. Infestin-4 has been used to antagonize FXIIa, while domains from protease nexin-2 have been used to inhibit FXIa[26–28].

1.5.3   FPR-Chloromethylketone (PPACK), Direct FXa inhibitors, Heparin

PPACK is a small molecule inhibitor of thrombin. PPACK (100 μM) provides strong and irreversible inhibition of thrombin for in vitro studies of platelet function. This approach is useful to solely examine platelet activation, adhesion, aggregation, and function in the absence of thrombin and fibrin. Furthermore, with the advent of novel oral direct FXa inhibitors (apixaban), these new anticoagulants can be used in vitro for direct inhibition of FXa. The use of apixaban (0.25 – 1 μM) becomes particularly useful when examining the effect of exogenously added thrombin on platelet activation and intracellular calcium signaling[29].

1.6   Microfluidic Technology

1.6.1   Motivation

Microfluidic technology was invented due to a need in industrial applications and academic laboratories to minimize reagent usage, evaluate novel drug therapeutic efficacy and toxicity, and increase throughput while maintaining the physiologic conditions in which most biological systems exist. Since blood flow occurs in a closed, high pressure, continuously circulating system, in vitro or ex vivo models that can capture the hemodynamics and flow characteristics offer better opportunities to accurately investigate the biological phenomena that occurs in vivo during thrombus formation. Furthermore,

current in vivo animal models of hemostatic and vascular injury are still not well-understood and the small volumes of blood collected from difficult to breed genetically modified animals mandates a low volume test of hemostasis and thrombosis[30,31].

Several previous technologies have been used to study the hemostatic process under flow ex vivo. Such technologies include parallel plate flow chambers, capillary flow chambers, and cone and plate viscometers. These technologies all have their own pitfalls with respect to volume requirements, experimental control and physiologic hemodynamics. By coupling very well-established micropatterning techniques with soft photolithography, microfluidic assays can be developed for whole blood perfusion over well-defined biomimetic injuries. With control over flow conditions, micropatterned protein/enzyme surface composition and inlet blood biochemistry, thrombi can be formed in vitro and examined with real time epifluorescence microscopy by a host of monoclonal antibodies, novel biosensors, and fluorescently conjugated peptides or proteins. Finally, the ability to measure multiple outputs in real-time with various fluorescent probes from a single blood sample over the course of an experiment provides control and reproducibility critical to the variable nature of hemostatic studies. This could serve as a basis for future automated preclinical diagnostic platforms.

A thorough discussion of PDMS and microcontact printing techniques is out of the scope of this dissertation and extensive reviews can be found elsewhere[32]. Generally speaking, microfluidic devices are made out of polydimethylsiloxane (PDMS) that was cured over master molds fabricated by photolithographic techniques. In brief, a photoresistive substrate is spin-coated onto a silicon wafer in a process known as spin-coating. This process

11

enables substrate adherence to the wafer to a height that will represent the microfluidic channel depth. The spin-coated wafer is then brought into close contact with a high-resolution transparency of the desired microfluidic geometry and channel device. UV light is then shun on the sample which then cross-links the photo-resistive substrate. Unexposed photoresist is then removed with a developing solution. This master mold can then be used to make PDMS casts of the microfluidic devices.

1.6.2 Microfluidic open systems for the study of hemostasis and thrombosis: Focal Injury Models, High Throughput Testing

Open microfluidic systems allow for exchange with the outside environment and offer excellent spatial and temporal control of the flow regime, surface protein/enzyme concentration, and perfused blood biochemistry. Such flow systems allow for high replicate testing of clotting events in vitro and utilizes low volumes of blood (< 1 ml). Microfluidic assays provide control of local flow environments by perfusion of whole blood over well-defined geometries and excellent command of sample flow rates via pre-programed syringe pumps that can also be automated via external LABVIEW interface[13]. Physiological venous (100-800 s^{-1}) and arterial shear rates (1000-2000 s^{-1}) can be used in microfluidic devices, and pathological shear rates (10,000-200,000 s^{-1}) have also been investigated too. Most microfluidic devices set-ups are single path perfusions and for square rectangular channels, the x-directed velocity field for steady flow over a domain of –w/2 y w/2 and 0 z h is given by

$$u(y,z) = \frac{48Q}{\pi^3 hw} \left\{ \frac{\sum_{n=1,3,5,\ldots}^{\infty} \frac{1}{n^3} \left[1 - \frac{\cosh(n\pi\frac{y}{h})}{\cosh(n\pi\frac{w}{2h})} \right] (\sin n\pi \frac{z}{b})}{1 - \sum_{n=1,3,5,\ldots}^{\infty} \frac{192h}{n^5\pi^5 w} \left[\tanh\left(n\pi \frac{w}{2h}\right) \right]} \right\}$$

(Equation 1-1)

PDMS allows for the creation of rectangular flow channels with microscopic features down to approximately 3 μm. Microcontact stamping has also allowed microprinting of proteins or lipids on various substrates down to a spatial resolution of < 1 μm. Neeves et al. have previously demonstrated the use of micropatterned collagen surfaces in a PDMS microchannel[33]. Collagen Type I was patterned onto a glass slide using a single channel device that was then removed to allow placement of a second 13 channel flow device[33]. The resulting protocol was an assay of thrombi formed over 13 individual flow paths each with a precisely patterned injury site where collagen was exposed to the flowing blood. Maloney et al. further advanced this design by making an 8-channel device through which blood was perfused by withdrawal through a single outlet[34]. Furthermore, Colace et al. also improved the biological complexity of the surface trigger in this model 8-channel microfluidic system. With regards to micropatterning, microchannels are usually filled with a protein of interest and rinsed with physiologic buffer before sample perfusion. Colace et al. used this technique to generate thrombogenic surfaces of collagen and immobilized TF in PDMS microchannels[35]. Briefly, Colace et al. modified the TF-bearing liposomes described by Smith et al. to produce TF-bearing biotinylated liposomal constructs which then could be bound to a collagen surface via biotinylated anti-collagen antibody and

13

streptavidin[36]. Such techniques are vital to study the simultaneous effect of platelet deposition and thrombin production under flow and characterize the roles of thrombin in platelet adhesion and fibrin generation in platelet plug formation[37]. Finally, it is important to note that the use of external syringe pumps only generates constant flow rate environments. Under these flow conditions, growing thrombi only obstruct the flow as large pressure drops develop eventually leading the partial and complete embolism of clots as even occlusive structures under flow cannot stop a syringe pump. Thus Colace et al. used the 8-channel device previously described to create a constant pressure drop flow regime by developing thrombi in four of eight channels which then diverted flow to the other four bifurcated channels due to the unreactive EDTA-treated blood that was being perfused simultaneously[37]. This was verified computationally with fluid dynamics simulations showing a drastic difference between clots formed in the presence or absence of fibrin.

2 MICROFLUIDIC ASSAY OF PLATELET DEPOSITION ON COLLAGEN BY PERFUSION OF WHOLE BLOOD FROM HEALTHY INDIVIDUALS TAKING ASPIRIN

2.1 Introduction

Antiplatelet therapies are commonly used in the acute treatment of coronary diseases and long-term prevention of cardiovascular events[38]. Inhibition of platelet cyclooxygenase-1 (COX-1) by aspirin (acetylsalicylic acid, ASA) and the subsequent attenuation of thromboxane A_2 (TXA$_2$) production causes a decrease in secondary platelet aggregation and reduces excessive thrombus formation[39]. ASA does not severely reduce the primary platelet response to the damaged vessel wall needed for homeostasis. Currently, about 50 million patients in the United States take ASA at typical doses of 81 or 325-mg per day to reduce cardiovascular risks[40].

Aspirin reduces the activation of platelets by irreversibly acetylating serine 529 of cycloxygenase-1 and therefore reducing TXA$_2$ production[39]. The inhibition of COX-1 is irreversible and permanent for the lifetime of platelets because platelets lack the synthetic machinery to produce new protein[41]. Recently, the bleeding risks associated with aspirin led to the development of anti-inflammatory drugs selective for COX-2. Several COX-2 selective inhibitors cause less gastrointestinal side effects than traditional non-steroidal anti-inflammatory drugs[42], but they cause cardiovascular risks via inhibition of COX-2 dependent endothelial prostacyclin. All approved COX-2 inhibitors have either been withdrawn or their prescription restricted[43].

However, with regards to COX-1 inhibitors, patients show a marked variability in laboratory responses to aspirin. Depending on the platelet function test, aspirin resistance has been reported in 5-60% of patients[44–46]. Failure to actually take the pill is a well-documented cause of apparent "aspirin resistance"[47,48]. Mutations in the thromboxane receptor would also cause aspirin insensitivity, but such mutations result in a modest bleeding phenotype that would be a contraindication for aspirin therapy[49]. Patients may also fail to benefit from aspirin therapy owing to increased platelet turnover, increased sensitivity to ADP and collagen[41], or increased COX-1 synthesis. However, an association between aspirin resistance detected by a laboratory test in patients and a higher vascular event rate in a group of resistant individuals has yet to be convincingly shown[50,51].

Determination of the anti-platelet effectiveness of pharmacological agents often occurs in closed systems, with or without flow. Measurement of platelet calcium mobilization upon TP stimulation is an example of a closed system with no flow[5]. Platelet aggregometry is a closed system with a poorly defined flow field. The efficacy of pharmacological agents in closed systems may not always predict anti-platelet therapeutic benefits under flow conditions. For example, apyrase is a potent inhibitor in a tube but can potentiate thrombosis under flow due to the dynamics of local levels of ATP and ADP in a concentration boundary layer[34]. During platelet deposition under flow conditions, the platelet deposit can reach platelet densities that are 50 to 200-fold greater than that of platelet rich plasma. Because of this dense platelet deposit, the potency of pharmacological agents may depend on the local concentration of platelet release products that occur under flow conditions[52]. The advent of microfluidic technology has enabled such platelet

deposits to be built under flow[34,53].Microfluidic patterning techniques allow for spatially

confined injury models distinct from current technologies such as perfusion of whole blood

through coated glass capillary flow chambers or parallel plate flow chambers. Furthermore,

microfluidic devices recreate the progression of signaling and thrombotic pathways as they

progress from a surface trigger, i.e. collagen and/or thrombin produced at the wall to

secondary aggregation processes driven by ADP and TXA_2[37,52]. Here we investigated the

utility of an 8-channel microfluidic device in assessing ASA phenotype using fluorescently

labeled platelets with ASA added to whole blood *in vitro*, either before ASA intake or at 24 h

after ASA intake by healthy individuals. We show a novel method to measure residual COX-

1 function and evaluation of the COX-1 mediated thromboxane A_2 pathway in a

microfluidic platelet function test under venous flow conditions.

2.2   Materials and Methods

2.2.1   Blood Collection, Labeling, and Drug Administration

Blood was collected at 0 h and 26 h by venipuncture from 28 healthy subjects (18-55

years), who self-reported non-smoking, free from oral medication and abstained from,

caffeine, alcohol, and high fat food for 24 h prior to the study and throughout the duration

of the study. All volunteers received a 325-mg loading dose of aspirin by mouth at 2 h.

Subjects returned after a 2 week washout period for a third blood draw (**Figure 2-1A**). For

arterial flow studies, blood was collected by venipuncture from 4 healthy individuals who

were free of oral medication for 10 days and self-reported free from disease or bleeding

disorders. All blood samples were drawn into H-D-Phe-Pro-Arg-chloromethylketone (100

µM PPACK final concentration, Haematologic Technologies). PPACK is a potent active site inhibitor of thrombin that irreversibly and specifically inactivates thrombin. All volunteers provided informed consent in accordance with IRB approval and the Declaration of Helsinki. The blood was treated with PE Mouse Anti-Human CD61 ($\alpha_{IIb}\beta_3$) antibody (BD Biosciences) in a ratio of 1:50. PPACK-treated whole blood was perfused through the microfluidic device within 1 h of phlebotomy. For *in vitro* additions to whole blood, acetylsalicylic acid (Sigma Aldrich) was dissolved in DMSO at 500 mM. Dilutions of ASA were then made to the desired final concentration in HBS within 1 h of the test. Final ASA concentrations used were: 0 µM, 0.05 µM, 0.5 µM, 1 µM, 5 µM, 10 µM, 50 µM, 500 µM (final 0.1 % DMSO in all samples). Blood was incubated for 30 min in ASA before initiation of the assay.

2.2.2   Fabrication of microfluidic devices, platelet deposition, and real-time imaging

Microfluidic devices were fabricated in poly(dimethylsioxane) (PDMS, Sylgard 184, Ellsworth Adhesives) according to previously described techniques[34]. The device was fed by 8 distinct wells, with perfusion by withdrawal into a syringe pump (Harvard Apparatus) from a single outlet (**Figure 2-1B**). The channels were spaced in close proximity to allow all channels to be imaged simultaneously with a 2X objective lens using an inverted microscope (IX81, Olympus America) equipped with a charge-coupled camera (Hamamatsu). A custom stage insert held 3 microfluidic devices allowing 24 simultaneous clotting events to be imaged in 15 sec intervals. A micropatterning device with a single channel (5 cm x 250 µm x 50 µm) was used for patterning collagen. Equine fibrillar collagen type 1 (Chronopar, Chronolog) was diluted to 250 µg/mL in isotonic glucose solution (Chronopar, Chronolog).

Prior to perfusion, channels were blocked with 0.5% bovine serum albumin (BSA) in 2-[4-(2-hydroxyethyl)piperazin-1-yl]ethanesulfonic acid (HEPES) buffered saline (HBS, 20 mmol/L HEPES, 160 mmol/L NaCl, pH 7.5) for 30 min. Samples were perfused at an initial venous wall shear rate of 200 s^{-1} (2 μL/min per channel) for 5 min. For arterial studies, an initial wall shear rate of 1000 s^{-1} (10 μL/min per channel) was used for 5 min. The respective shear rates for venous and arterial studies were established previously in other assays with the same microfluidic device[34,37].

2.2.3   IC$_{50}$ Calculation and ASA Sensitivity

Background-corrected fluorescence values were fit with a four parameter dose-response curve ((Equation 2-1):

(Equation 2-1)

$$FI = A + \frac{A-B}{1+10^{[(Log\ IC_{50}-C)\cdot D]}}$$

with *C* representing the ASA concentration, FI the background corrected fluorescence of the corresponding region of interest, *A* and *B* the minimum and maximum intensities, respectively, and *D* the Hill coefficient. The data were fit using a log(inhibitor) vs. response routine by GraphPad Prism 5.00 (GraphPad Software). Analysis of platelet deposition and total platelet accumulation on collagen was also calculated using the change in the background-corrected fluorescence values over time between time intervals 60 to 150 sec for collagen deposition and 150 to 300 sec for TXA$_2$-dependent secondary aggregation (F' = Δ F/Δ t between 60-150 sec or 150-300 sec). A ratio of these two slopes (R-value) was then taken as an internally normalized value for each subject with R > 1 when secondary

aggregation was prominent and R < 1 when secondary aggregation was attenuated relative to the primary response to collagen (primary deposition) (**Figure 8-2**, **Table 6**).
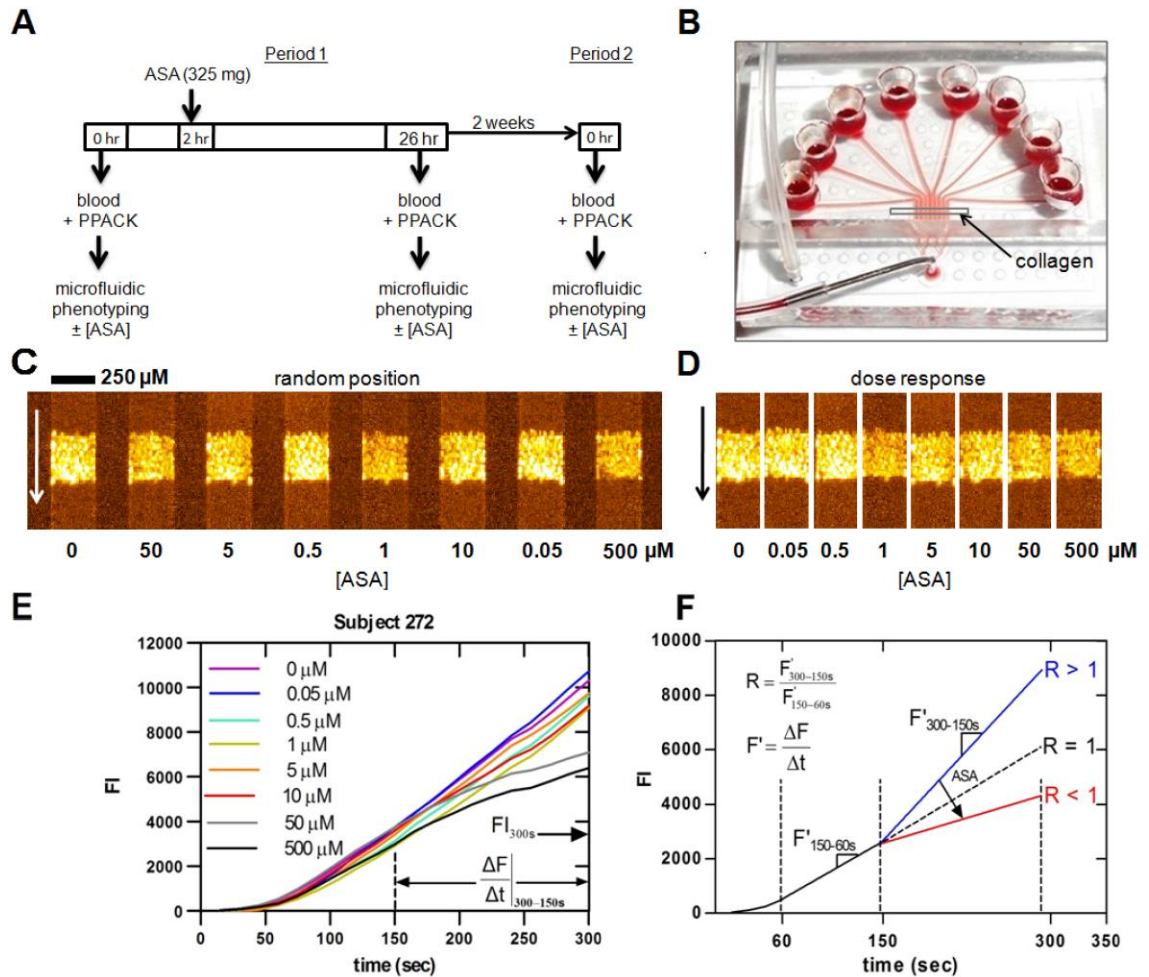
Figure 2-1 ASA phenotyping protocol and quantification of ASA concentration-response

(**A**), Study protocol. Blood samples were taken at t = 0 h and t = 26 h with ASA administration to each healthy donor at t = 2 h, followed by a second blood draw 2 weeks later. For each blood sample, increasing amounts of *in vitro* ASA was added to PPACK-inhibited WB prior to microfluidic testing (3 replicate tests per blood sample). (**B**), Photograph of the 8-channel microfluidic device with the micropatterned collagen strip digitally indicated. (**C & D**), Epifluoresence images of fluorescently labeled platelet accumulation on the collagen and

platelet interaction zone with various *in vitro* ASA concentrations, either in randomized positions (**C**) or ordered by ASA concentration (**D**). (**E**), Platelet fluorescence values over time for each in vitro ASA concentration. (**F**), Schematic summary of secondary platelet aggregation and definition of R value on the basis of platelet deposition rates (F').

2.3   Results

A protocol was established (**Figure 2-1A**) for the recruitment of healthy donors (n = 28, **Table 1**) to obtain 3 venous blood samples. Relevant characteristics of the subjects are reported (**Table 1**). The first blood sample was collected at t = 0 h, followed by ASA ingestion at t = 2 h, and collection of a second sample at t = 26 h, 24 h after *in vivo* ingestion of 325-mg of ASA by all subjects (Period 1). A third venous sample was collected after a 2 week washout period at t = 0 h (Period 2). With each of the 3 blood samples obtained from each donor during Period 1 and 2, ASA was added *in vitro* at increasing doses from 0 to 500 μM ASA prior to running the 300 sec microfluidic test (8 doses run in triplicate per blood draw at an initial wall shear rate of 200 s^{-1}), for a total of 2304 individual clotting events. All results shown are an average of triplicate measurements.

Subject ID	Age	BMI	Gender	Platelet Count Period 1 (x1000 platelets/µL)	Platelet Count Period 2 (x1000 platelets/µL)	% Hematocrit
217	25	27.08	M	190	187	43
246	30	24.28	F	183	171	36
272	22	21.65	F	280	275	39
259	43	20.14	M	220	247	39
262	37	24.18	M	274	233	41
225	31	24.47	F	216	217	36
250	44	24.77	F	227	216	38
241	26	19.47	F	204	227	40
283	37	28.28	F	206	176	38
268	31	27.59	M	293	262	44
203	33	29.71	M	216	226	44
248	33	20.84	F	300	288	38
239	52	24.58	F	225	301	37
216	27	24.98	F	182	195	36
226	51	23.51	F	226	222	34
235	21	20.73	F	189	216	36
238	26	17.54	F	150	183	37
240	48	31.79	M	182	149	40
255	25	20.02	F	183	181	44
212	29	23.92	M	272	191	44
231	35	27.33	M	209	209	45
243	23	19.46	F	235	230	40
278	22	20.37	F	261	258	36
293	37	20.59	F	283	285	39
253	44	26.18	M	224	245	46
256	29	19.12	M	176	176	40
277	25	20.34	F	196	182	36
282	44	28.52	M	243	234	45
Average	33 ± 9	23.62 ± 3.70	11M/17F	223 ± 40	220 ± 39	40 ± 3.5

Table 1. Donor Attributes

Healthy subject age, BMI, gender, platelet count for period 1 and 2, and %Hematocrit were measured and data is presented above.

2.3.1 IC$_{50}$ for ASA during thrombosis under flow

Ex vivo addition of ASA to whole blood was tested in the device in a concentration-dependent manner to calculate IC$_{50}$ values for collagen induced platelet deposition (**Figure 2-1**). In each experiment, a total of 24 simultaneously forming thrombi were imaged in real time. Fluorescently labeled platelets aggregated only at the site of micropatterned collagen, with no platelet deposition upstream or downstream of the micropatterned collagen (**Figure 2-1C,D**). Platelet adhesion due to collagen occurred within 60 sec and secondary platelet accumulation/aggregation continued after 150 sec of perfusion (**Figure 2-1E, Figure 8-2**). Inhibition of secondary platelet adhesion by ASA was measured through the R-value (**Figure 2-1F**). Determination of platelet surface fluorescence at 300 sec (FI$_{300s}$) allowed a measurement of an IC$_{50}$ of 22 μM ASA (**Figure 2-2A**Figure 2-1) for an *in vitro* ASA incubation time of 30 min for Subject 272. The collagen-induced platelet activation was temporally separated and preceded the ASA-sensitive deposition regime. A dose-dependent decrease in platelet deposition rate (F' from 150 to 300 sec) was observed with increasing ASA concentration while the initial platelet deposition rate (F' between 60 and 150 s) was ASA insensitive (**Figure 2-2B**). Finally, internal normalization (**Figure 2-2C**) of late stage F'$_{150-300s}$ divided by early stage F'$_{60-150s}$ provides a R-value of 1.0 near the ASA IC$_{50}$ of 10 μM. This R value showed more dynamic range and sensitivity related to secondary platelet aggregation due to TXA$_2$ release causing a minor left shift in the IC$_{50}$ value to 10 μM. The ASA dose-response was also obtained by *in vitro* addition of ASA to whole blood 24 h after a

23

single 325-mg dose was ingested by subjects. Representative subject 255 lacked response to *in vitro* addition of ASA demonstrating strong inhibition of platelet COX-1 activity by the 325 mg dose (**Figure 2-2D**).
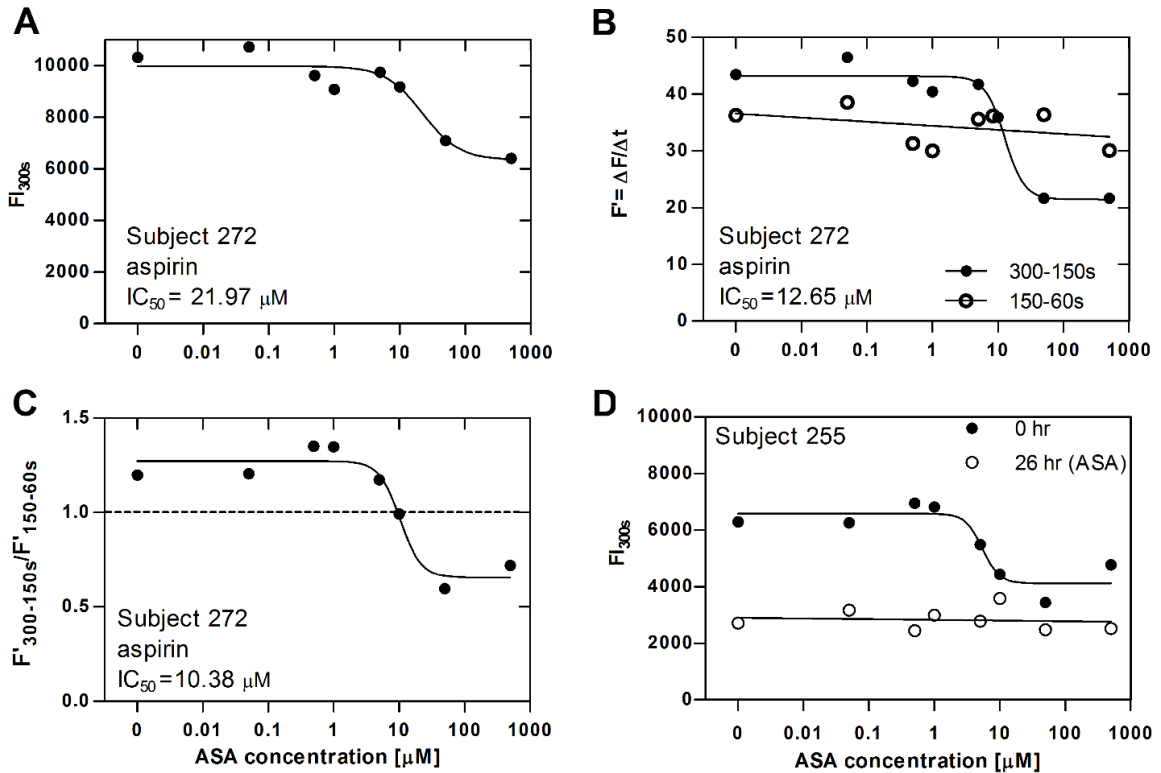
Figure 2-2 Platelet deposition from PPACK-inhibited WB treated with increasing *in vitro* ASA at 200 s^{-1} initial wall shear rate over fibrillar collagen for period 1 (t= 0 h, no ASA ingestion).

(**A**), Representative IC$_{50}$ curve for in vitro ASA dose-response. (**B**), In order to separate COX-1 mediated TXA$_2$ production from the platelet-collagen response, F' = $\Delta F/\Delta t$ was calculated for the initial time interval of 60 to 150 sec and secondary aggregation platelet deposition rate was calculated during the time interval of 150 to 300 sec. Initial platelet deposition rate from 60 to 150 sec was ASA-insensitive. (**C**), Normalization of subject response to *in vitro* ASA using the R-value. (**D**), *In vitro* addition of ASA at 26 h (open circle) had no efficacy after donors took ASA (325mg) at 2 h

2.3.2 Microfluidic ASA Phenotyping and in vitro addition of aspirin after oral administration

Microfluidic phenotyping of whole blood 24-h after a single 325-mg dose was ingested showed that 27 of 28 subjects had some reduction in total platelet accumulation relative to total platelet accumulation measured in blood prior to ASA ingestion (**Figure 2-3A**). Only Donor 253 displayed a slight increase in platelet deposit size, which was not statistically significant. Marked inter-subject variation in the amount of baseline platelet deposition was observed, with FI_{300s} values ranging from below 4000 to above 12000 FI. However, the microfluidic assay detected the decrease in total platelet accumulation following *in vivo* ASA ingestion. Platelet deposition from blood obtained 24 h after ASA ingestion (no additional *in vitro* ASA added) was inhibited relative to the platelet deposition measured for blood prior to ASA ingestion (**Figure 2-3B**). The degree of inhibition of platelet deposition for these 28 subjects at 24 h after ASA dosage ranged from 10 to 90 % (45 % ± 23%; $P < 0.001$, n = 28) (**Figure 2-3B)**. When comparing each subject at 26 h to their response at 0 h, subjects with ≥ 25 % inhibition (16 of 28 subjects) displayed statistically significant inhibition (**Figure 2-3B**, $P < 0.05$). In comparing platelet deposition (FI_{300s}) in response to *in vitro* 500 μM ASA addition relative to *in vitro* 0 μM ASA addition, the *in vitro* addition of high dose ASA was very potent in blood obtained from subjects prior to ASA ingestion where 24 of 28 subjects responded to *in vitro* ASA addition (**Figure 2-3C**, *solid bar*). Only 4 of 28 subjects (Donors 217, 250, 240, 253) lacked significant inhibition with *in vitro* ASA addition to blood obtained prior to in vivo ASA ingestion. In contrast, only 7

subjects of 28 displayed sensitivity to *in vitro* 500 μM ASA addition 24 h after ASA ingestion

(**Figure 2-3C**, *open bar*).
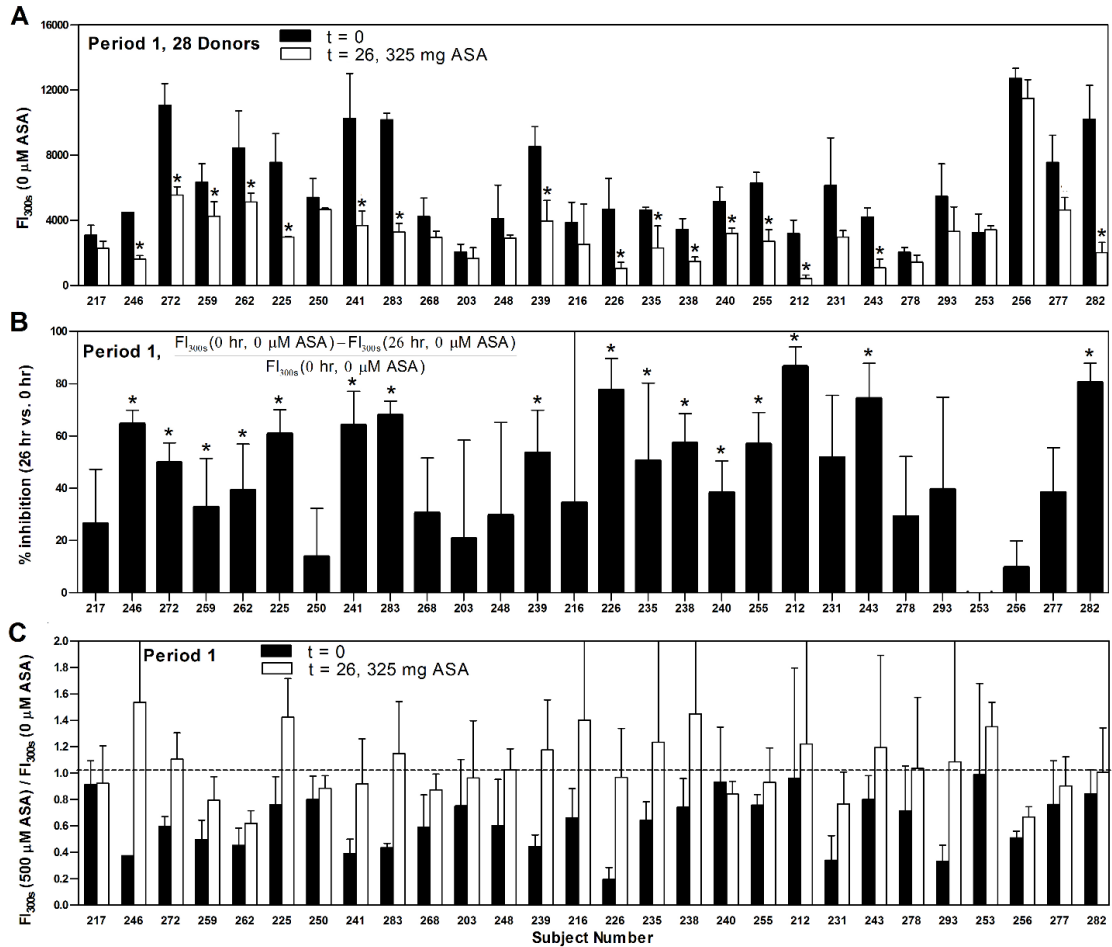
Figure 2-3 Microfluidic ASA Phenotyping of donors

(**A**), Ingestion of ASA at t = 2 h resulted in smaller platelet deposits compared to the response obtained from blood prior to ASA ingestion at t = 0 h (28 donors). *$P < 0.05$, relative to each donor at t = 0 h. Percent inhibition of platelet deposition as a measure of *in vivo* ASA efficacy at 26 h, as assessed by 8-channel microfluidic assay. *$P < 0.05$, relative to each donor at t = 0 h. (**B**). Comparison of high dose in vitro addition of 500 μM ASA measured for whole blood obtained before (t = 0 h) or 26 h after oral ASA administration (t = 2 h) (**C**). Data are mean ± SD (3 replicates).

2.3.3 Microfluidic Assay for measuring platelet deposition in the presence of aspirin

For the 28 healthy donors with platelet counts in the normal range, no correlation between the extent of platelet deposition on collagen and platelet count was observed (**Figure 2-4A**). Subject platelet counts were highly correlated between period 1 and period 2, indicating the ability of the body to tightly regulate total platelet count (**Figure 2-4B**). Total platelet deposition (FI_{300s}) showed a weak but positive correlation between period 1 and period 2 (**Figure 2-4C**).

Using the R-value as a normalized metric of secondary aggregation for each subject, 22 of 28 subjects had R > 1 in Period 1 and 23 of 28 subjects had R > 1 in Period 2 (**Figure 2-4D**). Interestingly, only 2 of 28 subjects had R < 1 in both trial periods (**Figure 2-4D**, *lower left quadrant*), suggesting that almost all donors have a secondary aggregation response (i.e. R > 1) that was detectable in a microfluidic assay when aspirin was absent. All 28 cohorts as a group had an average R = 1.21 ± 0.34 and 1.16 ± 0.22 in period 1, 0 h and period 2, 0 h respectively from 168 determinations of this metric displaying sensitivity and specificity to score secondary aggregation upon no *in vitro* ASA treatment in this microfluidic assay ($P < 0.05$, n = 28). In contrast, with 500 μM ASA added *in vitro*, only 3 of 28 donors displayed R(500 μM ASA) > 1 in both Period 1 and 2 (**Figure 2-4E**) demonstrating that almost all subjects had platelet function that were sensitive to inhibition by ASA. With respect to the *in vivo* activity of ASA, 21 out of 28 subjects had R < 1 at 24 h after ingestion of a 325-mg dose (no ASA added *in vitro*) (**Figure 2-4F**). In these subjects, the addition of 500 μM ASA *in vitro* did not further inhibit platelet function since the platelets had already been inhibited by ASA *in vivo*. Interestingly, the 7 of 28 subjects who had R>1 following

ASA ingestion also displayed insensitivity following *in vitro* ASA addition (*upper right quadrant*, **Figure 2-4F**).

A detailed Receiver-Operator Curve (ROC) analysis (**Figure 8-3**, **Figure 8-4**Figure 8-3) indicated that an R-value = 1 cut-off resulted in a true positive rate of 71 % (sensitivity) and a false positive rate of 36 % (or 64 % specificity) when comparing donors pre and post-ASA ingestion. Similarly, when comparing donors pre and post *in vitro* ASA addition, the R-value = 1 cut-off resulted in a true positive rate of 75 % (sensitivity) and a false positive rate of 33 % (or 67 % specificity).
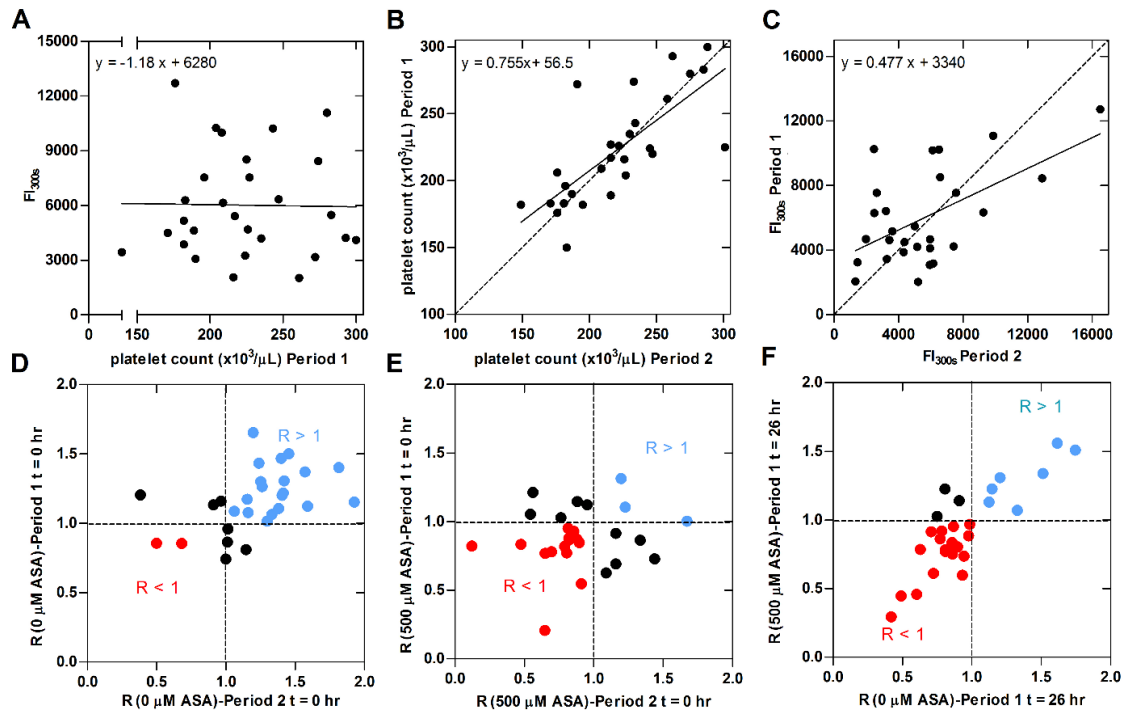
Figure 2-4 Microfluidic assay characterization of in vitro ASA response: R value

(**A**), Final thrombus size measured by final platelet fluorescence without in vitro ASA at t = 300 sec vs. donor platelet count in period 1 (no ASA ingestion). (**B**), Donor platelet count in period 1 vs. donor platelet count in period 2 after 2-week ASA washout period. (**C**), Final thrombus size without *in vitro* ASA addition at t = 300 sec in period 1 vs. final thrombus size without *in vitro* ASA addition at t = 300 sec in period 2. (**D**), R value for

secondary platelet aggregation (no ASA ingestion; no *in vitro* ASA added) in both periods. (**E**), R value for high-dose *in vitro* ASA inhibition of secondary platelet aggregation in both periods 1 and 2 (no ASA ingestion) (**F**), R value for high-dose *in vitro* ASA addition vs zero in vitro ASA addition in period 1 in blood exposed *in vivo* to ASA (ASA ingestion at 2 h).

2.3.4   Effect of in vitro ASA at arterial flow conditions

ASA is used to reduce the incidence of arterial thrombosis. In these microfluidic assays, we have observed that arterial shear rates of 1000 to 2000 sec^{-1} cause unstable thrombi with pronounced embolism, especially when thrombin or fibrin is absent (19). This is especially relevant for experiments conducted at constant flow rate (as opposed to constant pressure drop) where clot growth can cause high shear stresses to occur as the clot partially occludes the flow path. To investigate the pharmacological potency of ASA at arterial shear rates, IC_{50} curves were calculated using the same microfluidic assay by measuring platelet accumulation on collagen under the influence of *in vitro* ASA addition at 1000 s^{-1}. Comparison of the same 4 donors who did not participate in the study protocol previously mentioned at both venous (**Figure 2-5A**) and arterial (**Figure 2-5B**) shear rates indicate the efficacy of ASA under both flow conditions. The slightly lower IC_{50} at 1000 s^{-1}, although not significantly different, compared to the value found at venous shear rate may be due to the reduced levels of TXA_2 in the boundary layer at higher shear rates[34]. Further

work will be necessary to determine if the IC_{50} depends on wall shear rate.
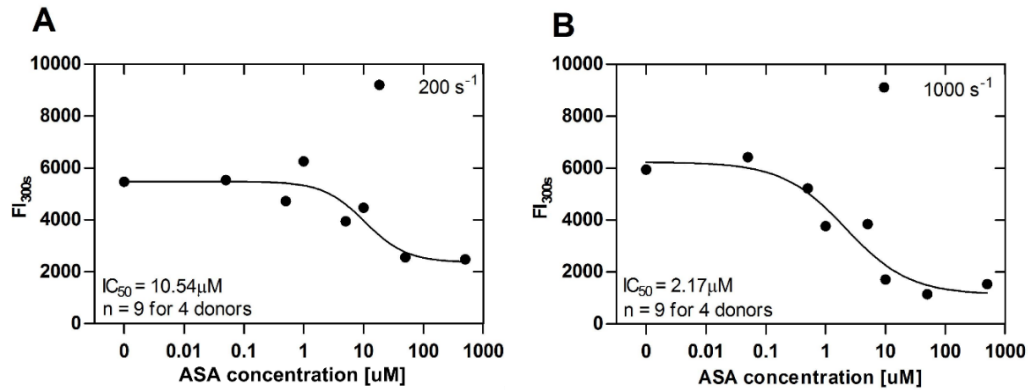
Figure 2-5 Response to *in vitro* ASA dosing: a comparison of venous vs. arterial initial wall shear rate

Representative IC_{50} curves for ASA at venous (**A**) and arterial (**B**) wall shear rates (4 donors). A total of 9 microfluidic assays were run at each initial wall shear rate for the 4 donors.

2.4 Discussion

We demonstrated that whole blood microfluidic assays and the data generated from these assays can produce an aspirin dose-response curve under flow conditions based upon: final platelet fluorescence (FI_{300s} in **Figure 2-2A**), platelet deposition rate between 150 and 300 sec ($F'_{300-150s}$ in **Figure 2-2B**), or the R-value which is a normalized metric of secondary platelet aggregation (**Figure 2-2C**). For each of these metrics, the IC_{50} of aspirin was between 10 and 20 μM which is quite consistent with the known $K_d = 4.5$ μM of ASA against COX-1 [54]. The effect of COX-1 inhibition on donor platelet function after 150 sec in this flow assay is consistent with previous findings in the same microfluidic device and a multi-scale neural network and Monte Carlo simulation of platelet deposition under flow

[52]. Furthermore, this onset of action of ASA is consistent with aggregometry results showing action of COX-1 inhibitors at the later stages after primary aggregation [55]. The assay partially detected the *in vivo* efficacy of ASA ingestion on platelet COX-1 when whole blood was tested *ex vivo* (**Figure 2-3**). Lack of statistical significance of *in vivo* modulation of platelet COX-1 activity due to ASA ingestion in 12 of the 28 subjects tested could be attributed to varying interdonor functionality of TP, $P2Y_1$, and $P2Y_{12}$ receptors. Interdonor changes in $P2Y_1$ and $P2Y_{12}$ receptor response modulate ADP flux from the growing thrombus under flow conditions hence causing variations in total platelet accumulation and the R value. Healthy subjects who ingested 325-mg ASA displayed 45 % smaller platelet deposits on average when the blood was tested 24 h after dosing (**Figure 2-3B**). Whereas healthy donors have platelets that display thromboxane-dependent secondary aggregation in the flow assay (only 2 of 28 donors had R < 1; **Figure 2-4D**), healthy donors have platelets that respond to ASA administered *ex vivo* (only 3 of 28 donors had R > 1 in duplicate tests of 500 μM ASA added *ex vivo*; **Figure 2-4E**).

These microfluidic assays bring together contributions from platelet collagen signaling, granule release, ADP signaling, thromboxane synthesis, and adhesion strength under flow conditions. Thus, the pharmacological effects of COX-1 inhibition were investigated under far more complex conditions than an assay that measures thromboxane synthesis. While the effects of aspirin ingestion or *in vitro* aspirin addition are clearly detectable in our assay, the capabilities of this microfluidic assay to detect "aspirin resistance" for patients with cardiovascular diseases remains unknown, as this study was limited to healthy subjects.

Several platelet function tests currently exist, however these technologies that assess aspirin sensitivity in whole blood have limitations, especially with regards to running a dose-response assay requiring multiple tests. Dose-response assays are fundamental pharmacological tools to quantify drug potency or remaining enzyme activity. The Platelet Function Analyzer (PFA-100) and VerifyNow are tests used to assess inhibition of platelet function by aspirin using whole blood. PFA-100 deploys a cartridge to create flow and measure puncture closure time with an activating coating of collagen/ADP or collagen/epinephrine [56]. The assay is highly dependent on plasma vWF, high shear stress, and epinephrine thus presenting difficulties in isolating the inhibitory effects of aspirin [57]. VerifyNow Aspirin is a point of care assay utilizing whole blood in standard cartridges containing a preparation of human fibrinogen-coated beads and arachidonic acid as agonists [56]. VerifyNow Aspirin is an assay based on light transmittance but lacks a hemodynamic flow field. Most recently development of a perfusion chamber allows for study of ASA dependent changes in platelet deposition [58]. Our methodology is distinct from Stephens et al. where whole blood was perfused through an entire glass capillary coated with human type III fibrillar collagen at 1000 or 1500 sec^{-1}. A collagen-coated capillary creates a long distance of many centimeters of collagen for platelets to activate, adhere, embolize, and recapture on the surface. Platelet deposition is a function of distance from the entrance in this assay due to boundary layer depletion of platelets over the long length of collagen. Since only one capillary is run at a time, dose-response testing is particularly cumbersome. In contrast, our 8-channel microfluidic perfusion of whole blood over fibrillar collagen exposes platelets to a spatially-confined 250 μm long "injury" site where all the data is collected with no

dependence on distance down the microfluidic channel. The 8-channel microfluidic device facilitated the *ex vivo* testing of anti-platelet drugs in a dose-dependent manner over a large cohort of healthy donors.

The biology of thrombosis includes the interaction of platelets with potent vessel wall-derived stimuli including collagen and thrombin. As a layer of platelets becomes activated on collagen, they recruit additional platelets via release of ADP and TXA_2. By targeting the secondary wave of platelet recruitment with $P2Y_{12}$ antagonists and/or cyclooxgenase-1 inhibitors, an anti-thrombotic effect is achieved with reduced risk of bleeding in comparison to other antithrombotic therapies that target biologically active clotting factors like warfarin. Few assays recreate the sequential process of collagen adhesion followed by the release of autocrine factors. Since platelet recruitment, adhesion, and the convective-diffusion of autocrine agents are dictated by prevailing hemodynamic conditions [34], microfluidic assays partially recreate the disease environment in which anti-platelet agents must act. We demonstrate the use of microfluidic assays to evaluate healthy subject response to aspirin. Supplemental discussion about this chapter, including additional discussion topics and data, is presented in the appendix of this dissertation.

3   DETECTION OF PLATELET SENSITIVITY TO INHIBITORS OF COX-1, P_2Y_1, and P_2Y_{12} USING A WHOLE BLOOD MICROFLUIDIC ASSAY

3.1   Introduction

Antiplatelet therapies are used in a variety of clinical settings from management of unstable angina to risk reduction of myocardial infarction or stroke. Aspirin is used by over 50 million patients in the United States to reduce the risk of cardiovascular events[40]. Aspirin irreversibly acetylates serine 529 of cyclooxygenase-1 (COX-1), blocking the enzyme active site for arachidonic acid and inhibiting the generation of prostaglandin H_2 and thus thromboxane A_2 (TXA_2) production from platelets[59]. Inhibition of platelet TXA_2 synthesis prevents platelet activation through the platelet TXA_2 receptor (TP), a receptor encoded by the TBXA2R gene.

In addition to TXA_2, adenosine disphosphate (ADP) receptors are another target of antiplatelet therapies. The platelet plasma membrane contains two ADP receptors, $P2Y_1$ and $P2Y_{12}$, which are purinergic G protein coupled receptors. $P2Y_1$ is linked to G_q and ADP signaling through this pathway results in rapid Ca^{2+} mobilization and platelet shape change [11,60]. $P2Y_{12}$ is linked to a G_i protein. ADP binding to $P2Y_{12}$ inhibits adenylate cyclase and stabilizes secondary platelet aggregation. Current therapies that target the $P2Y_{12}$ receptor range from prodrugs that irreversibly antagonize the $P2Y_{12}$ receptor to direct, reversible antagonists[60,61]. The thienopyridines clopidogrel and prasugrel are examples of the former, while ticagrelor is an example of the latter. Currently, no $P2Y_1$ antagonists are on the United States drug market, however, combined $P2Y_1$ and $P2Y_{12}$ antagonists are in

development[62]. To mimic the action of $P2Y_1$ and $P2Y_{12}$ antiplatelet therapies ex vivo, 2'-deoxy-N6-methyl adenosine 3',5'-diphosphate (MRS 2179) and 2-methylthioadenosine 5-monophosphate (2MeSAMP) are used in this study as highly selective $P2Y_1$ and $P2Y_{12}$ antagonists, respectively.

Targeting signaling pathways such as TXA_2 production and $ADP/P2Y_{12}$ signaling reduces secondary platelet aggregation while not severely altering primary hemostasis. However, the delicate balance between preventing excessive clotting and increasing bleeding risks requires careful monitoring of antiplatelet therapies. The evaluation of the effect of pharmacological agents on platelet function often rely on tests with poorly defined fluid mechanics and flow fields (eg. aggregometry) that fail to replicate platelet adhesive mechanisms under realistic and well geometrically-defined hemodynamic conditions. Under flow conditions, the efficacy of pharmacological agents greatly depend on granule release, platelet-platelet contacts, and convective removal of autocrinic agonists from the injury site. Microfluidic devices can recreate the hemodynamic conditions required to study anti-platelet agents. These devices offer spatially controlled focal injuries with collagen or collagen with tissue factor bearing surfaces[35,37]. Microfluidic devices have also been used to study clot contraction and clot permeability with precise control of wall shear stress and transthrombus pressure gradients [13,63]. In fact, the core-shell hierarchy of clots observed in vivo following laser injury [9] can be replicated in vitro with such devices[63].

Here we continue the development of microfluidic assay metrics found previously[64] and extend these metrics to examine two ADP antagonists and validate this assay for detection of anti-platelet therapies through Receiver-Operator Characteristic (ROC) analysis.

For flow assays to become a relevant clinical tool a large cohort of healthy donors must be tested with respect to response to antiplatelet agents. Toward that goal, we tested healthy subject platelet function with 38 donors and 66 independent blood draws (2 combined studies) following ex vivo addition of ASA. While coagulation assays can rely on stable pooled plasma for calibration, live platelet function assays have no available standard to calibrate the assay. We sought to define a self-normalized parameter, the R-value, to score platelet accumulation on collagen surfaces from a single blood sample test without reference to a prior test value or calibration fluid.

3.2 Materials and Methods

3.2.1 Blood collection, labeling, and antiplatelet agents

Blood was collected via venipuncture from 11 healthy subjects who self-reported as non-smoking, free of oral medication, and abstained from alcohol 48 h prior to donation. All subjects were free from illness and bleeding disorders. Blood samples were drawn into H-D-Phe-Pro-Arg-chloromethylketone (100 µM PPACK final concentration, Haematologic Technologies). All volunteers provided informed consent in accordance with IRB approval and the Declaration of Helsinki. Whole blood was treated with Phycoerythrin (PE) Mouse Anti-Human CD61 ($\alpha_{IIb}\beta_3$) antibody (BD Biosciences) in a ratio of (1:50) 7 min prior to perfusion. This antibody has no effect on platelet $\alpha_{IIb}\beta_3$ function in this microfluidic flow assay. PPACK-treated whole blood was perfused through the device within 25 min of phlebotomy. Blood was incubated with vehicle (0.1% DMSO final concentration) or indicated concentrations of ASA, 2MeSAMP, MRS 2179, or combined 2MeSAMP and MRS

2179 20 min prior to the assay. This time scale is consistent with previous studies done with these compounds[34,52,64]. Acetylsalicylic acid (ASA, Sigma Aldrich) was dissolved in DMSO at 500 mM, 2-methylthioadenosine 5′-monophosphate triethylammonium salt hydrate (2MeSAMP, Sigma Aldrich) was dissolved in HEPES buffered saline (HBS, 20 mM HEPES, 160 mM NaCl, pH 7.5) at 1 mM/L, and 2′-deoxy-N6-methyladenosine 3′, 5′-bisphosphate ammonium salt (MRS 2179, Tocris Bioscience) at 0.1 mM in HBS. A dilution of ASA was then made to the desired final concentration in HBS within 1 h of the test. Final concentrations of antiplatelet therapies used were: 500 μM ASA, 100 μM 2MeSAMP, and 10 μM MRS 2179, well in excess of their IC_{50}s in the assay of 10-20 μM ASA, 2.56 μM 2MeSAMP, and 0.23 μM MRS 2179 respectively[34,64]. Antiplatelet agent concentrations were used well in excess of their respective IC_{50} values to completely antagonize ADP receptors or abate COX-1 derived TXA_2.

3.2.2 Microfluidic devices and real time platelet deposition imaging

Microfluidic devices were fabricated in polydimethylsiloxane (PDMS, Sylgard 184, Ellsworth Adhesives) according to previously described techniques [34,64]. The microfluidic device has 8 parallel channels (250 μm wide by 60 μm high) that converge to a common outlet(**Figure 3-1A**). The device was fed by 8 distinct wells, with perfusion achieved by withdrawal into a single syringe pump (Harvard Apparatus). The channels run perpendicularly over a 250 μm long stripe of patterned equine fibrillar collagen type 1 (Chronopar, Chronolog). Channels were spaced in close proximity to image all 8 eight channels simultaneously with a 2X objective lens using an inverted microscope (IX81, Olympus America Inc.) equipped with a CCD camera (ORCA-ER, Hamamatsu). A custom

stage insert held 3 microfluidic devices allowing formation of 24 simultaneous thrombi to be imaged in 15 sec intervals. Prior to microfluidic assay, all channels were blocked with 0.5% bovine serum albumin (BSA) in HBS buffer. Blood samples were perfused at an initial venous wall shear rate of 200 s^{-1} for 5 min (2 μL/min per channel).

3.2.3 Platelet accumulation analysis

Background corrected fluorescence values were measured using MATLAB (MathWorks) as previously described [34]. Briefly, all eight platelet deposits on a single microfluidic device were identified and corrected with their corresponding background regions downstream of each platelet deposit by a custom MATLAB script. To calculate overall percent inhibition after a 300 s perfusion, platelet fluorescence values were normalized to each donor's baseline platelet adhesion to collagen ($FI_{300s}(Drug)/FI_{300s}$). Additionally, a R-value for ASA (R_{COX}) was defined as a ratio of platelet deposition rates that normalized the late stage platelet deposition rate ($F'_{300-150s}$) to early stage deposition rate ($F'_{150-60s}$) for all ex vivo ASA additions, as previously established[64]. The R_{COX} value is an internal intradonor standard to score secondary aggregation due to TXA_2 secretion, with values of $R_{COX} > 1$ indicating when secondary platelet aggregation was prominent and $R_{COX} < 1$ when secondary aggregation was attenuated by ex vivo ASA treatment (**Figure 3-1C**). In a previous work, a dose-dependent decrease in the rate of secondary platelet aggregation was found with increasing ex vivo ASA concentrations whereas the initial platelet deposition rate on collagen was unaffected by ASA. We now define an additional intradonor normalization metric R_{P2Y} as a ratio of platelet deposition rates normalizing late stage secondary platelet aggregation rate due to ADP release ($F'_{300-105s}$) to earlier stage platelet deposition rate ($F'_{105-60s}$)

(**Figure 3-1D**). The temporal onset for R_{P2Y} was based on previous work[52] establishing that the effect of ADP antagonism occurred after 100 sec, as was later confirmed in platelet dynamic traces for ADP antagonists for the 11 donors in this present study (**Figure 3-1B**).

Finally, sensitivity and specificity for detection of ASA, 2MeSAMP, or MRS 2179 was found through Receiver Operator Characteristic (ROC) analysis[65]. ROC curves were generated to detect the presence of each drug in the microfluidic assay through evaluation of the true positive and false positive fractions and the area under the curve (AUC) [65]. In this analysis, for each antiplatelet therapy tested, ROC curves were generated comparing 10 average R-values, one from each of the 10 healthy subjects with no ex vivo inhibition to 10 average measurements of the R-value for each anti-platelet drug tested.
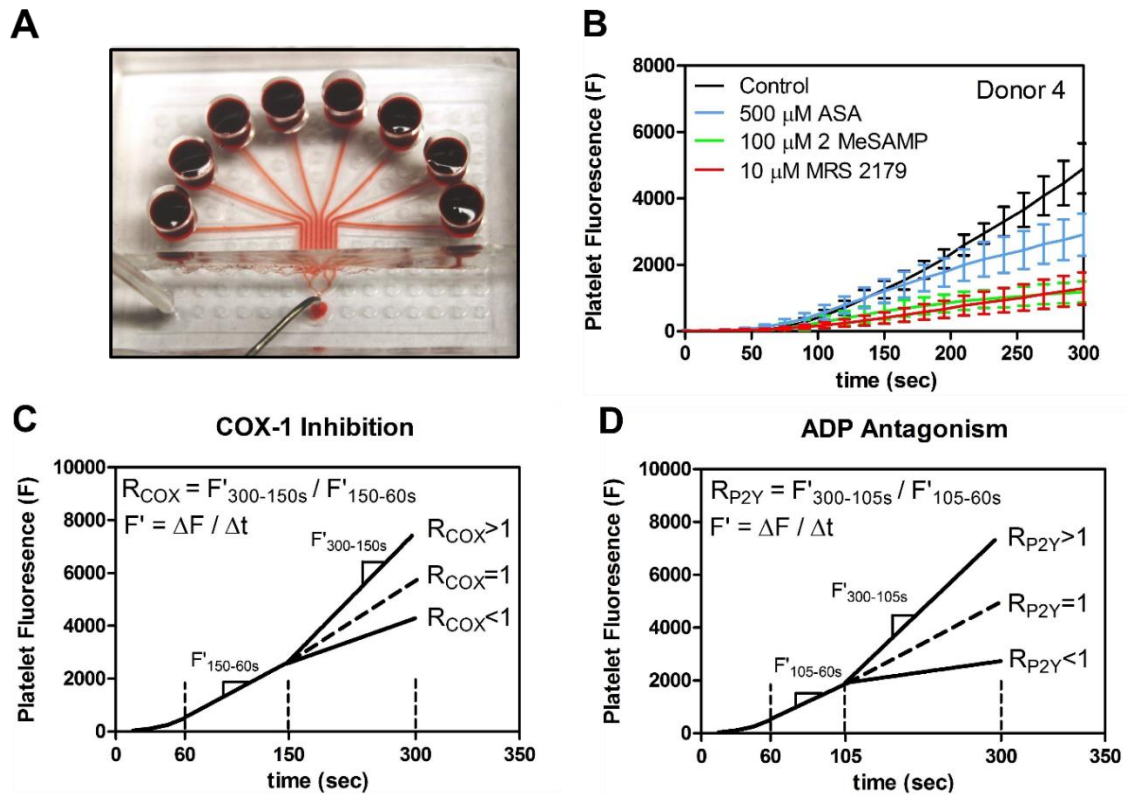
Figure 3-1 Eight-channel device, measured platelet fluorescence dynamics, and R_{COX}, R_{P2Y} schematic summaries.

(A), Photograph of the 8-channel microfluidic device, the device is fed by 8 wells converging into a single outlet. **(B)**, Platelet fluorescence values over time in the presence of aspirin, 2MeSAMP, and MRS 2179. Error bars indicate standard deviation from 6 measurements at each time point. **(C)**, Graphic representation of R_{COX} based on a ratio of platelet deposition rates (F') of secondary platelet aggregation to initial platelet deposition on collagen. **(D),** Graphic representation of $R_{P2Y.}$

3.3   Results

Ex vivo testing of anti-platelet agents occurred in duplicate on 3 separate microfluidic devices run simultaneously. For 11 subjects, a total of 432 individual thrombi were formed under flow on collagen, resulting in 108 events each for 3 individual conditions (control,

2MeSAMP, and MRS 2179), 60 events for ex vivo ASA addition, and 48 events for ex vivo addition of 2MeSAMP and MRS 2179. Statistical analysis was conducted to evaluate intradonor variations for duplicate control conditions on a single microfluidic device or 3 devices run simultaneously (6 conditions). Total platelet accumulation (FI_{300s}) and secondary aggregation [$R_{COX}(0)$] values for whole blood perfusion with vehicle buffer were tabulated from 11 blood samples and the coefficient of variation for each donor defined as standard deviation divided by the mean was found (**Table 7, Table 8**). Coefficients of variation for FI_{300s} ranged from 5.3% to 35.8% (mean = 13.1%) for replicate channels on a single device while values varied from 5.3% to 24.4% for triplicate microfluidic testing (mean = 16.3%). For $R_{COX}(0)$, coefficient of variation values were all < 20% for a single microfluidic device or triplicate device testing with the exception of donor 4 and donor 10. In 3 comparisons evaluating ex vivo ASA efficacy (**Figure 3-5**), prior supplementary data for 28 individuals [64] obtained in the same manner as this study was combined with data from 10 subjects from this work. Only 1 subject partook in both studies.

Platelets adhere substantially to the localized collagen surface within 1 minute and subsequent secondary platelet accumulation via platelet-platelet interactions over the 300 s perfusion time has been well-established in previous studies [34,52]. Growth in platelet coverage occurs in two dimensions on the collagen surface between 60 -105 sec. After 105 sec, thrombus growth continues in the third dimension and thrombus height under flow increases significantly due to secondary platelet-platelet aggregation mediated by soluble agonists such as ADP and TXA_2 at approximately 105 s and 150 s, respectively.

3.3.1 Platelet inhibition by ASA, 2MeSAMP, and MRS 2179

Platelet adhesion and subsequent secondary platelet aggregation were significantly reduced upon ex vivo addition of ASA, 2MeSAMP, or MRS 2179 (**Figure 3-1B**). Using R_{COX} or R_{P2Y} (**Figure 3-1C, D**), 8 out of 10 subjects displayed significant secondary platelet aggregation [R(0 drug) > 1] before ex vivo drug addition (**Figure 3-2A-C**). In contrast, 9 out of 10 subjects had $R_{COX} < 1$ upon ex vivo treatment with ASA **(Figure 3-2A)**. Furthermore, 9 out of 10 subjects had $R_{P2Y} < 1$ with ex vivo 2MeSAMP addition, demonstrating that most subjects had secondary platelet aggregation and primary platelet deposition that was sensitive to $P2Y_{12}$ antagonism (**Figure 3-2B**). R_{P2Y} was less reliable in scoring MRS 2179 inhibition of $P2Y_1$ with only 6 out of 10 subjects having $R_{P2Y} < 1$ (**Figure 3-2C)**, in part (ironically) due to the high potency of MRS 2179 in reducing Ca^{2+} mobilization through $P2Y_1$ signaling. Hence MRS 2179 drastically reduces primary platelet deposition in comparison to 2MeSAMP, thus the associated difficulty of taking a ratio of two small numbers as both primary platelet deposition and secondary platelet aggregation rate were inhibited by MRS 2179.

ROC curves were generated to examine the inhibitory effects of ASA, 2MeSAMP, and MRS 2179 in this assay (**Figure 3-2D-F)**. In comparing 10 measurements of $R_{COX}(0)$ (true full COX-1 activity, true full $P2Y_{12}$ and $P2Y_1$ function) to 10 measurements of R_{COX} (500 μM ASA) (true full COX-1 inhibition), the ROC curve had an AUC of 0.874 **(Figure 3-2D)**. Comparison of 10 R_{P2Y} values at baseline to 10 $R_{P2Y}(100$ μM 2MeSAMP) (true full $P2Y_{12}$ antagonism) gave an ROC curve AUC of 0.966 **(Figure 3-2E)**. Finally, in comparing the same 10 baseline R_{P2Y} values to $R_{P2Y}(10$ μM MRS 2179) an ROC curve AUC of 0.889 was

obtained. Calculated ROC AUC values indicate excellent diagnostic discrimination between populations upon ex vivo treatment with ASA, 2MeSAMP, or MRS 2179. ASA, 2MeSAMP, or MRS 2179 all decreased total platelet accumulation at 300 sec when normalized against baseline collagen response reaching statistical significance for the entire cohort ($p < 0.01$, $n = 10$ subjects) and each antiplatelet agent (**Figure 3-3**). The % inhibition of platelet function was much greater for 2MeSAMP and MRS 2179 than ASA. However, the effect of ex vivo 2MeSAMP and MRS 2179 were not statistically different from each other. While the % inhibition is very useful for measuring drug potency following ex vivo drug addition, it requires reference to a separate untreated blood sample which may not necessarily be available clinically with patients. In contrast, the R-value is self-normalized and can be used for a single blood sample obtained from a patient without the need to reference to a prior blood test to obtain % inhibition.
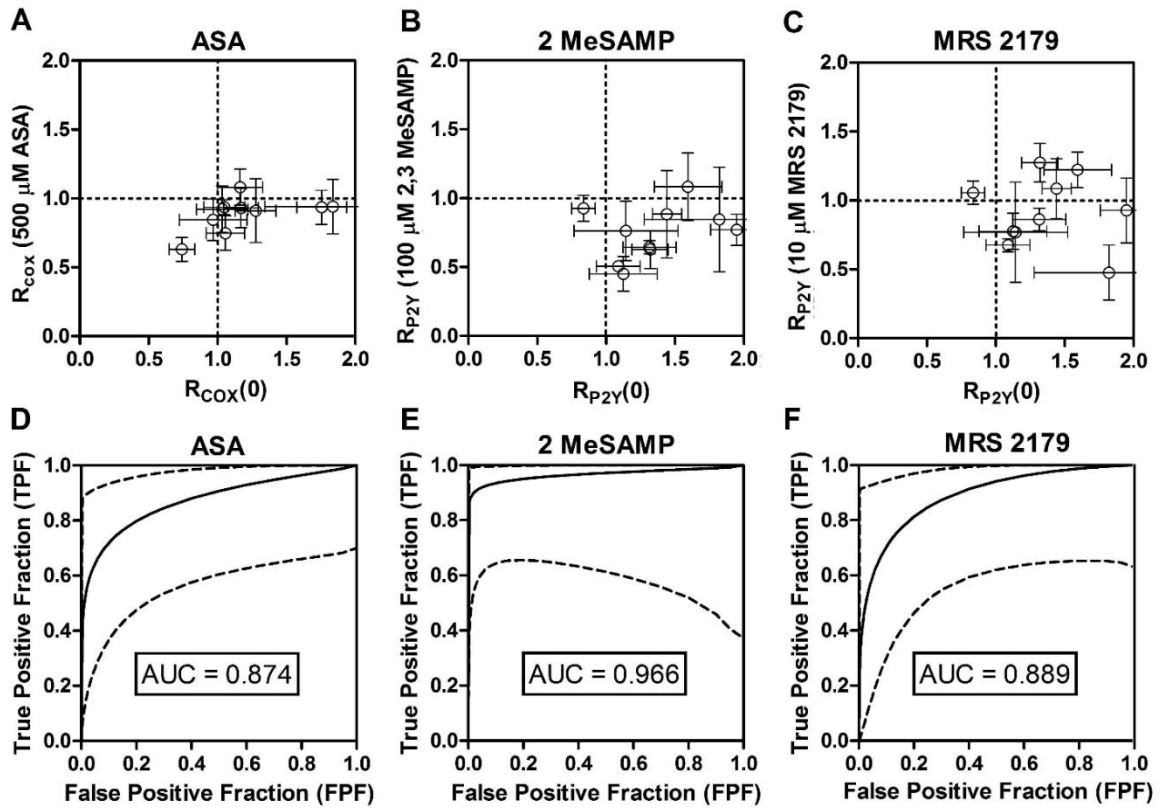
Figure 3-2 Microfluidic assay sensitivity and specificity of R_{COX} and R_{P2Y} to detect inhibition of primary platelet adhesion to collagen or secondary platelet aggregation

(A), R_{cox} for ex vivo ASA addition. **(B)**, R_{P2Y} for ex vivo 2MeSAMP addition. **(C)**, R_{P2Y} for ex vivo MRS 2179 addition. **(D)** ROC curve for detection of ex vivo ASA addition. **(E)**, ROC curve for detection of ex vivo 2MeSAMP addition. **(F)**, ROC curve for detection of ex vivo MRS 2179 addition. Error bars indicate standard deviation from 6 measurements of R_{COX} or R_{P2Y} for each donor. Dashed lines are 95% confidence intervals.

44
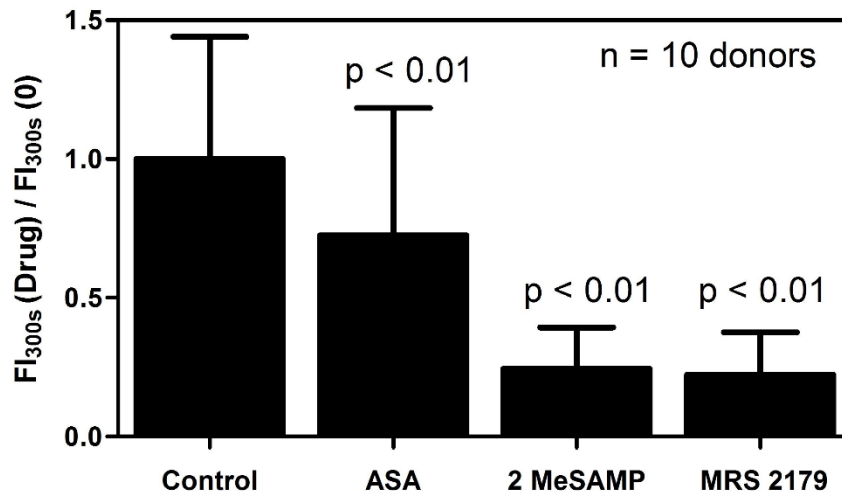
Figure 3-3 Effect of ex vivo ASA, 2MeSAMP, or MRS2179 on final platelet aggregate size normalized by baseline platelet aggregate size formed on collagen.

Ex vivo addition of ASA, 2MeSAMP, or MRS2179 resulted in smaller final platelet aggregate size compared to response measured with no drug ($p < 0.01$, n = 10 donors)

3.3.2   Platelet inhibition by combined 2MeSAMP and MRS 2179 ex vivo addition

To investigate the effects of combined $P2Y_1$ and $P2Y_{12}$ inhibition by MRS 2179 and 2MeSAMP respectively, 7 of the 10 subjects from the above study of ex vivo addition of either $P2Y_1$, $P2Y_{12}$, or COX-1 inhibitor alone were re-enrolled along with new subject #11. Platelet fluorescence traces over time representing thrombus buildup during the microfluidic assay were reduced in the case of combined $P2Y_1$ and $P2Y_{12}$ inhibition of platelet function in comparison to ex vivo $P2Y_1$ or $P2Y_{12}$ inhibition alone (**Figure 3-4A**). Using MRS 2179 and 2MeSAMP together, both primary deposition rate and secondary platelet aggregation rates were strongly reduced when compared to control or when MRS 2179 or 2MeSAMP were used individually to inhibit platelet function **(Figure 3-4A)**.

Combined ex vivo addition of 2MeSAMP and MRS 2179 dramatically reduced total platelet accumulation at 300 sec when normalized against control platelet response to collagen **(Figure 3-4B).** The platelet mass at the end of 300 sec due to combined $P2Y_1$ and $P2Y_{12}$ inhibition was significantly smaller than the platelet masses due to single $P2Y_1$ or $P2Y_{12}$ inhibition ($p < 0.001$, n = 8 subjects) **(Figure 3-4B)**. Because the primary deposition rate was so strongly attenuated, R_{P2Y} was not suited to score combined $P2Y_1$ and $P2Y_{12}$ inhibition (**Figure 3-4C**). This is due to the high efficacy of combined MRS 2179 and 2MeSAMP treatment on the primary platelet deposition rate on collagen in this microfluidic thrombosis model. The primary deposition rate becomes exceedingly low once ADP is completely attenuated under flow conditions through inhibiting both $P2Y_{12}$ and $P2Y_1$ signaling pathways. ADP is a potent modulator of platelet recruitment to the initial monolayer of platelets adherent to collagen. The R-value was originally intended to score secondary aggregation, hence the difficulties in using R_{P2Y} to detect a ratio of platelet deposition rates over the two temporal ranges.
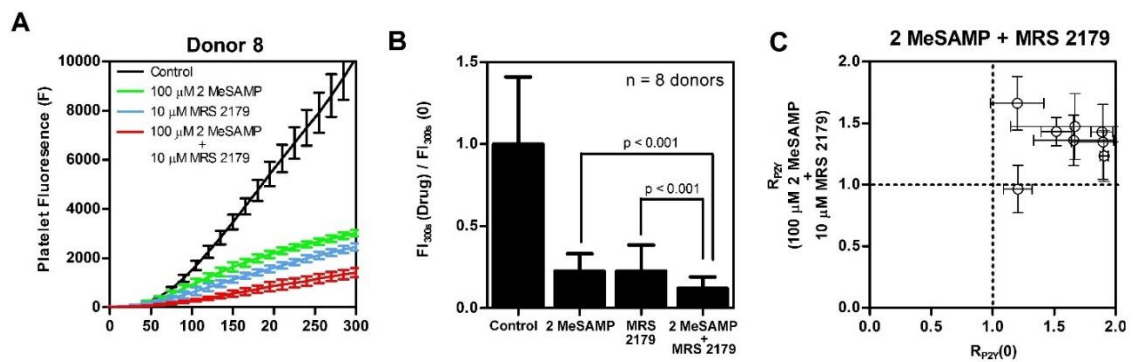
Figure 3-4 Effect of combined ex vivo addition of 2MeSAMP and MRS2179 on platelet function in comparison to ex vivo addition of 2MeSAMP or MRS2179 alone.

(A) Platelet fluorescence dynamics over time in the presence of ex vivo 2MeSAMP, MRS 2179, or combined 2MeSAMP and MRS 2179. **(B)** Ex vivo addition of 2MeSAMP and MRS 2179 reduced final thrombus size more significantly than 2MeSAMP or MRS 2179 treatment alone when normalized against final control thrombus size over collagen ($p < 0.01$, $n = 8$ donors). **(C)** R_{P2Y} for combined ex vivo 2MeSAMP and MRS 2179 addition. Error bars indicate standard deviation for 6 measurements of R_{P2Y} for each donor.

3.3.3   Statistics of platelet phenotyping with microfluidics using ASA

Finally, we incorporate and quantify historical supplementary data from a previous work [64] into this study with intent to show the full distribution of microfluidic platelet function metrics (total platelet accumulation, primary and secondary platelet deposition rates, R_{COX}). Distribution of these metrics is optimal with maximum data in assessing the capabilities of this microfluidic assay to detect the inhibitory effects of ex vivo ASA on platelet function.

Microfluidic phenotyping of 37 donors, 10 from the current study and 28 from a previous study [64] showed a broad distribution of primary platelet deposition rates on collagen with no ex vivo ASA treatment (**Figure 3-5A**). Late stage secondary platelet aggregation also distributed broadly **(Figure 3-5A)**. Binning of total platelet accumulation showed varied inter-subject platelet function response to collagen with FI_{300s} values ranging from 2,000 to 16,000 **(Figure 3-5B)**. Interestingly, the 10 healthy subjects from this study exhibited FI_{300s} values all below 6000 while the larger unique subset of 28 subjects from the previous study showed a wider range of FI_{300s} values. The stochastic Gaussian-like distribution of $R_{COX}(0)$ values centered above 1 indicated that R_{COX} was a robust measurement of secondary platelet aggregation response in untreated whole blood **(Figure**

47

3-5C). The use of $R_{COX} = 1$ as the decision value was previously reported as the microfluidic assay for detection of in vivo and ex vivo ASA had high discrimination (high true positive rate with low false positive rate) at this anchoring point [64]. In a total of 66 determinations of $R_{COX}(0)$, 52 measurements were above the $R_{COX} = 1$ cutoff demonstrating a majority of donors had a strong secondary platelet aggregation response in the assay. Observation of 14 values of $R_{COX} < 1$ indicate some donors lack detectable secondary aggregation by this assay, a phenomena potentially attributable to low levels of released ADP and TXA_2 in the boundary layer formed above the platelet deposit [52]. In contrast, with 500 μM ASA added ex vivo, 49 of 66 determinations of $R_{COX} < 1$ demonstrated that most subjects had platelets that were sensitive to ASA inhibition of platelet TXA_2 production **(Figure 3-5C)**. The 17 determinations of R_{COX} where $R_{COX} > 1$ with 500 μM ASA added ex vivo could be due to non COX-1 mediated ASA effects on platelets when they are activated by collagen with autocrinic ADP present [66]. Such blood samples may be worthy of further study with respect to the phenotype of functional insensitivity to ASA despite COX-1 acetylation. A notable left shift of the distribution away from $R_{COX}(0)$ was evident for the 66 determinations of $R_{COX}(500$ μM ASA$)$ **(Figure 3-5C)**.
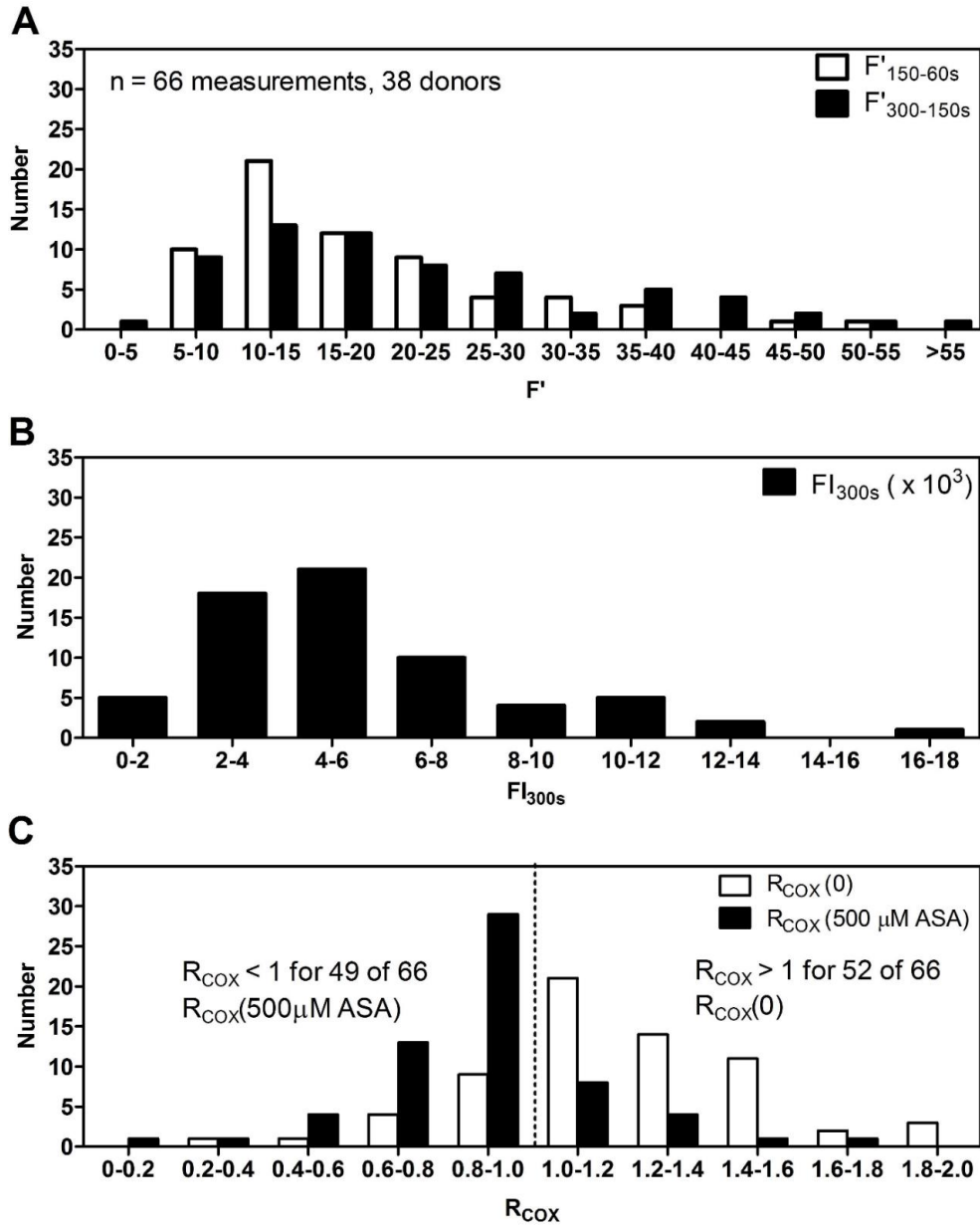
Figure 3-5 Distribution of microfluidic metrics in the assessment of platelet adhesion to collagen and ASA's inhibition of platelet function under flow.

(A), Binning of primary and secondary platelet deposition rates. **(B)**, Binning of final platelet accumulation as measured by platelet fluorescence at t = 300s (FI_{300s}). **(C)**, Binning of R_{COX} values in assessment of the effect of ASA on secondary platelet aggregation in the microfluidic perfusion assay.

3.4 Discussion

We demonstrated the utility of whole blood microfluidic assays run on an 8-channel microfluidic device to assess the effect of various anti-platelet agents on platelet function under flow. We extended from a previous study [64] the R_{COX} value, a normalized metric to detect reduction in secondary platelet aggregation due to ex vivo ASA addition (**Figure 3-1C**). We now define R_{P2Y} a ratio of secondary platelet aggregation rate to primary platelet deposition rate (with a different temporal profile than R_{COX}) to quantify $P2Y_1$ and $P2Y_{12}$ antagonists **(Figure 3-2)**. Examination of R_{P2Y} and ROC curve testing establish 2MeSAMP and MRS 2179 as potent anti-platelet drugs that target both initial platelet adhesion to collagen and secondary platelet aggregation by attenuating the autocrine ADP pathway (**Figure 3-6**).
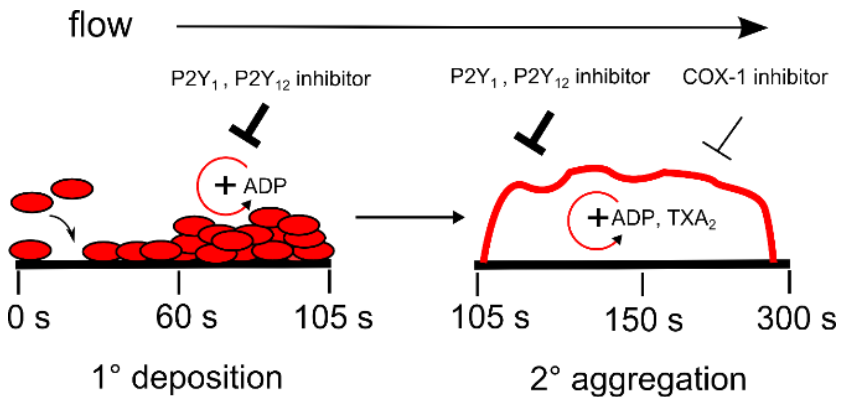
Figure 3-6 Effect of P_2Y_1, P_2Y_{12} antagonists and ASA on primary platelet adhesion to collagen and secondary platelet aggregation due to ADP and thromboxane autocrine and paracrine signaling.

COX-1 inhibitor ASA reduced secondary aggregation between 150 and 300 s without an effect on primary platelet deposition to collagen from 60 to 150 s. 2MeSAMP and MRS 2179 reduced primary deposition between 60 and 105 s and secondary platelet aggregation between 105 and 300 s. Time intervals marked are indicators for R_{COX} and R_{P2Y}, 60- 150 sec & 150 sec-300 sec and 60-105 sec & 105 sec-300 sec respectively. X-axis is not to scale.

The effect of ASA on secondary platelet-platelet interactions has been well-characterized in platelet aggregometry [55]. Under flow, ADP and TXA_2 are complex and interacting modulators since both can become elevated in a concentration boundary layer [52]. Additionally, R_{P2Y} was shown to be unsuited to score the potency of combined $P2Y_1$ and $P2Y_{12}$ antagonism of platelet function because primary deposition rate was so strongly inhibited in this microfluidic thrombosis model. Measured platelet fluorescence dynamics and normalization of final platelet mass against control platelet masses formed over collagen for 8 healthy donors showed ex vivo dual treatment with $P2Y_{12}$ and $P2Y_1$ inhibitors to be significantly more potent than single ex vivo $P2Y_1$ or $P2Y_{12}$ antagonism (**Figure 3-4B**).

We report findings with some similarities and differences to the prior flow studies of Lucitt et al. [67] and Mendolicchio et al. [68]. Lucitt et al. found no effect on the rate of platelet coverage of the collagen surface with in vitro ASA addition at 1500 s^{-1}. However, percent surface coverage may be a less sensitive measure of secondary aggregation which also increases the height of platelet deposits. Menolicchio et al. also reported a limited reduction of platelet aggregate growth above the layer of platelets adherent to collagen with in vitro addition ASA at 1500 s^{-1}. Since there was no thrombin/fibrin generation allowed in Lucitt [67] who used 300 ATU hirudin or Menolicchio [68] who used 68 USP heparin,

arterial shear rates of 1500 s^{-1} may limit the detection of ASA action because thrombin/fibrin dramatically stabilize the platelet deposit at arterial conditions[37]. As a platelet deposit grows in height in a flow channel, the shear rates become exceedingly high during a constant flow rate perfusion and embolization is likely, especially at an initial arterial wall shear rates, with or without fibrin present[37]. At the venous shear rate used with antiplatelet agents in the present study, partially occlusive deposits formed in the absence of thrombin/fibrin are more reliably measured since there is no embolization, even under constant flow conditions. In prior work, we have shown that the IC$_{50}$ of ASA measured at venous shear rates was quite similar to that measured at arterial shear rates [64]. In addition, the IC$_{50}$ of 2MeSAMP and MRS 2179 at venous wall shear rates were also on the same order of magnitude to that found at arterial shear rates (1000s^{-1}) (**Figure 8-5**).

Lucitt et al. also reported an effect of in vitro 2MeSAMP on initial platelet recruitment on collagen surfaces delaying the time to reach 2.5% platelet surface coverage to 56 sec as compared to 33 sec for the control case in an 8 min assay at 1500 s^{-1}. Lucitt et al. found that in vitro ASA had no effect on this initial stage of platelet adhesion. We report findings consistent with Lucitt et al. but at 200 s^{-1}. We found that ASA does not affect primary platelet deposition to collagen ($F'_{150-60s}$), while 2MeSAMP and MRS 2179 inhibit primary platelet response to collagen ($F'_{105-60s}$) but more significantly affects secondary platelet aggregation ($F'_{300-105s}$) requiring R_{P2Y} as a new internally normalized metric to characterize platelet response to ADP antagonists under flow. ADP antagonists were found to inhibit platelet function by ~ 105 sec as compared to ~ 150 sec due to ASA inhibition of TXA$_2$ release. Also, Lucitt et al. determined 2MeSAMP significantly reduced the rate of

platelet aggregate formation on collagen by impairing recruitment of additional platelets. Menolicchio et al. reported marked reduction of platelet aggregation above the initial platelet surface on collagen due to in vitro addition of 2MeSAMP. Both report these results at $1500s^{-1}$. This is consistent with our findings at $200s^{-1}$ with R_{P2Y} and ROC curves detecting significant impairment of secondary platelet aggregation due to either 2MeSAMP or MRS 2179.

Monitoring of $P2Y_{12}$ inhibition by clopidogrel or other $P2Y_{12}$ antagonists can be achieved through assays such as vasodilator-stimulated phosphoprotein phosphorylation (VASP), turbidometric platelet aggregometry, or the VerifyNow P2Y12 test. Although platelet aggregometry remains the gold standard for platelet function testing, several disadvantages exist such as poor reproducibility, high sample volume, and complex sample preparation[44]. Turbidometric platelet aggregometry testing uses ADP induced platelet aggregation to measure the effect of clopidogrel. However, ADP can illicit platelet aggregation through $P2Y_1$ while VASP requires flow cytometry and an experienced technician[44]. Point of care assays are especially advantageous in clinical settings as they enable immediate decision making for dosing of antiplatelet drugs. The VerifyNOW P2Y12 is the only device that meets the various constraints to be considered a point of care assay. Interestingly, in comparing the clinical utility of this microfluidic assay to the VerifyNow P2Y12 system, ROC curve AUC values were strikingly similar. A ROC curve value of 0.929 was found in the assessment of the VerifyNow P2Y12 assay to detect antiplatelet effects during clopidogrel therapy, comparable to the 0.966 value found for 2MeSAMP in this study[69].

53

With regards to microfluidic flow assays, microfluidic chambers often utilize a single flow path comprised of a millimeter length collagen coated cover slip or capillary tube enabling platelets to tether, activate, and re-adhere along the entire length[67]. With such long zones available for adhesion, the platelet coverage is often a function of distance along the collagen. The current microfluidic injury model exposes platelets to a narrow 250 μm long collagen strip with no dependency on distance down the "injury" site as the image capture zone is the entire prothrombotic surface. Furthermore, the type of collagen used as the adhesive substrate impacts platelet-surface interactions. Previous reports utilize bovine soluble collagen type I, porcine type I collagen, or equine tendon fibrillar type I collagen[13,37]. The equine fibrillar type I collagen used in this study is a thoroughly established prothrombogenic surface as a recent study examined sources of variability over this collagen type in microfluidic flow assays for n = 104 healthy donors[70].

Several previous flow systems have been examined for the detection of $P2Y_1$, $P2Y_{12}$ antagonists and COX-1 effects under various shear rates[67,68,71]. However, distinct in our studies are the eight channels comprising this single microfluidic device capable of performing dose-response experiments for 8 different concentrations on a single antiplatelet agent or high throughput testing of three antiplatelet agents in duplicate with simultaneous testing across three devices. Single channel platelet function measurements make dose response testing and high replicate testing of multiple drugs cumbersome. Dose dependent testing of the inhibitory effects of antiplatelet therapies on platelet function is crucial in narrowing the therapeutic window for these drugs. This would be an additional step towards personalized medicine in a clinical setting.

While antiplatelet agents are used for the prevention of arterial thrombosis, the monitoring of antiplatelet agents in anticoagulated whole blood (that lacks fibrin stabilization) is perhaps most precisely detected at venous shear rate, especially when constant flowrate perfusion is used. The action of antiplatelet agents on thrombus build-up in the presence of fibrin generation at arterial shear rates remains an area of active investigation. Such arterial thrombosis studies will be best conducted under microfluidic conditions of constant pressure drop (not constant flow rate) where channel occlusion is a natural and important endpoint to the experiment [37]. Further work would be required to examine whether the presence of thrombin and fibrin in this microfluidic thrombosis model affects the inhibitory capabilities of 2MeSAMP and MRS 2179 on platelet function and as well as the compounds' respective IC_{50} values at venous and arterial wall shear rates. A constant pressure drop microfluidic thrombosis model at initial arterial wall shear rates would be more physiologically relevant. This could be a future avenue to investigate the efficacy of $P2Y_1$ and $P2Y_{12}$ inhibitors over increasingly complex surface triggered prothrombogenic surfaces such as lipidated recombinant tissue factor on collagen[35].

The 8-channel microfluidic phenotyping of healthy subject response to anti-platelet therapies in this study was able to reproduce the biochemical signaling pathways and transport processes under which antiplatelet therapies must act. Quantification through platelet deposition rates, total platelet fluorescence and the all encompassing R value self-normalizes donors without requiring donor specific measurements of vWF levels, platelet count, and hemoatocrit. However, quantification of secondary platelet aggregation using R_{P2Y} or R_{COX} has not been tested with patients on clopidogrel or combined clopidogrel and

aspirin regiments. Translation of these values to quantify patients treated for coronary heart disease remains an area of future study. This work represents another step towards a functional high throughput point of care platelet function assay to detect patient-specific response to various antiplatelet therapies.

4 MICROFLUIDIC ASSAY OF HEMOPHILIC BLOOD CLOTTING: DEFICITS IN PLATELET AND FIBRIN DEPOSITION AT LOW FACTOR LEVELS AND POTENTIATION OF rFVIIa-INDUCED FIBRIN DEPOSITION BY THE CONTACT PATHWAY

4.1 Introduction

Hemophilia A and B are X-linked genetic disorders resulting in deficiencies of coagulation factor VIII (FVIII) or FIX, respectively[72]. The inheritance of FXI deficiency, also known as hemophilia C, is autosomal, and mostly leads to a bleeding risk during trauma[73]. Bypass therapies are used when neutralizing antibodies develop against FVIII, FIX, or less commonly FXI in hemophilic patients. Bypass therapies, including activated prothrombin complex concentrates (aPCC) and recombinant factor FVIIa (rFVIIa) supplant FXa generation from the intrinsic tenase (FIXa/FVIIIa) by increasing prothrombinase levels or activating FX on the platelet surface that then leads to thrombin generation[74]. Evaluations of responses to infused rFVIIa in hemophilia A and B patients reveal phenotypic differences in the drug's capacity to restore hemostasis[75]. Previous studies show that addition of rFVIIa to washed platelets increases platelet adhesion and aggregation to collagen at arterial shear rates attributable to the binding of rFVIIa to activated platelets[76]. Others showed a significant decrease in lag time and an increase in total fibrin deposition[77]. However, the effect of rFVIIa on fibrin generation under flow conditions

and the potential role of the contact pathway in rFVIIa efficacy has not yet been investigated.

Recent developments in microfluidics have allowed low volume, high-throughput hemostatic assessment of platelet function[23,64,78]. We have previously described a microfluidic model evaluating contact pathway-driven coagulation using whole blood (WB) from patients with congenital bleeding disorders perfused over collagen without exogenously added tissue factor[23]. Platelet and fibrin deposition in WB from patients with FVIII and FIX-deficiencies displayed deficits in both platelet and fibrin deposition at <1% critical factor level activity[23].

In the current study, the efficacy of rFVIIa was tested in high and low corn trypsin inhibitor (CTI, 4 or 40 μg/ml) inhibited WB from healthy or clotting factor-deficient hemophilia patients. CTI is a potent and selective inhibitor of βFXIIa[79]. Normal or hemophilic WB was perfused over collagen type I surfaces at an initial venous wall shear rate of 100s^{-1}. We observed rFVIIa potentiation of platelet adhesion to collagen in hemophilic patients and healthy donors independent of CTI. However, with strong inhibition of the contact pathway (high CTI), exogenous rFVIIa was unable to rescue fibrin generation in cases of severe or moderate factor-deficiencies. The low levels of thrombin generated by rFVIIa alone indicate a novel role for the contact pathway in potentiating platelet-rFVIIa function. Thus in the absence of exogenous tissue factor, rFVIIa promotes platelet deposition on collagen by production of "signaling" levels of thrombin, but does not rescue fibrin deposition to normal levels unless the contact pathway participates.

4.2 Materials and Methods

4.2.1 Blood collection, labelling, rFVIIa addition and patient recruitment

Blood was drawn from healthy donors (n = 10) and coagulopathic patients (n = 8) under Internal Review Board approval of the University of Pennsylvania. Information regarding patient sex, age, bleeding phenotype, and recent therapy was collected(**Table 2**). Laboratory testing of hemophilic patients included a platelet count, residual coagulation factor activity, prothrombin time (PT), and activated partial thromboplastin time (aPTT). Residual FVIII, FIX, or FXI activity were measured in Hemophilia A and VWD disease, Hemophilia B, and Hemophilia C diagnoses respectively. The aPTT test assesses contact pathway function by measuring the time to clot formation in platelet-poor plasma in the presence of contact activators. aPTT values (reference range: 20.9-34.4 sec) were negatively correlated with residual factor activity levels as previously established[23]. Healthy donors were self-reported free of oral medication for 7 days and abstained from alcohol 48 h prior to blood donations.

Patient ID#	Diagnosis	Residual Coagulation Factor %*	aPTT (Sec)	Platelets ($10^3/\mu L$)	Timing of Most Recent Therapy	Replacement Therapy Dosage
50	Moderate Hemophilia C	3%	58.7	274	None	N/A
51	Severe Hemophilia A	<1%	78.6	233	1 wk	35 IU/kg rFVIII
52	Severe Hemophilia A	15%	43.5	204	20 hr	26 IU/kg rFVIII
53	Severe Hemophilia A	15%	39.9	239	24 hr	30 IU/kg rFVIII
54	Moderate Hemophilia B	5%	48.2	250	30 hr	50 IU/kg rFIX
55	Severe Hemophilia A	3%	51.8	201	4 days	30 IU/kg rFVIII
56	Moderate Hemophilia A	10%	46	333	4 wk	51 IU/kg rFVIII
57	Severe Hemophilia A	9	57.1	145	3 days	27 IU/kg rFVIII

Table 2. Eight patients were examined with respect to ex vivo rFVIIa addition in the microfluidic hemostasis model with high or low CTI-inhibited WB.

Time since last hemostatic therapy, % residual coagulation factor activity, PTT, and platelet count are as reported. *Reflects in some cases recent administration of factor concentrate.

WB was drawn into 4 µg/ml and 40 µg/ml CTI (Haematologic Technologies, Essex Junction, VT) containing polypropylene test tubes, a material which minimally activates the contact pathway. A low 4 µg/ml CTI is a concentration sufficient to prevent visible clotting in the test tube for approximately 30 min but insufficient to completely inhibit contact pathway activation at the micropatterned microfluidic injury site[23]. A high 40 µg/ml CTI concentration, while not perfect in abolishing contact activation, will prevent visible clotting for 60 to 120 min allowing studies of TF-dependent extrinsic pathway with minimal participation of the contact pathway[35,37,80]. Both concentrations of CTI allow sufficient time for completion of all assays with no clotting in the 35 µL entrance reservoirs of the microfluidic devices.

Blood samples were treated with 0.125 µg/ml fluorescently conjugated non-function blocking anti-CD41a antibody (clone VI-PL2, Becton Dickson, Franklin Lakes, NJ, 0.125 µg/ml final concentration) to label platelets and fluorescently conjugated anti-fibrin antibody (clone T2G1, Dr. Mortimer Poncz laboratory, Children's Hospital of Philadelphia, 0.5 µg/ml final concentration) to label fibrin. WB samples were also treated with vehicle HEPES buffered saline (HBS, 20 mM HEPES, 160 mM NaCl, pH 7.5) or indicated concentrations of rFVIIa. Recombinant FVIIa (NovonSeven, Novo Nordisk, Plainsboro NJ, 1 mg/ml final concentration) was reconstituted in histidine diluent. A dilution of rFVIIa was made to the final desired concentration in HBS within 1 hr of the assays. Whole blood perfusion in microfluidic devices started within 15 min of venipuncture.

4.2.2 Microfluidic haemostasis model

Microfluidic devices were fabricated in polydimethylsiloxane (PDMS, Sylgard 184, Ellsworth Adhesives) according to previously described techniques[33,34]. The 8-channel microfluidic device has 8 channels fed by 8 wells with perfusion by withdrawal from a single outlet into a syringe pump (PHD 2000, Harvard Apparatus, Holliston, MA). The channels (250 μm by 60 μm) run perpendicularly over a 250 μm wide strip of patterned equine fibrillar collagen type I (Chronopar, Chronolog). A custom stage insert held two microfluidic devices allowing replicate testing of 4 conditions at each concentration of CTI in 60 sec intervals. Microfluidic devices were mounted on an inverted microscope (IX81, Olympus, Center Valley, PA). Microfluidic channels were spaced in close proximity to allow two channels to be imaged simultaneously with a 10X objective lens equipped with a CCD camera (ORCA-ER, Hamamatsu, Bridgewater, NJ). Prior to initiation of the flow assay, all channels were blocked with 0.5% bovine serum albumin (BSA) in HBS buffer. Blood samples were perfused at an initial local wall shear rate of $100s^{-1}$ (1 μL/min per channel) for 15 min. In constant flow rate mode, the local wall shear rate monotonically increases as thrombi grow to the channel height[37].

4.2.3 Platelet and fibrin accumulation analysis

Platelet and fibrin fluorescence intensities, which are proportional to the total platelet and fibrin masses respectively were measured in 60 sec intervals for 15 min through Image J software (Image J, NIH, Bethesda, MD). The initial image was taken as background and subsequent images were background corrected. Platelet and fibrin masses were measured in an area comprising of 70% center zone of the 250 μm by 250 μm collagen surface due to the

slightly non-uniform shear profiles along the side of the microfludic channels[33]. Platelet

adhesion and fibrin formation was not observed upstream or downstream of the collagen

strip prior to full channel occlusion. Statistical significance was assessed using a two tailed

Student's t test.

4.3 Results

4.3.1 Exogenous rFVIIa enhances platelet adhesion to collagen, but does not restore fibrin generation in a moderately FXI-deficient patient

The hemostatic effect of rFVIIa was evaluated by ex vivo addition to the WB of

hemophilic patients. High or low CTI-treated WB from a moderately FXI-deficient patient

(#50) with 3% FXI activity produced no detectable levels of fibrin (**Figure 4-1B,D**). As

expected, high or low CTI had little effect on fibrin generation, which was already strongly

attenuated in this patient because of the FXI deficiency. In the flow assay over collagen,

fibrin generation is dependent on contact pathway engagement (FXIIa→FXIa) which is

nearly absent in this patient. Fibrin generation due to the contact pathway was confirmed

with perfusion of low CTI-treated recalcified healthy pooled plasma or factor-deficient

plasma over collagen (**Figure 8-6**).

Exogenous rFVIIa addition increased platelet deposition on collagen at high and low

CTI (**Figure 4-1A,C**). However, ex vivo supplementation with rFVIIa failed to rescue fibrin

formation at either CTI concentration (**Figure 4-1B,D**). Without contact pathway

engagement (high CTI and FXI deficiency), rFVIIa strongly promoted platelet deposition

with little effect on fibrin production. To rule out inhibition of rFVIIa function by CTI, a

62

fluorogenic substrate for FVIIa was tested with rFVIIa and high or low CTI showing no

effect of CTI on rFVIIa function (**Figure 8-7**).
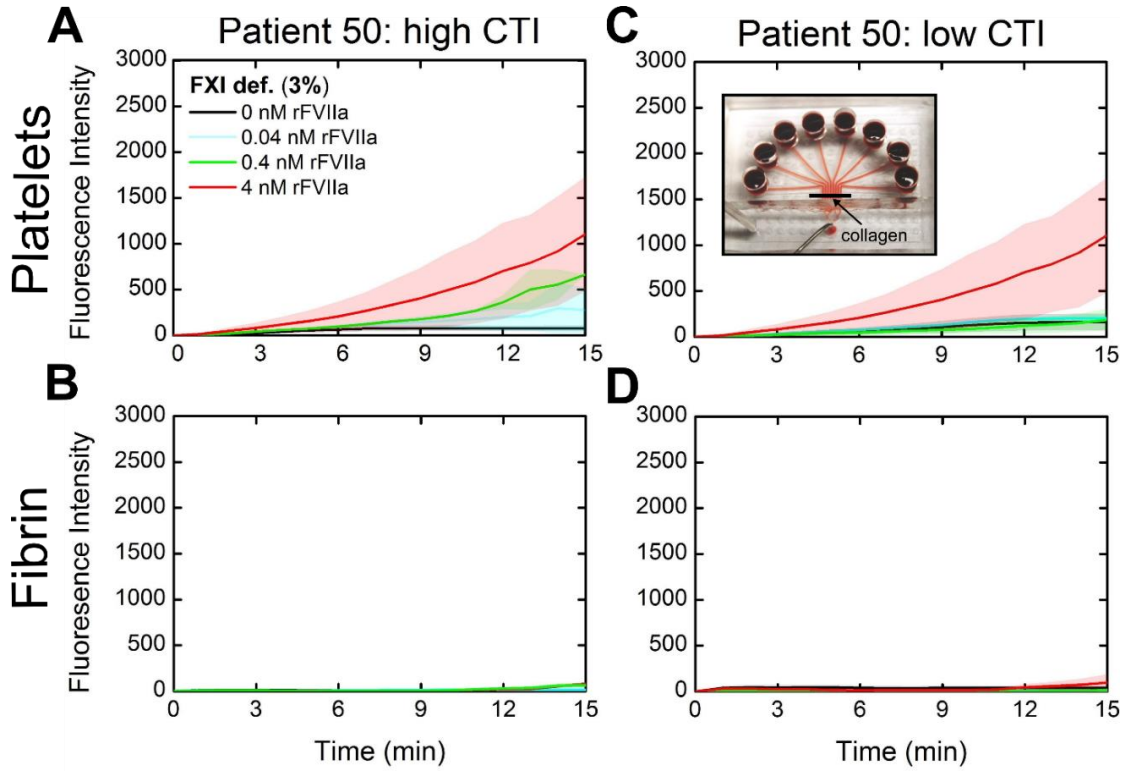
Figure 4-1 Moderately FXI-deficient (3%) patient #50 response to exogenous rFVIIa

(A & B), Platelet and fibrin fluorescence at various exogenous rFVIIa concentrations in high CTI (40 μg/ml).

(C & D), Platelet and fibrin fluorescence with ex vivo rFVIIa addition in low CTI (4 μg/ml). Shaded traces are

the standard deviation of two clotting events measured in 60 sec intervals over 15 min. Insert: 8-channel

microfluidic device with location of the collagen strip as indicated.

4.3.2 Exogenous rFVIIa enhances platelet adhesion to collagen, but does not restore fibrin generation in a severely FVIII-deficient patient

WB from a severely FVIII-deficient patient (#51; <1% FVIII) tested at one week following administration of FVIII concentrate, showed a deficit in fibrin production that was not rescued by rFVIIa at either CTI concentration. Recombinant FVIIa enhanced platelet deposition but had no effect on fibrin production (**Figure 4-2**). Despite FXa generation due to rFVIIa binding to activated platelets, insufficient thrombin was produced to cause robust fibrin formation. Robust fibrin formation, especially in the absence of exogenous tissue factor, requires intrinsic tenase formation (FIXa/FVIIIa) which clearly did not occur with <1% FVIII levels. The level of CTI had no effect since the contact pathway can proceed downstream from FXIIa to FIXa but will not result in sufficient intrinsic tenase.
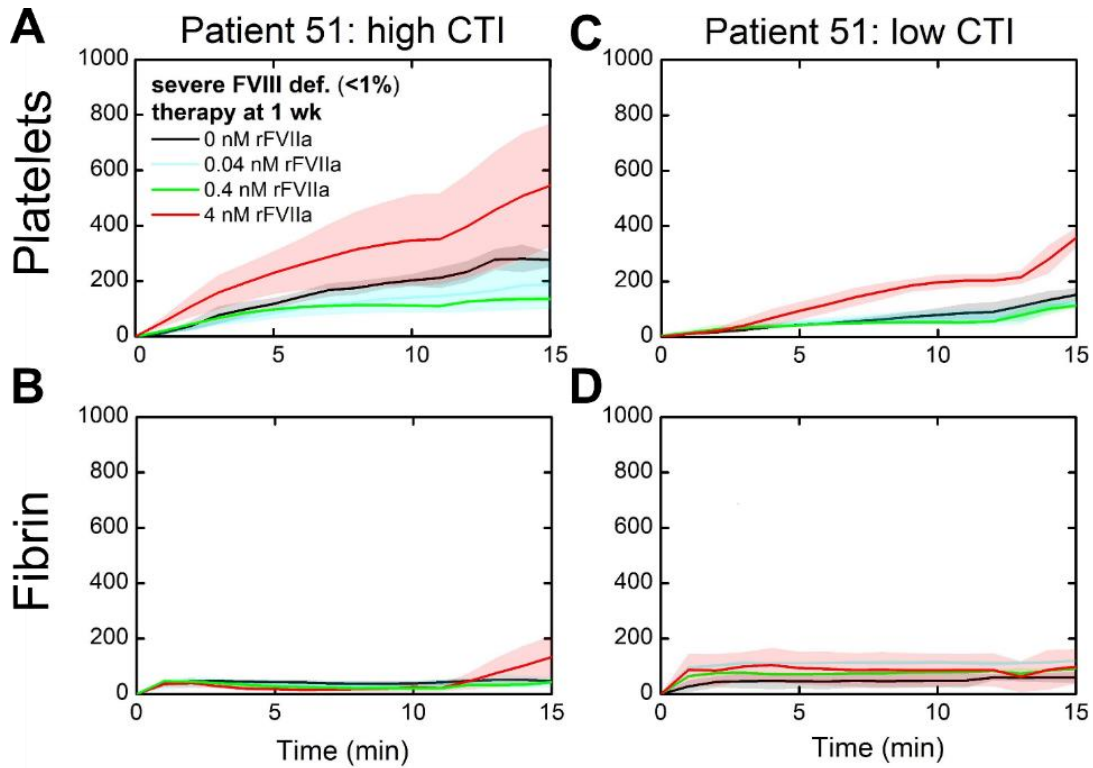
Figure 4-2 Severely FVIII-deficient (<1%) patient #51 response to exogenous rFVIIa

(A & B), Platelet and fibrin fluorescence over time in high CTI at indicated concentrations of ex vivo rFVIIa.

(C & D), Platelet and fibrin fluorescence over time in low CTI at indicated concentrations of ex vivo rFVIIa.

Timing of recent hemostatic therapy is as indicated. Shaded traces are the standard deviation of two clotting

events measured in 60 sec intervals over 15 min.

4.3.3 Moderate deficiency of FVIII or FIX allows rFVIIa to enhance platelet and fibrin generation when the contact pathway is available

In high CTI, rFVIIa augmented platelet deposition in a severely FVIII-deficient

patient (#55; 3% FVIII) who was treated with FVIII concentrate 4 days prior to testing

(**Figure 4-3A, upper left**). However, ex vivo rFVIIa addition again did not produce

substantial fibrin accumulation with strong inhibition of the contact pathway (**Figure 4-3A,**

lower left). In contrast, fibrin generation occurred upon addition of rFVIIa at low CTI **(Figure 4-3A, lower right)**. Contact pathway engagement (FXIIa→FXIa→FIXa) and intrinsic tenase assembly was productive enough to make sufficient thrombin to generate fibrin when rFVIIa was used at a 3% FVIII deficiency.

Similarly, a moderately FIX-deficient patient (#54; 5%) displayed nearly identical results as patient (#55) (**Figure 4-3B**). Recombinant FVIIa potently amplified platelet deposition in either CTI concentration (**Figure 4-3, upper panels**) whereas fibrin formation was highly dependent on contact pathway activity (low versus high CTI; **Figure 4-3, lower panels**). A similar role for the contact pathway was discovered when two additional severely FVIII-deficient patients treated with FVIII concentrate were tested (#57 & 56) (**Figure 8-8**). In three of these patients a peak in platelet deposition as measured by platelet fluorescence with contact pathway engagement and rFVIIa was found at 7-11 min followed by a drastic dip in the signal(Patient #54,57,56). This is due to downstream movement of the platelet-fibrin aggregates past the collagen surface as the clots formed under a constant flow regime cannot stop flow driven by a syringe pump.
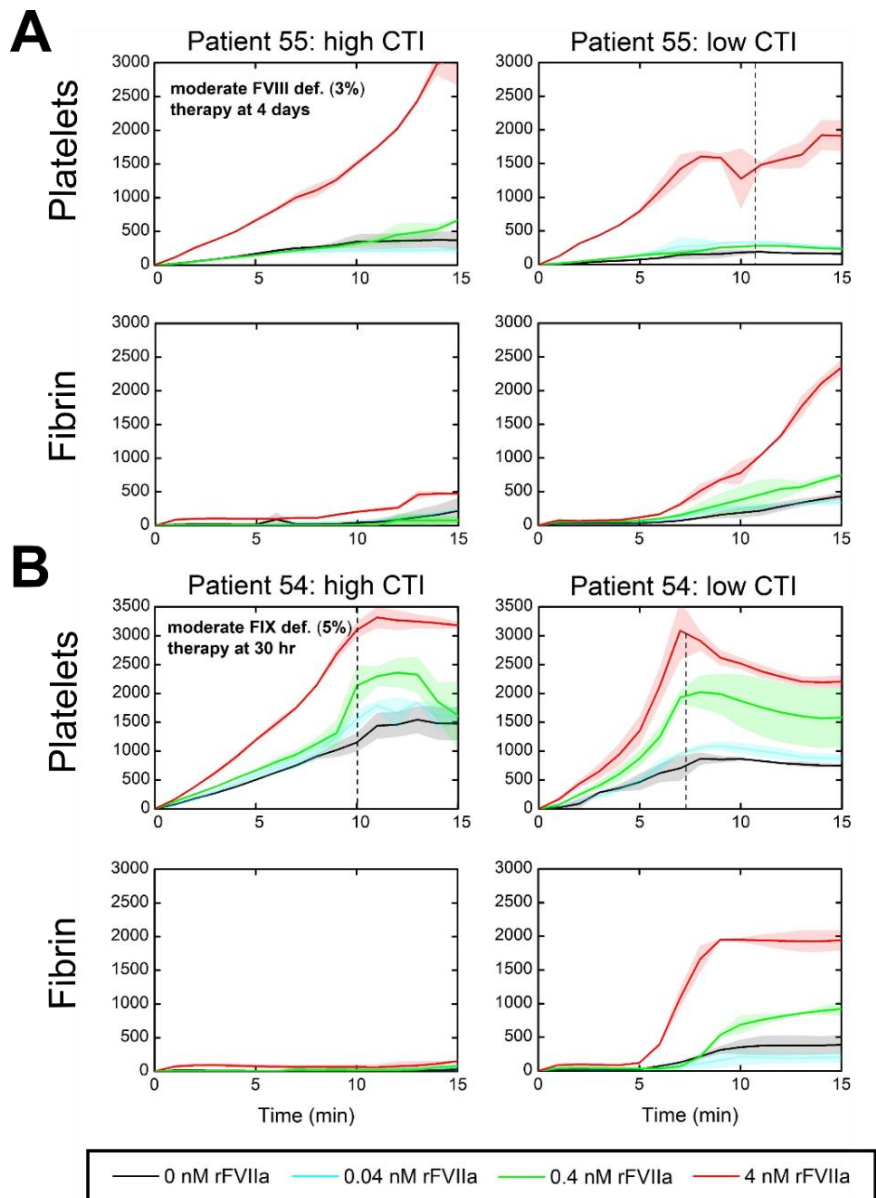
Figure 4-3 Effect of ex vivo rFVIIa in severely FVIII-deficient patient #55 and moderately FIX-deficient patient #54 after recovery of critical factor levels to 3 and 5% respectively

(A), Platelet and fibrin fluorescence over time in high or low CTI-inhibited WB for patient #55. **(B),** Platelet and fibrin fluorescence in high or low CTI-inhibited WB for patient #54. Timing of recent hemostatic therapy

is as indicated. Shaded traces are the standard deviation of two clotting events measured in 60 sec intervals over 15 min. Dashed lines indicate full channel occlusion.

4.3.4 Recovery of FVIII levels to 15% in patients allows rFVIIa to potentiate both platelet and fibrin deposition with less requirement for the contact pathway

When severely FVIII-deficient patients (#53 and #52) were recently treated (<24 hr) with therapy to increase their FVIII levels to 15%, exogenous rFVIIa addition caused substantial increases in platelet deposition and fibrin generation. The two FVIII-deficient patients displayed identical responses to rFVIIa. Increases in platelet deposition, fibrin initiation, and fibrin generation were measured in both patients; concentration dependent increases in platelet and fibrin accumulation were statistically significant at 4 nM rFVIIa (**Figure 4-4**). As residual clotting factor levels reach 15%, a level clinically considered as a mild deficiency, the influence of FXIIa was less prominent. However, the effects of FXIIa were still detectable as fibrin was generated faster and more abundantly in low CTI compared to high CTI in both patients (**Figure 4-4A, B, lower panels**).

In examining total platelet accumulation at 15 min (or prior to full channel occlusion), rFVIIa increased final platelet accumulation independent of CTI in all 8 patients (#50-57) (**Figure 4-5A**). Recombinant FVIIa showed robust effects on total fibrin accumulation with contact pathway-initiated coagulation at low CTI and >3% factor levels and minimum effect with strong inhibition of the contact pathway (high CTI) or at <3% factor levels (**Figure 4-5B)**. The levels of fibrin production in FVIII or FIX-deficient patients in low CTI and the lack of fibrin generation in high CTI with rFVIIa indicate a novel role for contact pathway potentiation of platelet-rFVIIa function.

68
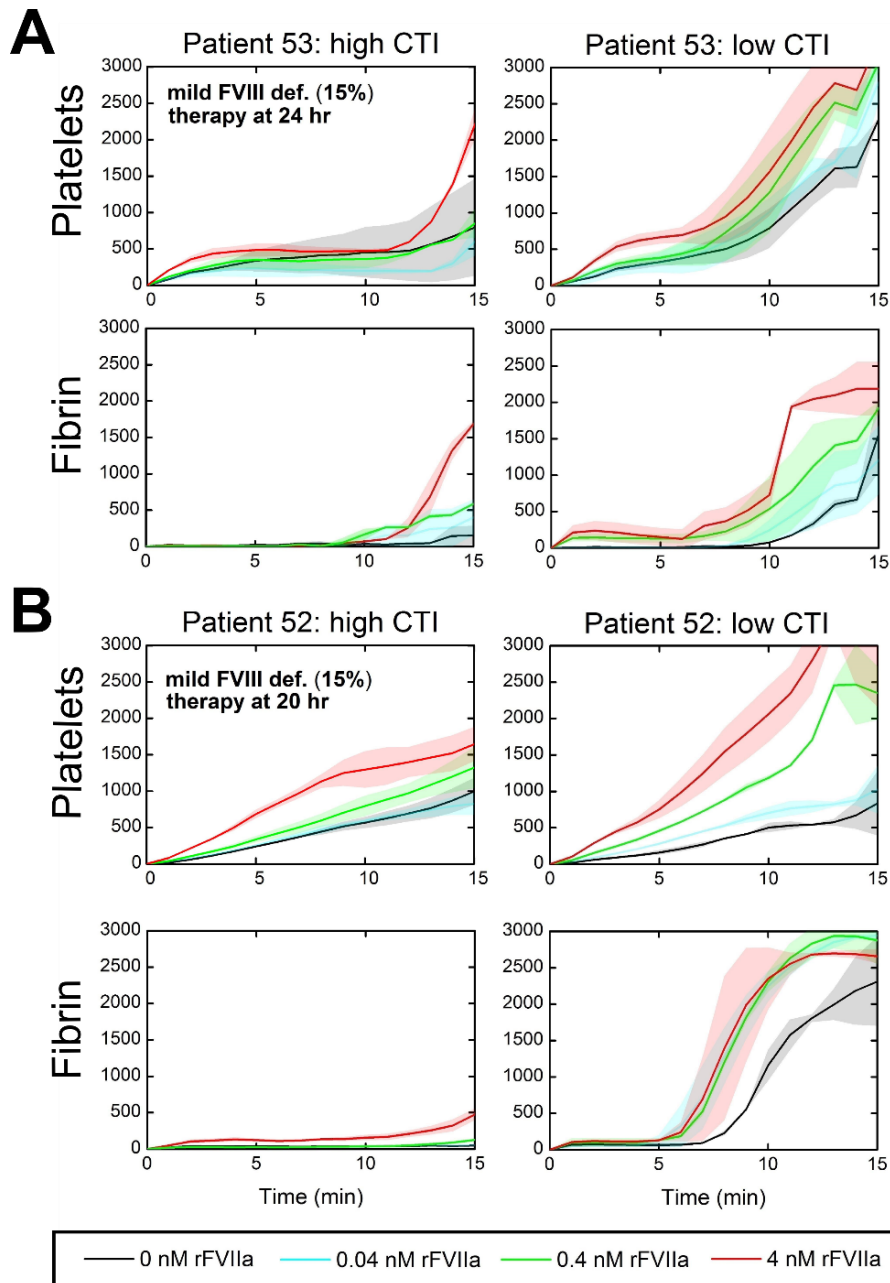
Figure 4-4 Effect of ex vivo rFVIIa in 2 severely FVIII-deficient patients after recovery of FVIII activity to 15%

(A), Platelet and fibrin fluorescence dynamics in high or low CTI-inhibited WB for severely FVIII deficient patient #53. **(B)**, Platelet and fibrin fluorescence dynamics in low or high CTI inhibited WB for severely

FVIII-deficient patient #52. Timing of recent hemostatic therapy is indicated. Shaded traces are the standard deviation of two clotting events measured in 60 sec intervals over 15 min.
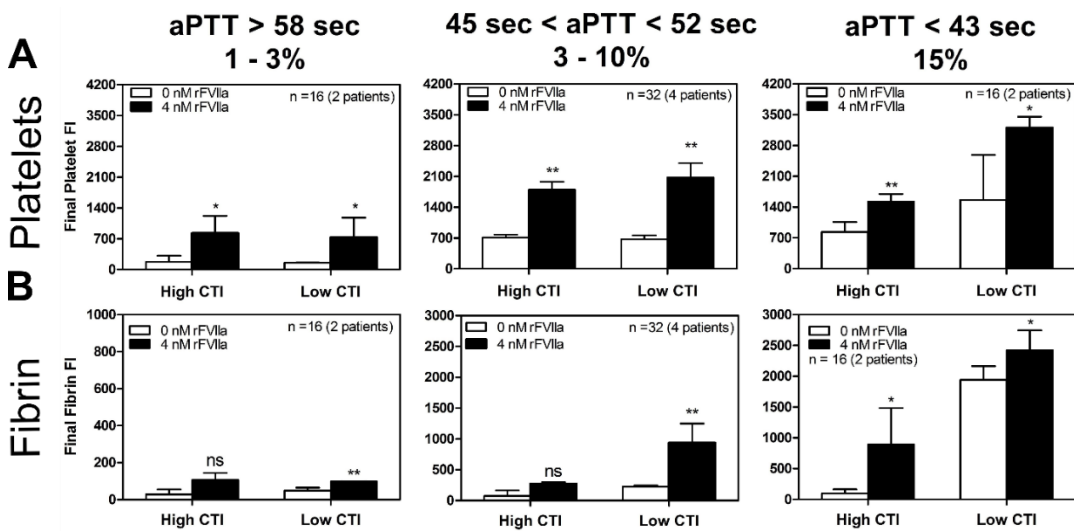
Figure 4-5 rFVIIa response in CTI-inhibited WB from 8 factor-deficient patients (#50-57; Table 2. Eight patients were examined with respect to ex vivo rFVIIa addition in the microfluidic hemostasis model with high or low CTI-inhibited WB.): Platelet and fibrin accumulation at t = 15 min or just prior to full channel occlusion sorted by residual factor activity and aPTT results

(A), Average final platelet mass as measured by platelet surface fluorescence at 0 or 4 nM rFVIIa in 8 intrinsic clotting factor deficient patients. Error bars are standard deviation of a minimum of 4 clotting events. **(B)**, Average final fibrin mass as measured by surface fibrin fluorescence at 0 or 4 nM rFVIIa in 8 intrinsic clotting factor deficient patients. Error bars are standard deviation of a minimum of 4 clotting events. (*p<0.05, **p<0.01, ns: non-significant)

70

4.3.5 Contact activation and rFVIIa enhance platelet and fibrin deposition in healthy blood

Eight healthy donors were subsequently tested in the same manner as the coagulopathic patients to further investigate the role of the contact pathway in exogenous rFVIIa function. Consistent with the platelet response to rFVIIa in hemophilic patients, healthy donor platelet deposition increased due to rFVIIa addition independent of the contact pathway (high or low CTI) (**Figure 4-6A, upper panels**). However, the contact pathway (low CTI) was required to generate sufficient levels of thrombin for robust fibrin formation (**Figure 4-6A, lower panels**). Similar to some hemophilic patients (#54, 56, 57), a combination of the contact pathway and ex vivo rFVIIa resulted in peak platelet deposition at 7 min followed by a drastic drop in signal. This is indicative of increasing shear stresses on the clots which eventually causes them to tear from the collagen surface, restructure, and embolize downstream.

Recombinant FVIIa significantly increased total platelet accumulation at 15 min or prior to full channel occlusion in low CTI, showing efficacy in enhancing platelet deposition independent of the contact pathway (**Figure 4-6B; p<0.01**). Total fibrin accumulation increased by three fold with rFVIIa when FXIIa was engaged (**Figure 4-6C; p<0.01)**, while no increase was observed when FXIIa was strongly inhibited.
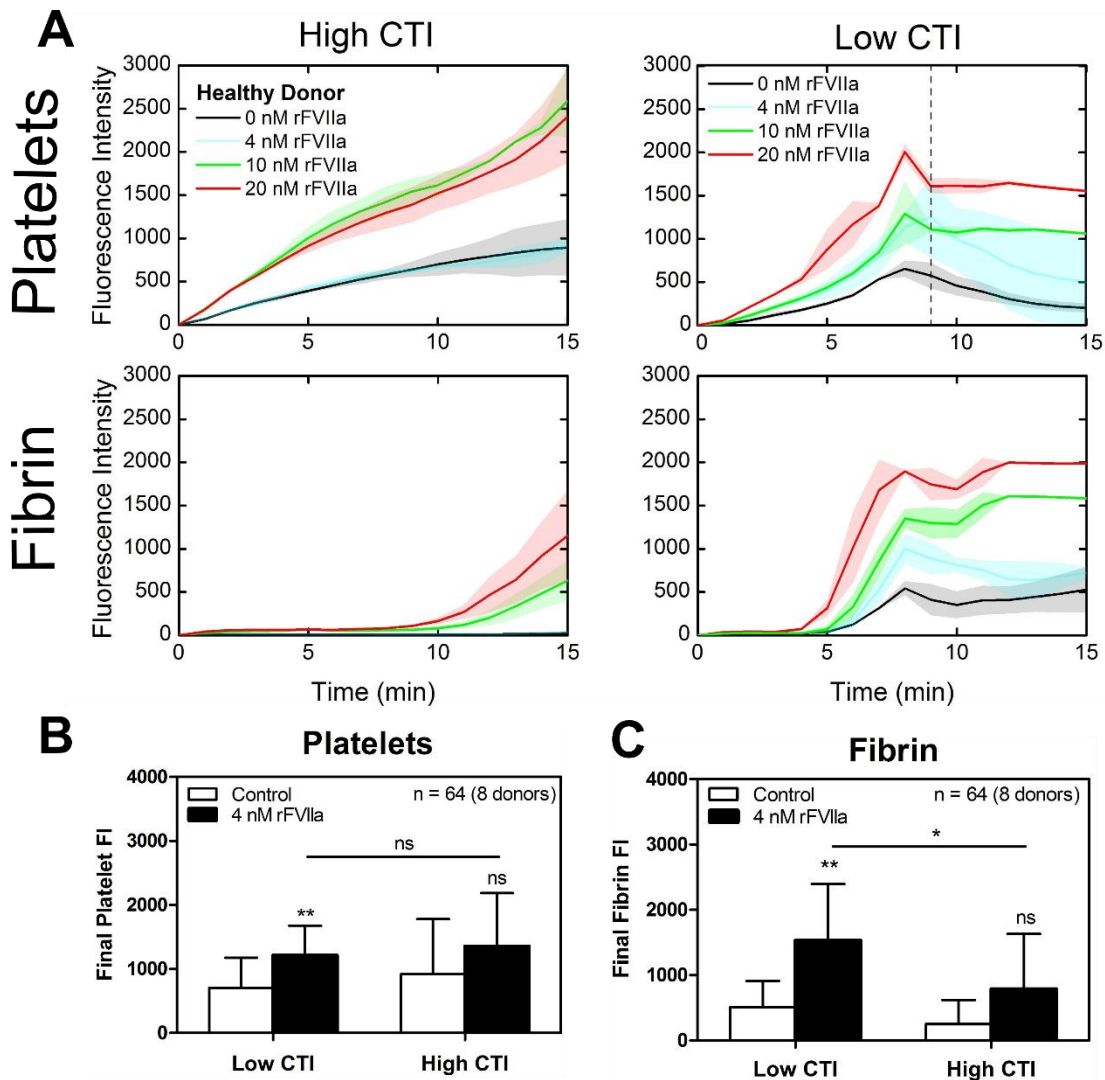
Figure 4-6 Healthy donor WB (n = 8 donors) platelet and fibrin accumulation response to rFVIIa

(A), Platelet and fibrin fluorescence over time as a function of rFVIIa concentrations in high or low CTI. Dashed line indicates full channel occlusion (B), Average final platelet mass at t = 15 min or just prior to full channel occlusion in the presence or absence of ex vivo rFVIIa in high or low CTI-inhibited WB. (C), Average final fibrin mass at t = 15 min in the presence or absence of ex vivo rFVIIa in high or low CTI-inhibited WB. Bars are average and standard deviation from n = 8 healthy donors and 16 clotting events. (*p<0.05, **p<0.01, ns: non-significant)

4.4 Discussion

Microfluidic models of hemostasis comprised of high or low CTI anti-coagulated WB perfused over collagen at venous shear rates were used to assess platelet and fibrin deposition in response to exogenous rFVIIa. Under these conditions, we investigated the role of rFVIIa under flow. We observed significantly increased platelet adhesion in the presence of rFVIIa but an inability of rFVIIa to potentiate fibrin formation unless the contact pathway was engaged.

Results from hemophilic patients (#50,51,54,55,56,57) indicate that rFVIIa function on platelets generate low "signaling" levels of thrombin to amplify platelet deposition but these levels were insufficient to generate fibrin. If contact engagement was blunted in the case of severe FXI or FVIII-deficiency (**Figure 4-1,Figure 4-2**) or at high CTI in FVIII or FIX-deficient patients (**Figure 4-3A, B, lower left**), rFVIIa did not lead to ample fibrin formation. However, with engagement of the contact pathway (low CTI), rFVIIa may crosstalk with the contact pathway to facilitate strong fibrin production in FVIII or FIX-deficient patients (**Figure 4-3A, B lower right**).

In addition, rFVIIa can generate FXa on the platelet surface and to a very minimal extent in solution[81]. In severely FVIII-deficient WB (< 1%), thrombin made distally from platelet-bound rFVIIa (4 nM added) is sufficient to promote greater platelet activation but is insufficient to generate fibrin (**Figure 4-2**). In moderately hemophiliac blood (3% FVIII or 5% FIX), strong inhibition of the contact pathway prevented fibrin formation although platelet deposition was still enhanced by rFVIIa (**Figure 4-3**). The initiation of the contact pathway in low CTI dramatically enhanced fibrin formation in moderate hemophiliac blood

(3% FVII or 5% FIX) treated with rFVIIa **(Figure 4-3)**. Similar results were found in mild

hemophilic blood (15% FVIII) (**Figure 4-3**) and even in healthy WB (**Figure 4-6**) where

strong inhibition of the contact pathway significantly blunted fibrin production following

exogenous rFVIIa treatment.

Recombinant FVIIa can enhance FXa generation at the site of bleeding by a variety of

pathways. If TF is exposed to WB, formation of the extrinsic tenase TF/rFVIIa would be

extremely procoagulant. Furthermore, the heterogeneous response to rFVIIa amongst

hemophiliacs can also be potentially attributable to variable quantities of circulating lipids or

procoagulant TF-containing microparticles, two variables known to put hemophiliacs at risk

for cardiovascular diseases as they age[82,83]. However, hemophiliacs bleed into joints,

which are presumably sites of low cellularity and low TF[84]. The results derived from FXI-

deficient blood (**Figure 4-1**) argue against bloodborne TF as a kinetically significant trigger

that produces detectable changes in our intrinsically driven microfluidic hemostasis model.

In contrast to the present study, prior work by Onasoga-Jarvis et al. perfused rFVIIa-

supplemented hemophiliac blood over TF-containing collagen to drive thrombin and fibrin

production [77].

We predict that for in vivo situations where wall-derived TF and contact activation are

both minimal, rFVIIa can promote hemostasis in severe hemophilia via platelet activation by

low levels of thrombin (distal of platelet bound rFVIIa) in the absence of substantial fibrin

generation. When the contact pathway is engaged through FXII[85], collagen[86], activated

platelets[87], or nucleic acid[88], it can promote the efficacy of rFVIIa by providing

additional FXa or by inactivation of an inhibitor, such as recently reported FXIa-mediated cleavage of tissue factor pathway inhibitor (TFPI)[89].

A level of 4 nM rFVIIa enhanced platelet deposition under flow by 2 to 3-fold in all patients tested (**Figure 4-5A; p<0.05**). At <10% factor level (aPTT > 45 sec), the contact pathway alone (no rFVIIa) at either high or low CTI produced essentially no fibrin (**Figure 4-5B**). However, for <10% factor level, low CTI inhibition of WB potentiated the ability of rFVIIa to promote fibrin formation. Distinct from hemophilia, conditions of trauma that promote contact activation may enhance the ability of rFVIIa to cause fibrin generation. Furthermore, while incidences of venous thrombosis are rare in factor-deficient patients[90], we quantified partial movement and remodeling of clots at low CTI with ex vivo rFVIIa in 3 hemophilic patients. As embolized thrombi are clinically significant, future work should assess the risk of venous thromboembolism with rFVIIa under a pressure relief flow regime in this microfluidic device[37]. In pressure relief mode, full channel occlusion is a natural endpoint as flow diversion to open channels allows thrombi to grow to full occlusion. This work highlights the ability of rFVIIa to generate low levels of FXa on platelets to drive platelet deposition via thrombin even when that thrombin is sufficient to drive fibrin deposition under flow. If the contact pathway is not engaged and TF is absent, rFVIIa may display its efficacy in severe hemophiliacs (<1%) by enhancing only platelet function.

5 RECOMBINANT FACTOR VIIA ADDITION TO SEVERE HEMOPHILIC BLOOD PERFUSED OVER COLLAGEN/TISSUE FACTOR CAN SUFFICIENTLY BYPASS THE FACTOR IXA/VIIIA DEFECT IN ORDER TO RESCUE FIBRIN

5.1 Introduction

Hemophilia A and B are X-linked genetic disorders resulting in deficiencies in coagulation factor VIII (FVIII) or factor IX (FIX), respectively[72]. These deficiencies cause a wide range of bleeding phenotypes depending on severity [75,91–93]. Current treatment strategies for hemophilic patients include recombinant clotting factors or bypass therapies. Bypass therapies such as activated prothrombin complex concentrates (aPCC) or recombinant factor VIIa (rFVIIa) were developed to treat hemophilic patients who develop inhibitors[74]. Bypass therapies can supplant FXa generation from the intrinsic tenase (FIXa/FVIIIa) by increasing prothrombinase levels or by activating FX on the platelet surface via rFVIIa. Though rFVIIa is approved for treating hemophilia patients with antibodies to FIX or FVIII, its mechanism of action is complex[94]. Past work has indicated that rFVIIa requires tissue factor to function and its requisite high doses are due to its competition with endogenous FVII for TF[95,96]. Other studies indicate that rFVIIa can also bind monocytes and activated platelets to generate FXa independent of TF[97–99].

Thus, further studies can help elucidate the roles of intrinsic tenase, extrinsic tenase, and rFVIIa in platelet rich thrombus formation and fibrin generation in hemophilic patients

under the hemodynamics conditions found in vivo. In hemophilia, deficits in thrombin generation impact platelet activation[100], fibrin formation[101], and clot stabilization[102]. In vitro flow models with perfusion of human blood deficient in FVIII or with inhibition of FVIII resulted in decreased platelet aggregation and fibrin formation at low shear conditions[103–105]. With in vivo models of vascular injury (ferric chloride or laser injury), mice deficient in FVIII or FIX produce unstable thrombi that fail to reach full vessel occlusion[106–108]. While the extrinsic pathway is classically thought of as the arm of the coagulation cascade that mitigates deficits in hemophilia A and B, TF expression varies greatly in human tissues[109,110]. High TF levels may compensate for a lack of FVIII or FIX in some but not all subendothelial vascular beds. Studies have shown bleeding in hemophilia is common in the joints where TF expression is considered to be low[110]. The contribution of FXa and thrombin stemming from residual intrinsic tenase in various TF-laden backgrounds has not been studied extensively using hemophilic blood. Previous studies only assessed the most severe cases of human FVIII or FIX deficiency (<1%) often with FXIIa function uncontrolled or utilized blood from mice deficient in FVIII or FIX[104,105,111]. Few have examined how mild or moderate deficiencies in FVIII or FIX levels affect platelet adherence, clot stability, and fibrin formation under flow in the presence or absence of bypass therapy[77] and surface TF.

Previously we have developed a contact pathway-driven microfluidic model that evaluated the role FVIII and FIX in patients with congenital bleeding disorders[23,24]. Platelet adhesion and fibrin formation under flow was significantly reduced in whole blood from these patients at <1% critical factor level activity[23]. Furthermore, in a second study

we concluded that rFVIIa generates low levels of 'signaling' thrombin sufficient to enhance platelet deposition on collagen, but is insufficient to drive fibrin polymerization unless the contact pathway is engaged. In this present study, we aimed to unify our previous two studies and firmly establish the role of the intrinsic tenase and rFVIIa in the regulation of platelet-fibrin thrombus development under flow. We measured healthy or hemophilic WB perfusion over collagen type I surfaces bearing well-controlled low or high concentrations of lipidated tissue factor at an initial venous wall shear rate of 100 s^{-1}. We also measured the differential effect of exogenously added rFVIIa on platelet deposition, fibrin initiation, and fibrin accumulation. This study confirms that FIXa/FVIIIa is required for fibrin generation under healthy WB flow, even when TF is abundant at the wall. In severe hemophilic blood with CTI-inhibited FXIIa, high levels of rFVIIa are required to rescue fibrin formation through the combined generation of FXa via TF/rFVIIa and platelet/rFVIIa function.

5.2   Materials and Methods

Blood was drawn from healthy donors (n = 5) and hemophilic patients (n = 10) under Internal Review Board approval of the University of Pennsylvania. Data regarding patient bleeding phenotype and recent therapy was collected (Table 3)

Patient ID#	Diagnosis	Residual Coagulation Factor %*	aPTT (Sec)	PT	Platelets (10^3/μL)	Timing of Most Recent Therapy	Replacement Therapy Dosage
62	Severe Hemophilia A	3	56.1	13.3	172	3 days	rFVIII (35 IU/kg)
63	Severe Hemophilia A	32	32.7	12.9	291	5 hrs	rVIII (25 IU/kg)
64	Severe Hemophilia B	14	34.4	13.7	252	96 hrs	rFIX (unknown)
65	Severe Hemophilia B	6	51.2	14.9	200	3 days	rFIX (47 IU/kg)
67	Mild Hemophilia A	18	37.4	12.9	244	None in past 5 years	rFVIII (unknown)
68	Moderate Hemophilia A	6	50.8	14.1	173	None in past 10 months	N/A
69	Moderate Hemophilia A	2	53.5	12.5	217	None since 2012	N/A
70	Severe Hemophilia A	24	40.1	12.8	273	26 hrs	rFVIII (50 IU/kg)
71	Moderate Hemophilia B	5	51.1	15.9	208	None in past 5 years	N/A
29	Severe Hemophilia B	**<1	133.6	14.5	125	8 hrs	rFIX (50 IU/kg)

Table 3. 10 patients were examined with respect to exogenous rFVIIa efficacy by perfusion of high CTI inhibited WB on TF$_{low}$ and TF$_{high}$ collagen surfaces.

Time since last hemostatic therapy, % residual coagulation factor activity, PTT, and platelet count are as reported. *Reflects in some cases recent administration of factor concentrate.

Laboratory testing of hemophilic patients included a platelet count, residual coagulation factor activity, prothrombin time (PT), and activated partial thromboplastin time (aPTT). Residual FVIII, FIX, or FXI activity were measured in Hemophilia A and VWD disease, Hemophilia B, or Hemophilia C diagnoses respectively. The aPTT test assesses intrinsic

pathway function by measuring the time to clot formation in platelet-poor plasma in the presence of exogenous intrinsic pathway activators such as kaolin[112]. aPTT values (reference range: 20.9-34.4 sec) were negatively correlated with residual factor activity levels as previously established[23]. Healthy donors were self-reported free of oral medication for 7 days and abstained from alcohol 48 h prior to blood donations.

WB was drawn into 40 μg/ml CTI (Haematologic Technologies, Essex Junction, VT) containing polypropylene plastic syringes, a material which activates the contact pathway minimally. At 40 μg/ml, CTI will almost completely abolish contact pathway activation and prevent visible clotting for 30 to 45 min allowing studies of surface-trigged TF-dependent coagulation under flow with minimal participation of FXIIa[80]. This concentration of CTI allows sufficient time for completion of all assays with no clotting in the 35 μL entrance reservoirs of the microfluidic devices.

Preparation of TF bearing collagen surfaces

Glass slides were first functionalized with Sigmacote (Sigma, St. Louis, MO) to create a hydrophobic surface. Acid-insoluble equine type I collagen fibrils (Chrono-Par, Chrono-log, Havertown, PA) were introduced into a previously described single channel microfluidic patterning device (250 μm by 1 cm) [33,34]. This patterning device was then filled with 5 μL of Dade Innovin PT reagent (Siemens Healthcare USA, Malvern, PA. 20 nM stock concentration) diluted 300 or 5 fold with 2-[4-(2-hydroxyethyl)piperazin-1-yl] ethanesulfonic acid (HEPES)-buffered saline (HBS, 20 mM HEPES, 160 mM NaCl, pH 7.4) to obtain low or high TF surface concentrations. TF surface concentrations were measured by the staining of TF vesicles with fluorescein isothiocynate labeled annexin V as previously described[113].

In all microfluidic experiments TF bearing collagen surfaces were incubated for 30 minutes in the absence of flow and then washed with 5 µl of 0.5% bovine serum albumin (BSA) in HBS. Nominal low and high TF surface concentrations ($[TF]_{wall}$) were ~0.1 and ~2 molecules per $µm^2$, respectively, as previously reported[113]. This single channel patterning device was then removed to allow placement of microfluidic flow devices onto the micropatterned TF bearing collagen strip.

Extrinsic pathway triggered microfluidic flow assay on TF bearing collagen surfaces

An 8-channel microfluidic device was fabricated in polydimethylsiloxane (PDMS, Sylgard 184, Ellsworth Adhesives) according to previously described techniques[33,64]. The device has 8 channels fed by 8 wells with perfusion by withdrawal from a single outlet into a syringe pump (PHD 2000, Harvard Apparatus, Holliston, MA). This 8-channel device was placed over TF bearing collagen surfaces and reversibly sealed by house vacuum. The channels (250 µm by 60 µm) of the device run perpendicularly over a 250 µm wide strip of patterned equine fibrillar collagen type I bearing TF. This forms platelet and prothrombotic protein interaction zones measuring 250 µm by 250 µm. A customized stage insert held two microfluidic devices allowing replicate testing of 4 conditions in 60 sec intervals. Microfluidic devices were mounted on an inverted microscope (IX81, Olympus, Center Valley, PA). Microfluidic channels were spaced in close proximity to allow two channels to be imaged simultaneously with a 10X objective lens equipped with a charged-coupled device (ORCA-ER, Hamamatsu, Bridgewater, NJ). Prior to initiation of the flow assay, all channels were blocked with 0.5% bovine serum albumin (BSA) in HBS.

Blood samples were treated with fluorescently conjugated non-function blocking anti-CD41a antibody (clone VI-PL2, Becton Dickson, Franklin Lakes, NJ, 0.125 μg/ml final concentration) to label platelets and fluorescently conjugated anti-fibrin antibody (clone T2G1, Dr. Mortimer Poncz laboratory, Children's Hospital of Philadelphia, 0.5 μg/ml final concentration) to label fibrin. WB samples were also treated with vehicle HBS or indicated concentrations of rFVIIa. Recombinant FVIIa (NovonSeven, Novo Nordisk, Plainsboro NJ, 1 mg/ml final concentration) was reconstituted in histidine diluent. WB samples were treated with detection antibodies and rFVIIa 5 min prior to initiation of flow assays. A dilution of rFVIIa was made to the final desired concentration in HBS within 1 hr of the tests. Whole blood perfusion in microfluidic devices started within 15 min of venipuncture. Blood samples were perfused at an initial local wall shear rate of $100s^{-1}$ (1 μL/min per channel) for 15 min. In constant flow rate mode the local wall shear rate monotonically increases as thrombi grow to the channel height[37].

Platelet and fibrin accumulation analysis

Platelet and fibrin fluorescence intensities, which are proportional to the total platelet and fibrin masses respectively were measured in 60 sec intervals for 15 min through ImageJ software (ImageJ, National Institute of Health, Bethesda, MD). The initial image was taken as background and subsequent images were background-corrected. Platelet and fibrin masses were measured in an area comprising of 70% center zone of the 250 μm by 250 μm TF collagen surface due to the slightly non-uniform shear profiles along the side of the microfluidic channels[33,34]. Platelet adhesion and fibrin formation was not observed

upstream or downstream of the TF collagen strip prior to full channel occlusion. Statistical

significance was assessed using a two tailed Student's t test.

5.3 Results

5.3.1 Surface-triggered extrinsic pathway under flow does not rescue platelet adherence or fibrin generation at <3% factor activity.

The hemostatic potential of surface-triggered TF under flow to rescue deficits in

FVIII or FIX was evaluated through perfusion of hemophilic or healthy WB over collagen

bearing TF_{low} or TF_{high} surfaces.
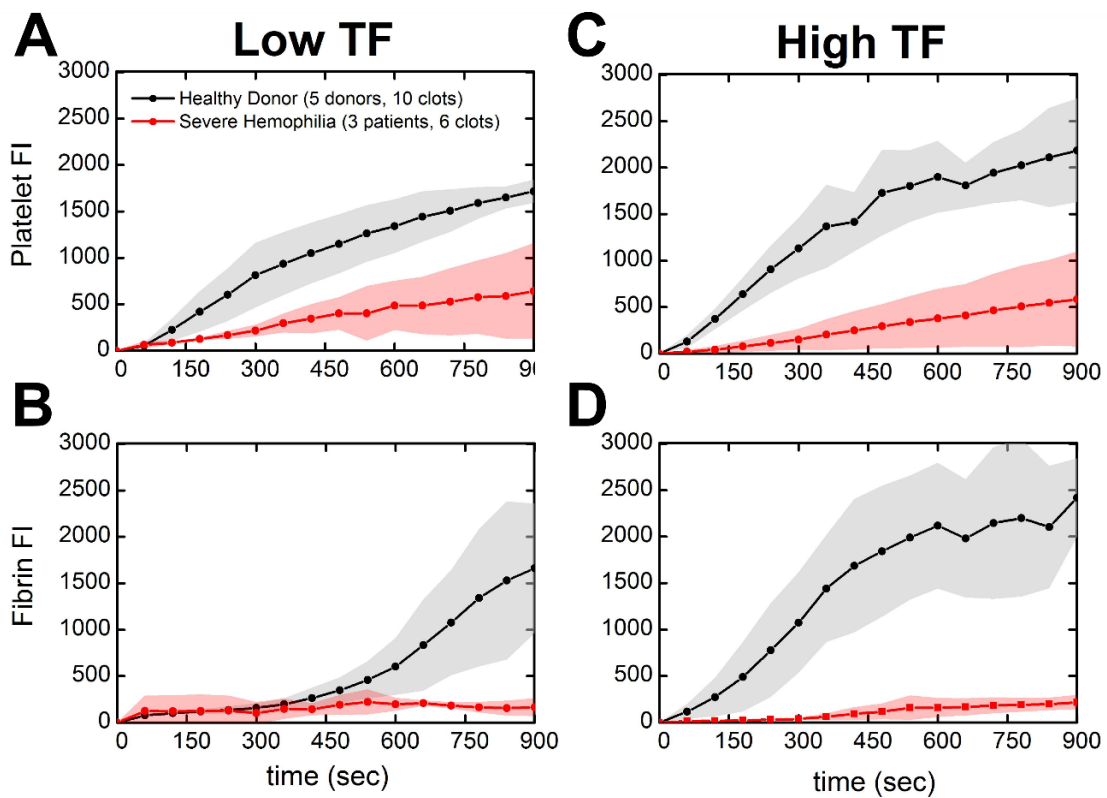
Figure 5-1 Comparison of severely and moderately factor-deficient (1-3%) patients against healthy donor response to TF_{low} or TF_{high} bearing collagen surfaces

(**A & B**), Platelet adherence and fibrin deposition dynamics measured by platelet and fibrin fluorescence respectively. WB inhibited with 40 μg/ml CTI was perfused over TF_{low} bearing collagen surfaces at 100 s^{-1}. (**B & C**), Platelet adherence and fibrin deposition dynamics over time. WB inhibited with 40 μg/ml CTI was perfused over TF_{high} bearing collagen surfaces at 100 s^{-1}. Lines with shaded traces and points are the mean and standard deviation of 6 clotting events measured in 60 sec intervals over 15 min for three distinct hemophilic patients (red) or 10 clotting events measured in 60 sec intervals over 15 min for five distinct healthy subjects (black).

High CTI-inhibited WB from two severely factor-deficient patients and one moderately factor-deficient patient (#62, 69, 29) with 3, 2, and <1 % factor activity respectively produced no detectable levels of fibrin (**Figure 5-1B,D**, **red lines**) as opposed to healthy controls where robust platelet deposition and fibrin generation was measured regardless of surface TF concentration (**Figure 5-1B, D: black lines**). Fully consistent with TF/FVIIa as the primary trigger of coagulation in this microfluidic model, time to fibrin initiation in healthy donors decreased when surface TF concentration increased (**Figure 5-1B, D: black lines**). Platelet deposition over time was also elevated on TF_{high} collagen surfaces indicating that thrombin generation was occurring at a concentration sufficient to drive platelet deposition and facilitate fibrin formation (**Figure 5-1C,D: black line**). Interestingly, at < 3% factor activity, hemophilic patient platelet deposition was reduced compared to healthy blood independent of surface TF concentration (**Figure 5-1A, C: red lines**).
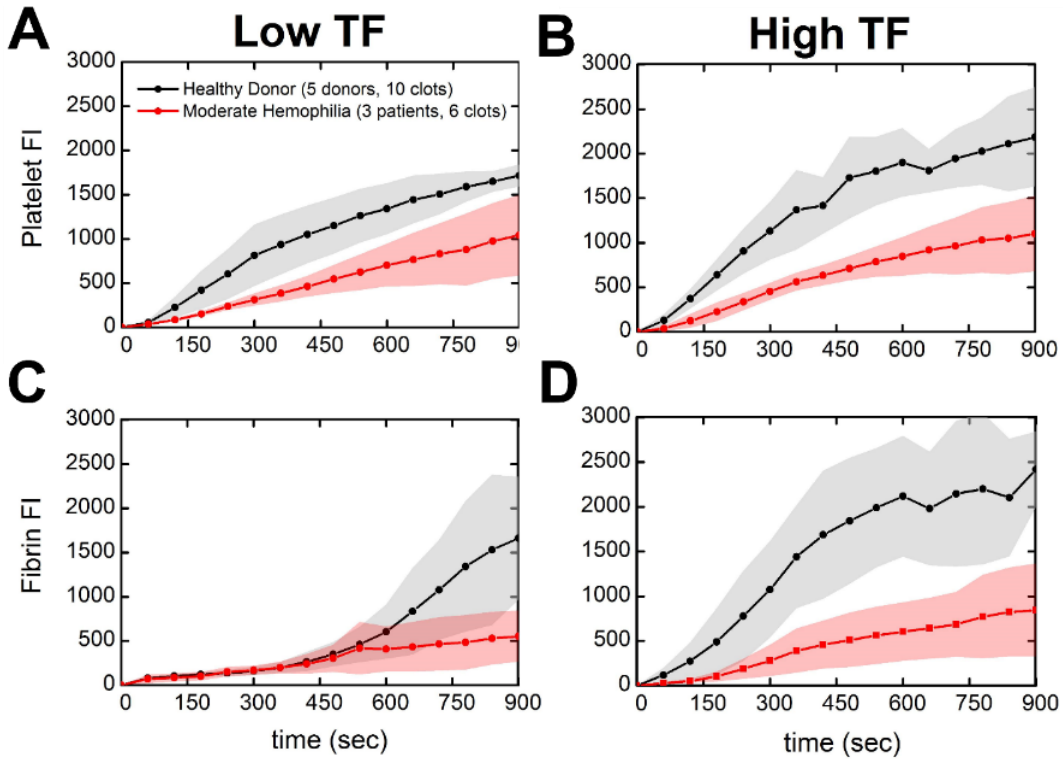
Figure 5-2 Comparison of 3-14% clotting factor activity patients against healthy donor response to TF$_{low}$ or TF$_{high}$ bearing collagen surfaces

(**A & B**), Platelet adherence and fibrin deposition dynamics measured by platelet and fibrin fluorescence respectively. WB inhibited with 40 μg/ml CTI was perfused over TF$_{low}$ bearing collagen surfaces at 100 s^{-1}. (**B & C**), Platelet adherence and fibrin deposition dynamics over time. WB inhibited with 40 μg/ml CTI was perfused over TF$_{high}$ bearing collagen surfaces at 100 s^{-1}. Lines with shaded traces and points are the mean and standard deviation of 6 clotting events measured in 60 sec intervals over 15 min for three distinct hemophilic patients (red) or 10 clotting events measured in 60 sec intervals over 15 min for five distinct healthy subjects (black).

5.3.2   Extrinsic pathway triggered coagulation under flow partially restores platelet adhesion and fibrin generation at 3-14% factor activity.

Perfusion of moderately and mildly FVIII or FIX-deficient patient WB (#64, 65, 68, 71) resulted in poorly detectable or low levels of fibrin accumulation under flow on TF$_{low}$ or

85

TF$_{high}$ surfaces, respectively (**Figure 5-2C,D: red lines**). Additionally, significant decreases in platelet adhesion on TF collagen surfaces were again observed in these patients independent of surface TF concentration (**Figure 5-2A, B: red lines**). However, these levels of platelet adhesion were higher than those observed with the 1-3% factor activity group (**Figure 5-1A, C: red lines**). These results indicate that engagement of the intrinsic tense (FIXa/FVIIIa → FXa) in combination with FXa production from TF/FVIIa under flow on TF$_{high}$ collagen surfaces was sufficient to initiate some fibrin formation and produce low amounts of fibrin accumulation (**Figure 5-1D: red lines**).
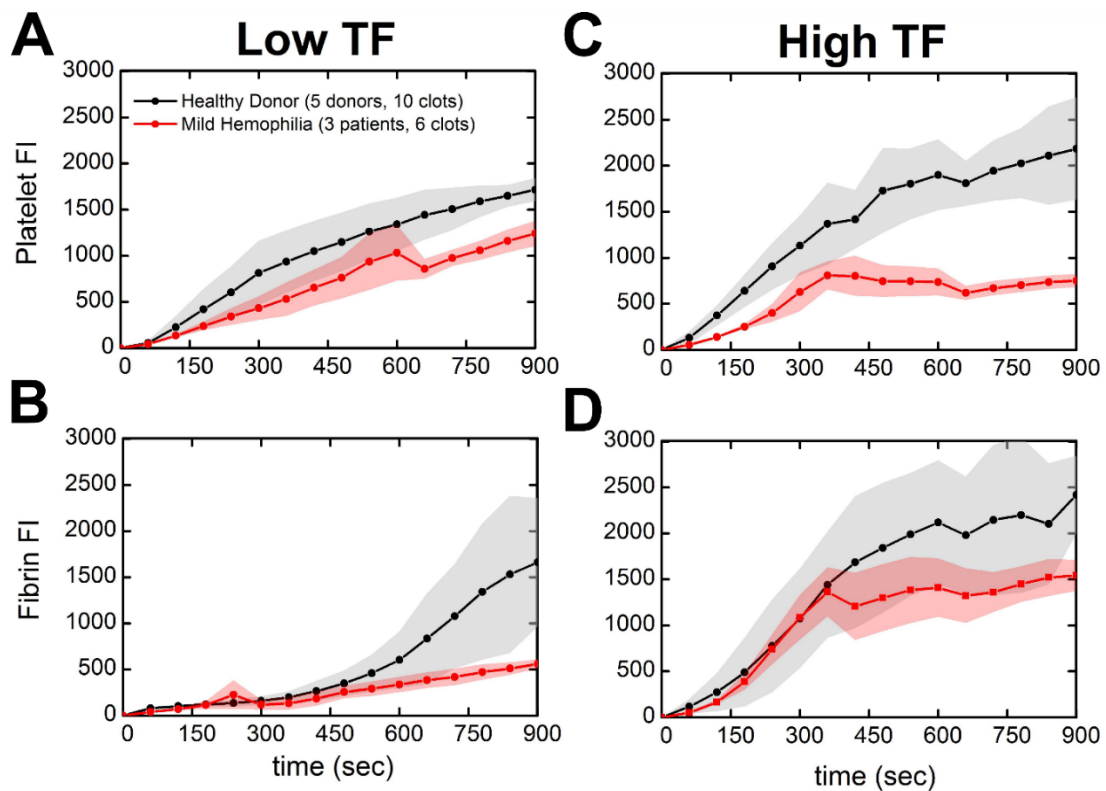
Figure 5-3 Comparison of >14% clotting factor activity against healthy donor response to TF$_{low}$ or TF$_{high}$ bearing collagen surfaces

(**A & B**), Platelet adherence and fibrin deposition dynamics measured by platelet and fibrin fluorescence respectively. WB inhibited with 40 µg/ml CTI was perfused over TF_{low} bearing collagen surfaces at 100 s^{-1}. (**B & C**), Platelet adherence and fibrin deposition dynamics over time. WB inhibited with 40 µg/ml CTI was perfused over TF_{high} bearing collagen surfaces at 100 s^{-1}. Lines with shaded traces and points are the mean and standard deviation of 6 clotting events measured in 60 sec intervals over 15 min for three distinct hemophilic patients (red) or 10 clotting events measured in 60 sec intervals over 15 min for five distinct healthy subjects (black).

Figure 5-4 Total platelet or fibrin accumulation for different clinical severities of hemophilia

(**A & B**), Maximum platelet or fibrin accumulation on TF_{low} bearing collagen surfaces at 100 s^{-1} measured by platelet or fibrin fluorescence at t = 15 min or just prior to full channel occlusion. Data is ordered by severity

of factor deficiency (1-3%, 3-14% & >14%) and compared to mean healthy subject maximum platelet or fibrin accumulation. (**C & D**), Maximum platelet or fibrin accumulation on TF_{high} bearing collagen surfaces at $100s^{-1}$ measured by platelet or fibrin fluorescence at t = 15 min or just prior to full channel occlusion. Data is ordered by severity of factor deficiency (1-3%, 3-14% & > 14%) compared to mean healthy subject maximum platelet or fibrin accumulation. Error bars are the standard deviation of 6 clotting events for each clinical severity of hemophilia and 10 clotting events for five healthy subjects. (** $p < 0.01$, * $p < 0.05$, ns: non-significant)

5.3.3 Platelet adhesion is partially rescued by the extrinsic pathway independent of TF concentration while fibrin formation is fully restored on TF_{high} collagen surfaces at >14% factor activity

Platelet deposition from WB of mildly FVIII or FIX-deficient patients (#63, 67, 70) remained attenuated in comparison to the platelet deposition from healthy controls although it was not statistically significant with low surface TF concentrations (**Figure 5-3A, C**). Interestingly, we observed residual defect in fibrin production at >14% factor activity in the presence of TF_{low} collagen surfaces (**Figure 5-3B: red line**). Time to fibrin initiation and total fibrin accumulation under flow was fully restored with TF_{high} collagen surfaces (**Figure 5-3: red line**). The influence of FVIIIa and FIXa become more prominent as residual clotting factor levels reach >14%.

In examining total platelet and fibrin accumulation under flow at 15 min for all cohorts, platelet and fibrin accumulation on TF_{low} and TF_{high} surfaces was highly defective for blood from patients with 1-3% normal factor level when compared to healthy blood (**Figure 5-4A-D**). High levels of TF do not rescue clotting in severely factor-deficient patients (**Figure 5-4D**) whose blood generated essentially no fibrin.
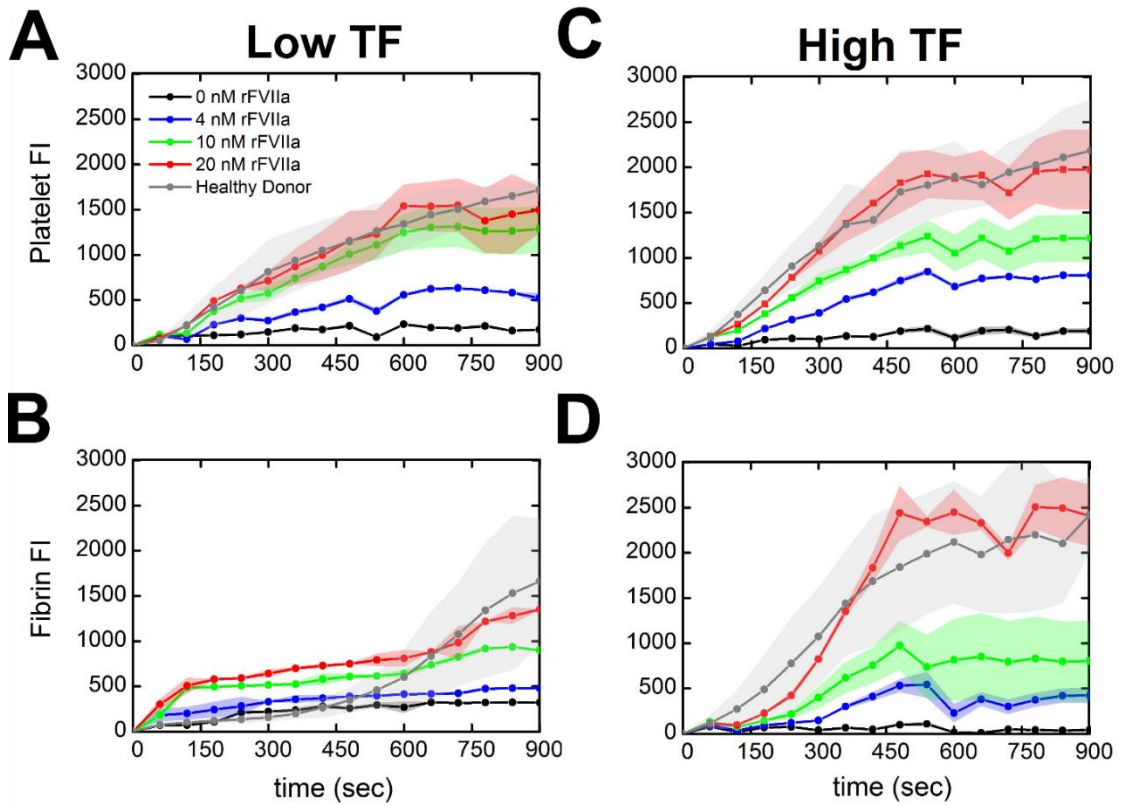
Figure 5-5 Effect of in vitro rFVIIa (0-20 nM) in severely FVIII-deficient patient

(**A & B**), Platelet adherence and fibrin deposition in the presence or absence of exogenous rFVIIa measured by platelet and fibrin fluorescence at t = 15 min or just prior to full channel occlusion. WB treated with exogenous rFVIIa (0-20 nM) and inhibited with 40 μg/ml CTI was perfused over TF_{low} bearing collagen surfaces at 100 s^{-1}. (**C & D**), Platelet adherence and fibrin deposition in the presence or absence of exogenous rFVIIa measured by platelet and fibrin fluorescence. WB treated with exogenous rFVIIa (0-20 nM) and inhibited with 40 μg/ml CTI was perfused over TF_{high} bearing collagen surfaces at 100 s^{-1}. Lines with shaded traces and points are the mean and standard deviation of 2 clotting events measured in 60 sec intervals over 15 min for each concentration of rFVIIa (colored) or 10 clotting events measured in 60 sec intervals over 15 min for five distinct healthy subjects (gray).
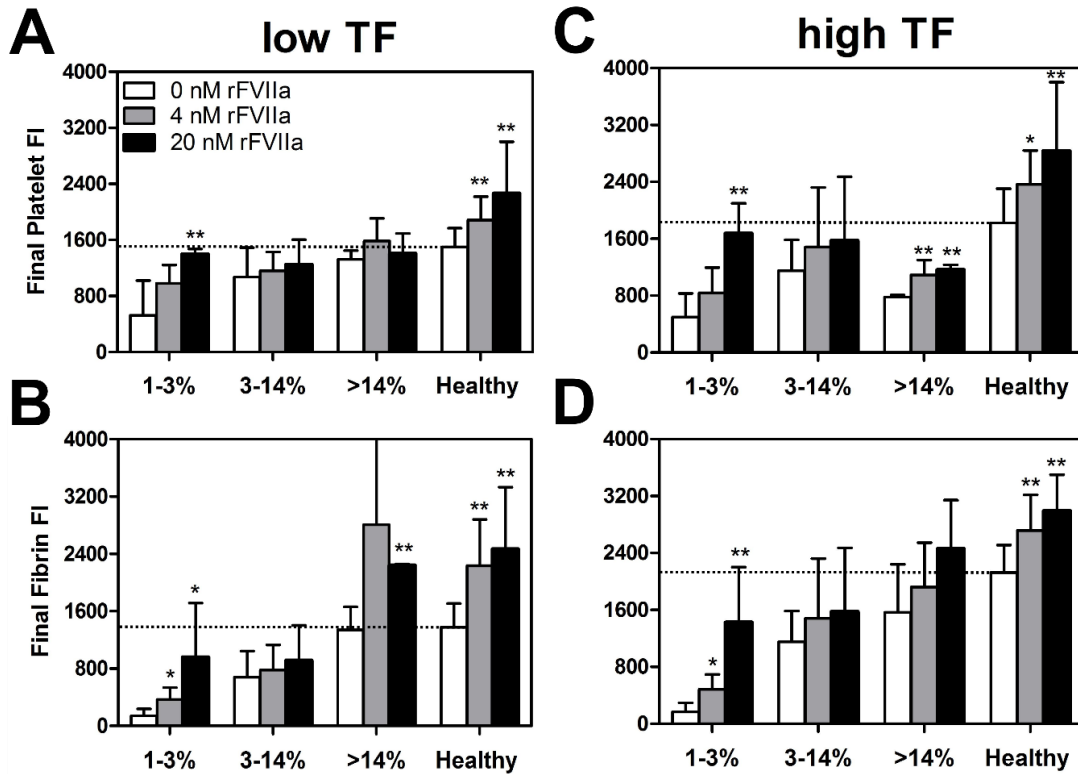
Figure 5-6 Total platelet or fibrin accumulation in response to in vitro rFVIIa (0-20 nM) for different clinical severities of hemophilia

(**A & B**), Maximum platelet or fibrin accumulation in the presence or absence of exogenous rFVIIa measured by platelet or fibrin fluorescence. WB treated with exogenous rFVIIa (0-20 nM) and inhibited with 40 μg/ml CTI was perfused over TF_{low} bearing collagen surfaces at $100s^{-1}$. Data is ordered by severity of factor deficiency (1-3%, 3-14% & >14%) and compared to mean healthy subject maximum platelet or fibrin accumulation. (**C & D**), Maximum platelet or fibrin accumulation in the presence or absence of exogenous rFVIIa measured by platelet or fibrin fluorescence. WB treated with exogenous rFVIIa (0-20 nM) and inhibited with 40 μg/ml CTI was perfused on TF_{high} bearing collagen surfaces at $100s^{-1}$. Data is ordered by severity of factor deficiency (1-3%, 3-14% & >14%) and compared to mean healthy subject maximum platelet or fibrin accumulation. Data is ordered by severity of factor deficiency (1-3%, 3-14% & > 14%) compared to mean healthy subject maximum platelet or fibrin accumulation. Error bars are the standard deviation of 6 clotting events for each clinical

severity of hemophilia and 10 clotting events for five healthy subjects. (** $p < 0.01$, * $p < 0.05$, ns: non-significant)

5.3.4 Exogenous rFVIIa enhances platelet deposition on collagen with TF$_{low}$ and TF$_{high}$, but only fully restores fibrin accumulation at 20 nM on TF$_{high}$ collagen in a severely FIX-deficient patient

Perfusion of WB from a severely FIX-deficient patient (#29; <1% FIX) showed negligible fibrin accumulation that was only partially rescued by even 20 nM rFVIIa on TF$_{low}$/collagen (**Figure 5-5B**). Addition of rFVIIa strongly enhanced platelet deposition at either TF concentration (**Figure 5-5. 5A,C**). The combination of high exogenous rFVIIa (20 nM) and TF$_{high}$/collagen was able to fully restore fibrin initiation and accumulation under flow (**Figure 5-5D**).

The effect of exogenously added rFVIIa was tested on patients with a range of hemophilic severity using TF$_{low}$ and TF$_{high}$ surfaces. A level of 20 nM rFVIIa significantly increased final platelet and fibrin accumulation at 1-3% factor activity (**Figure 5-6**) to levels commensurate with that observed with untreated healthy blood. With increasing rFVIIa supplementation, healthy whole blood also displayed increased platelet and fibrin deposition on TF$_{low}$ and TF$_{high}$(**Figure 5-6**).
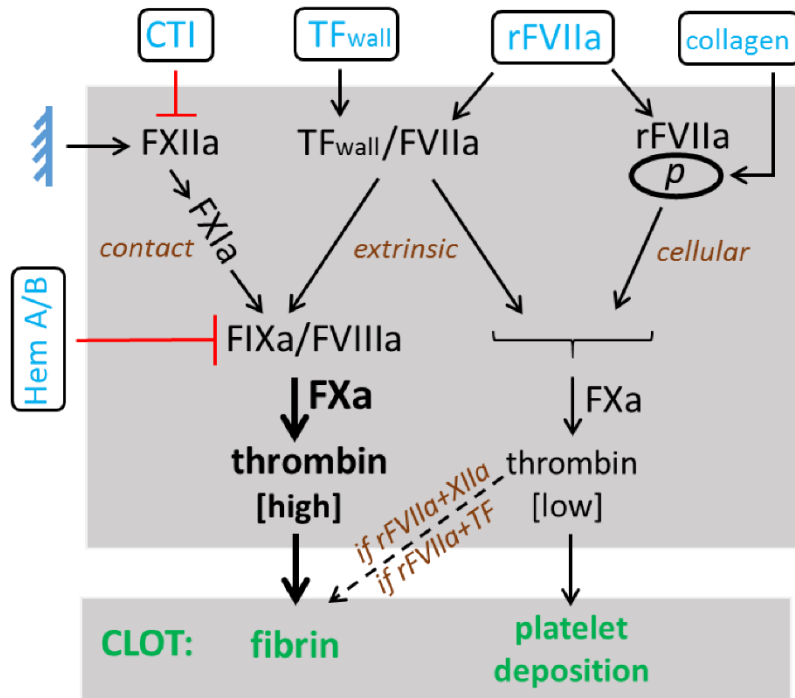
Figure 5-7 Signaling pathways of hemophilic blood when triggered by surface TF/collagen in the presence or absence of rFVIIa.

In hemophilic blood clotting under flow conditions over TF, most FXa comes from the intrinsic tenase (FIX/FVIIIa) even when some FXa can be initially generated by the extrinsic tenase TF$_{wall}$/FVIIa and platelet/rFVIIa.

Condition				Clotting at 100 s^{-1}		
Phenotype	**Surface**	**Contact pathway**	**rFVIIa**	**Platelets**	**Fibrin**	**[ref.]**
Severe (< 3%)	Collagen	No (high CTI)	0	low	none	[24]
		No (high CTI)	+	modest rescue	none	
		Yes (low CTI)	0	Low	none	
		Yes (low CTI)	+	slight rescue	~none	
Moderate (3-10%)	Collagen	No (high CTI)	0	modest	none	[24]
		No (high CTI)	+	rescue	none	
		Yes (low CTI)	0	modest	very low	
		Yes (low CTI)	+	rescue	rescue	
Severe (<3 %)	Collagen + [TF]low	No (high CTI)	0	very low	none	*
	Collagen + [TF]low		+	rescue	rescue	
	Collagen + [TF]high		0	very low	none	

	Collagen + [TF]high		+	rescue	rescue	
Moderate	Collagen + [TF]low	No (high CTI)	0	modest	modest	*
	Collagen + [TF]low		+	modest	modest	
(3-10%)	Collagen + [TF]high		0	moderate	moderate	
	Collagen + [TF]high		+	moderate	moderate	

Table 4. Clotting potential of severe or moderate hemophilic A or B blood when triggered by the low or high levels of contact activation or extrinsic activation in the presence and absence of rFVIIa.

Rescue indicates return to response levels of healthy blood. Low CTI: 4 μg/mL corn trypsin inhibitor; High CTI: 40 μg/mL corn trypsin inhibitor. Mild hemophilic blood (>14-15%) preforms without large functional deficit when compared to healthy blood in this assay under conditions of contact or extrinsic activation with reduced sensitivity to added rFVIIa. *, this study.

5.4   Discussion and Conclusion

Microfluidic assays consisting of high CTI (40 μg/ml)-inhibited WB perfusion on TF$_{low}$ or TF$_{high}$/collagen surfaces at venous wall shear rates were used to evaluate platelet deposition and fibrin formation in hemophilic patients. A broad cohort of patients were tested representing a large spectrum of clinical phenotypes of hemophilia A or B (severe, moderate, and mild(Table 3). Under these ex vivo hemodynamic conditions, we observed significantly decreased platelet deposition and fibrin formation on TF$_{low}$ and TF$_{high}$ collagen

surfaces in severe hemophilic samples.   Taken together, these results indicate that in healthy

blood clotting under flow conditions over TF, most Factor Xa comes from the intrinsic

tenase (FIXa/FVIIIa) even when some FXa can be initially generated by the extrinsic tenase

TF/FVIIa (**Figure 5-7**).

   With respect to factor-deficient patients at 1-3% factor activity (**Figure 5-1**), we

observed severe deficits in platelet adherence and fibrin formation that was not rescued by

perfusion on TF_{high} collagen surfaces. With the intrinsic tenase severely blunted as in the case

of severe FVIII or FIX-deficiency, surface TF-triggered coagulation failed to produce

adequate levels of thrombin for detectable fibrin formation (**Figure 5-1B,D**). At high

surface TF concentrations of ~ 2 TF molecules/μm^2 as measured in a prior study [113], the

extrinsic tenase could not support fibrin formation when critical residual clotting factor

activity was <3% (**Figure 5-1D**). Interestingly, we did not observe similar trends when we

tried to recreate the conditions of acquired severe hemophilia in these microfluidic assays

through the use of function-blocking antibodies against FVIII or FIX (**data not shown**)

added to healthy blood. Under flow conditions on TF_{low} or TF_{high} collagen surfaces, normal

blood treated with function-blocking antibodies against FVIII or FIX only displayed

decreases in fibrin formation on TF_{low} collagen surfaces while no effect was seen on platelet

deposition. This suggests large functional differences between true factor deficiencies, factor

deficiencies plus inhibitors, and laboratory experiments with antibodies added to healthy

blood.

   At 3-14% factor activity, TF collagen surfaces were able to partially restore platelet

adhesion and fibrin formation under flow, yet these levels were still significantly below

healthy WB controls (**Figure 5-2**). This restoration of platelet adhesion and fibrin generation was likely due to sufficient intrinsic tenase (FVIIIa/FIXa) functioning on platelets to generate sufficient FXa for thrombin and fibrin production. Finally, at >14% factor activity, platelet adhesion was moderately suppressed while TF_{high}/collagen fully restored fibrin formation (**Figure 5-3**). This is consistent with previous studies which report adequate local thrombin concentrations that support fibrin formation under flow in the case of mild FVIII deficiencies and high surface TF concentrations[77]. These findings are also consistent with previous studies that report FVIII/FIX dependent enhancement of platelet procoagulant activity as a limiting step in fibrin formation under flow[111].

We also assessed the role of rFVIIa in platelet deposition and fibrin formation under flow in hemophilic and healthy WB samples. Results from a severe hemophilic patient indicate that rFVIIa amplifies platelet deposition but was not fully sufficient to support fibrin generation if the contact pathway was inhibited (**Figure 5-5**) [24]. However, a combination of 20 nM exogenous rFVIIa and TF_{high}/collagen facilitated strong fibrin production in the severely FVIII-deficient patient (**Figure 5-5D**). A consideration of final platelet and fibrin deposit size in the presence of exogenous rFVIIa indicates enhancement of platelet and fibrin accumulation in the severely factor-deficient hemophilic patients tested (**Figure 5-6**). A similar trend was observed when rFVIIa was exogenously added to the WB of healthy donors followed by perfusion on TF_{low} and TF_{high} collagen surfaces (**Figure 5-6**). In summary, we took a systems approach by modulating the following inputs: contact pathway engagement, the procoagulant surface trigger, and exogenous concentrations of rFVIIa. We then explored the impact of these inputs and found distinct changes in platelet

deposition and fibrin generation under flow as a function of these inputs (**Table 4**). Based on this study and our earlier study[24], rFVIIa cannot rescue fibrin deposition via the cellular pathway alone, unless FXIIa or TF is participating.

Distinct from the studies of Swieringa et al. who added TF directly into blood prior to perfusion, the micropatterning of TF-rich collagen surfaces generates localized regions of thrombosis in microfluidic channels which ensures that blood does not come into contact with extraneous prothrombogenic surfaces prior to the region of interest. This enables study of platelet deposition in conjunction with surface-triggered coagulation akin to the laser cremaster injury[114–116]. In contrast, addition of exogenous TF into blood fails to recreate the hemodynamic aspects of thrombosis which are highly dependent on surface presentation of TF to the flowing blood[35]. Furthermore, the present work extends previous studies by directly examining the contribution of platelet bound rFVIIa on platelet and fibrin formation under flow in a wide range of hemophilic patients[77].

In conclusion, our microfluidic assay results from WB of FVIII or FIX-deficient patients indicate a critical role of the intrinsic tenase in driving platelet adhesion and fibrin formation on TF-laden collagen substrates at venous shear rates (**Figure 5-7**). FVIII/FIX dependent thrombin production on the platelet surface and the subsequent thrombin activation of platelets along with fibrin formation are potent, key pathways in thrombus formation under flow.

6 EX VIVO RECAPITULATION OF TRAUMA-INDUCED COAGULOPATHY UNDER FLOW AND PRELIMINARY ASSESSMENT OF PLATELET FUNCTION FOLLOWING TRAUMA USING MICROFLUIDIC TECHNOLOGY

6.1 Introduction

Trauma is the leading cause of death in people under the age of 36 years old[117]. Many severely injured patients exhibit trauma induced coagulopathy (TIC), a hemorrhagic state that accounts for 40% of trauma deaths[117]. TIC is multifactorial and associated with tissue injury, inflammation, shock, hemodilution, acidosis, hypoxia, and hypothermia[117]. Tissue injury and shock result in hyperfibrinolysis due to the acute release of tissue plasminogen activator (tPA) from endothelial cells. Systemic fibrinolysis results in fibrinogen consumption and limits clot formation and stability at the site of vascular injury, resulting in increased bleeding risk[118]. Furthermore, blood loss followed by resuscitation with colloids or packed red blood cells (PRBCs) leads to the hemodilution of clotting factors.

Current research in TIC has focused on coagulation factors and proteases, with the role of platelet function during trauma not as well-defined[119,120]. Platelet function studies of trauma patients have been difficult to implement due to the technical complexities of current platelet function tests. Although recent advances in platelet aggregometry and thromboelastography (TEG) have enabled important studies of platelet function and clot strength in trauma patients [121–125]. These techniques, however, are closed systems lacking flow or are comprised of poorly defined flow fields.

Microfluidic systems are open systems where blood flows over a zone of defined procoagulant surface, thereby recreating the unique spatial and compositional attributes of blood clotting found in vivo [23]. Microfluidic technology in conjunction with micropatterning techniques enable low volume and high throughput testing of platelet function and fibrin generation over a range of physiological shear stresses [34,37,126–128]. Microfluidic whole blood assays have been previously used to evaluate platelet and clotting function in hemophiliacs and healthy donors taking antiplatelet therapeutics [23,24,77,129].

In regards to current resuscitation strategies, the administration of PRBCs with or without fresh frozen plasma (FFP) and the optimal FFP:PRBCs ratio remain active areas of investigation [130]. Prospective studies have shown that platelets may serve as the third component of resuscitation strategy [130–133]. PRBC administration not only increases hemoglobin, but also contributes biorheologically by driving platelet margination towards the vessel wall.

In this study, we applied microfluidic technology to investigate resuscitation-driven hemodilution, hyperfibrinolysis, and plasmin-inhibitor therapy, all topics relevant to TIC risk and treatment. Additionally, we evaluated platelet function under flow using whole blood from trauma patients during the acute phase of TIC.

6.2   Methods

6.2.1   Microfluidic evaluation of hemodilution and hyperfibrinolysis

Following approval from the Internal Review Board approval at the University of Pennsylvania, healthy donors (n = 15) were recruited to donate whole blood using standard

phlebotomy techniques. Donors were required to refrain from all oral medications for 7 days and abstain from alcohol for 48 h prior to donation. Blood was drawn into corn trypsin inhibitor (CTI, Haematologic Technologies, Essex Junction, VT, 40 µg/ml final concentration) or FPR-chloromethylketone (PPACK, Haematologic Technologies, Essex Junction, VT, 100 µM final concentration). CTI inhibits the contact pathway for studies of surface-triggered coagulation while PPACK inhibits thrombin generation in order to examine platelet function in the absence of thrombin in vitro. Blood samples were treated with fluorescently conjugated anti-CD61a antibody (clone VI-PL2, Becton Dickson, Franklin Lakes, NJ, 0.125 µg/ml final concentration) to label platelets and fluorescently conjugated fibrinogen (Invitrogen, Life Technologies, Carlsbad, CA, 75 µg/ml) to label fibrin(ogen) 5 min prior to initiation of flow assays. All healthy donor microfluidic experiments were completed within 45 min of phlebotomy.

Microfluidic fabrication methods and device specifications were previously described [24,33,34]. Microfluidic channels ran perpendicularly over a 250 µm wide strip of patterned equine fibrillar collagen type I (Chronopar, Chronolog) or Tissue Factor (TF) bearing collagen type I surfaces (Dade Innovin, Siemens Healthcare USA, Malvern, PA). Epifluorescent microscopy and image acquisition were performed in real-time as previously described [23,24]. Dilution of the hematocrit to simulate resuscitation-induced hemodilution was achieved with exogenous addition of HEPES buffered saline (HBS, 20 mM HEPES, 160 mM NaCl, pH 7.5), donor specific platelet poor plasma (PPP) or platelet rich plasma (PRP). Isolation of PRP or PPP was previously described [24,80]. HBS, PPP or PRP was added in 1:3, 1:1, 3:1 ratio to whole blood to obtain Hct levels of 30%, 20%, 10%

respectively 5 min prior to initiation of the flow assay. Fibrinolysis was promoted by exogenously adding 10X stock solutions of tPA (abcam, Cambridge, MA, 0-50 nM). Blood samples were perfused at an initial venous wall shear rate of 200 s^{-1} or an initial arterial wall shear rate of 1222 s^{-1} in a previously designed pressure relief mode for 20 min [37]. Platelet and fibrin accumulation were analyzed as previously described [24].

6.2.2 Microfluidic Assessment of Trauma patient platelet function

Following Institutional Review Board approval, blood was collected from trauma patients (n = 20) who had sustained injuries requiring evaluation at the Hospital of University of Pennsylvania (HUP) Level 1 Trauma Center. Exclusion criteria included failure to obtain an initial blood draw and death within 24 h of admission. Patient demographics, clinical laboratory test results, and outcomes were recorded (**Table 5**). All trauma patients had Hct levels and platelet counts within physiologic ranges (**Table 5**). All clinical laboratory tests were obtained at the same time as the microfluidic assessment of trauma patient platelet function. All trauma patient samples were collected within one hour of injury. A blood sample was drawn upon patient arrival using 21-guage or larger needle into a 10 ml plastic syringe (Becton Dickson, Franklin Lakes, NJ) containing no anticoagulant. Blood samples were aliquoted into vacationers for clinical assays and residual blood was transferred into a single vacutainer containing 100 μM PPACK. The effects of this collection method and the delay between phlebotomy and inhibition by PPACK (average ~ 3 min) were assessed and found to have negligible effects on platelet activation and thrombin generation (**Figure 8-16**, **Figure 8-17**).

	Patient #	Mechanism	Age	Medication affecting plt function	Blood products prior to admission	Pre-existing conditions	Hct	Platelets ($10^3/\mu L$)	ISS	TBI	PTT (secs)	PT (secs)	INR	Blood alcohol (mg/dL)	Blood products post microfluidic	24 h Mortality	In -hospital
1	3	MCC	23	No	No	None	36	238	22	No	27.3	15.1	1.3	<10	PRB CS	N	N
2	4	Stroke	83	No	No	hypertension	40	251	0	No	22.3	11.7	0.9	72	FPP & Platelets	N	N
3	5	Fall	84	Aspirin, Plavix	No	peripheral vascular disease, diabetes, hypertension, chronic kidney disease	36	142	11	Yes	29.8	13.2	1.1	0	None	N	N
4	6	MVC	60	coumadin	No	DVT, depression,	39	186	27	Yes	27.2	19.2	1.7	263	None	N	N
5	7	MCC	25	No	4U PRBC	None	42	126	43	Yes	25.5	14.5	1.2	<10	PRB CS	N	N
6	9	Fall	68	No	No	hypertension, diabetes	34	171	30	Yes	44	15.3	1.3	<10	PRB CS	N	N
7	11	Fall	29	No	No	Haemophilia A	36	281	0	No	81.6	13.7	1.1	<10	None	N	N
8	13	Assault	47	No	No	schizophrenia, etoh abuse,	40	207	34	Yes	26	14.5	1.2	178	PRB CS & FFP	N	N
9	15	Fall	88	No	No	coronary artery disease, hypertension	40	163	5	No	27.8	14.9	1.2	0	None	N	N
10	17	GSW	31	No	No	None	47	320	26	No	X	X	X	139	None	N	N
11	19	Fall	47	Lovenox, Aspirin	No	Hypertension, cardiomyopathy,	40	295	1	No	26.9	13.2	1.1	0	None	N	N
12	20	Fall	77	No	No	Atrial Fib	36	142	2	No	20.3	12.4	1	<10	None	N	N
13	22	MVC	28	Heroin	No	asthma	43	188	2	No	28.4	13.5	1.1	<10	None	N	N
14	24	SW	27	No	No	asthma	39	224	10	No	25.5	13.7	1.1	<10	None	N	N
15	26	MVC	31	No	No	alcohol abuse	49	245	2	No	21.9	13.9	1.2	439	None	N	N
16	28	Fall	80	Aspirin	No	hypertension, hyperlipidemia	38	58	2	No	29.5	14.1	1.2	0	None	N	N
17	31	Fall	55	No	No	hypertension	33	247	27	No	28.9	14.3	1.2	<10	PRBC, FFP, & Platelets	N	N
18	34	MVC	26	No	1U PRBC	asthma	29	93	26	No	31.2	15.2	1.3	0	PRB Cs, FFP, & Platelets	N	N
19	35	SW	45	No	No	Seizure disorder, on dilantin	38	193	1	No	30.9	12.8	1	307	None	N	N
20	36	Pedestrian Struck	50	No	No	None	37	348	1	No	30.1	13.6	1.1	96	None	N	N

Table 5. Twenty trauma patient characteristics and clinical data

Twenty trauma patients were examined in WB microfluidic assays with PPACK-inhibited WB perfusion over collagen. Trauma patient characteristics and clinical data are as reported, blood products post microfluidic testing were administered within the first hour of evaluation by Hospital of University of Pennsylvania (HUP) Level 1 Trauma Center. Medications altering coagulation, blood product use, pre-existing conditions, Hct, platelet count, Injury Severity Score (ISS), diagnosis of traumatic brain injury (TBI), PT, PTT, INR, blood alcohol level, and blood products post microfluidic testing are as reported. (MCC, motorcycle crash; MVC, motor vehicle crash; GSW: gun shot wound; SW, stab wound.)

PPACK anticoagulated blood samples were treated with fluorescently conjugated anti-CD61a antibody (clone VI-PL2, Becton Dickson, Franklin Lakes, NJ, 0.125 μg/ml final concentration) to label platelets and anti-human CD62P (P-Selectin) antibody (BioLegend, San Diego, CA, 4 μg/ml final concentration) to stain for P-Selectin. Blood samples were subsequently treated with either HBS or 100X stock solutions of the indicated antagonists. MRS 2179 (2'-deoxy-N6-methyladenosine 3', 5'-bisphosphate ammonium salt (MRS 2179, Tocris Bioscience, Minneapolis, MN), S-Nitrosoglutathione (GSNO, Santa Cruz Biotechnology, Dallas TX), and iloprost (Tocris Bioscience) were the antagonists used and dissolved at 0.1 mM, 10 mM, 0.2 mM in HBS respectively. Whole blood perfusion in microfluidic devices started within 10 min of blood collection in constant flow mode at 100 s^{-1}.

6.2.3   Statistical significance analysis

Statistical significance was assessed using a two-tailed unpaired Student's t-test. Data sets were considered significantly different from each other if the calculated p-value < 0.05. Exact p-values are reported in the results where $p > 0.001$, otherwise $p < 0.001$ is denoted.

6.3 Results

6.3.1 Hemotocrit reduction: dilution reduces platelet deposition on collagen (no thrombin) and platelet-fibrin accumulation on TF/collagen

Our healthy volunteer study population had a mean age 26.2 ± 1.52y (10M/5F). The effect of hematocrit dilution on platelet deposition was evaluated by ex vivo dilution of healthy whole blood with either saline, PPP, or PRP (**Figure 8-11**). In the absence of thrombin with PPACK-inhibited whole blood at 200 s^{-1}, platelet deposition was strongly inhibited by hemodilution with saline ($p < 0.001$), PPP ($p < 0.001$), or PRP ($p < 0.001$: 10 & 20% Hct, $p = 0.01$: 30% Hct) (**Figure 6-1A,C,E**). As expected in the microfluidic flow assay over collagen, fibrin generation was dependent on thrombin production and was negligible in PPACK-inhibited whole blood in the absence of surface-patterned TF on collagen (**Figure 6-1B, D, F**).
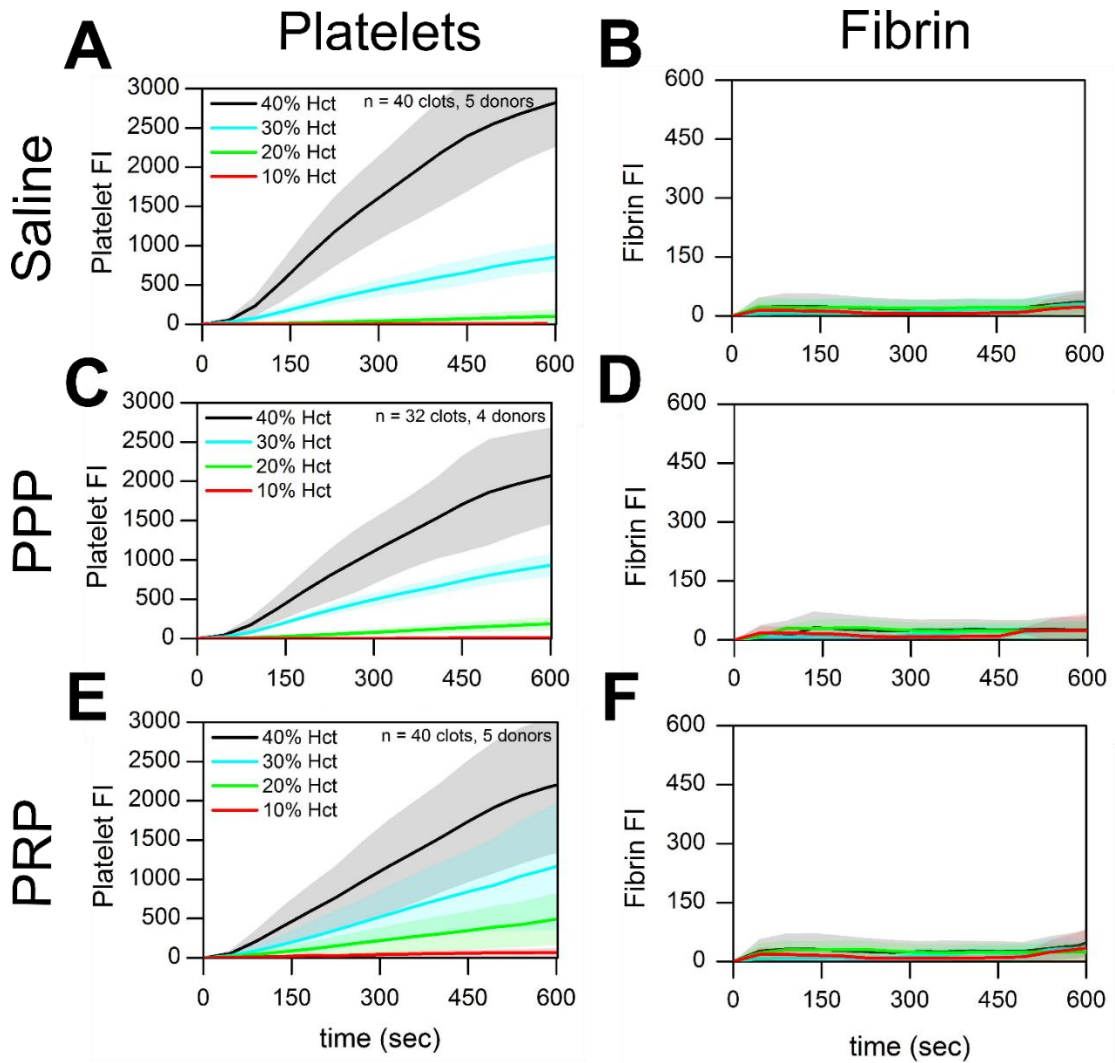
Figure 6-1 Platelet accumulation on collagen in healthy donors following Hct dilution in the absence of thrombin.

(A & B), Platelet and fibrin fluorescence intensities vs. time with saline dilution of Hct. (C & D), Platelet and fibrin fluorescence vs. time with PPP dilution of Hct. (E & F), Platelet and fibrin fluorescence intensities vs. time with PRP dilution of Hct. Shaded traces are the mean and standard deviation of 10 clotting events from 5 donors.

Similarly, in the presence of surface-triggered coagulation (**Figure 6-2**), we detected significant decreases in platelet accumulation for all lowered Hct levels when whole blood was diluted with saline ($p < 0.001$: 10 & 20% Hct, $p = 0.0154$: 30% Hct), PPP ($p < 0.001$: 10 & 20% Hct, $p = 0.002$: 30% Hct or PRP ($p < 0.001$: 10% Hct, $p = 0.0035$: 20% Hct, $p = 0.0316$: 30% Hct) (**Figure 6-2A, C, E**). Total fibrin accumulation at lower Hct levels was also significantly reduced when whole blood was supplemented with saline ($p < 0.001$: 10, 20 & 30% Hct) or PPP ($p < 0.001$: 10% Hct, $p = 0.005$: 20% Hct, $p = 0.0064$: 30% Hct) or PRP ($p < 0.001$: 10% & 20% Hct, $p = 0.3576$: 30% Hct) to reduce Hct (**Figure 6-2B, D**). The reduced fibrin accumulation observed with reduced Hct cannot be due to a reduction in coagulation factors since the concentration of coagulation proteins remains constant when whole blood is diluted with PPP or PRP (as opposed to saline dilution). In this experiment, reduced platelet deposition was highly correlated with reduced fibrin production as Hct was reduced, regardless of how Hct was lowered (**Figure 6-2**).
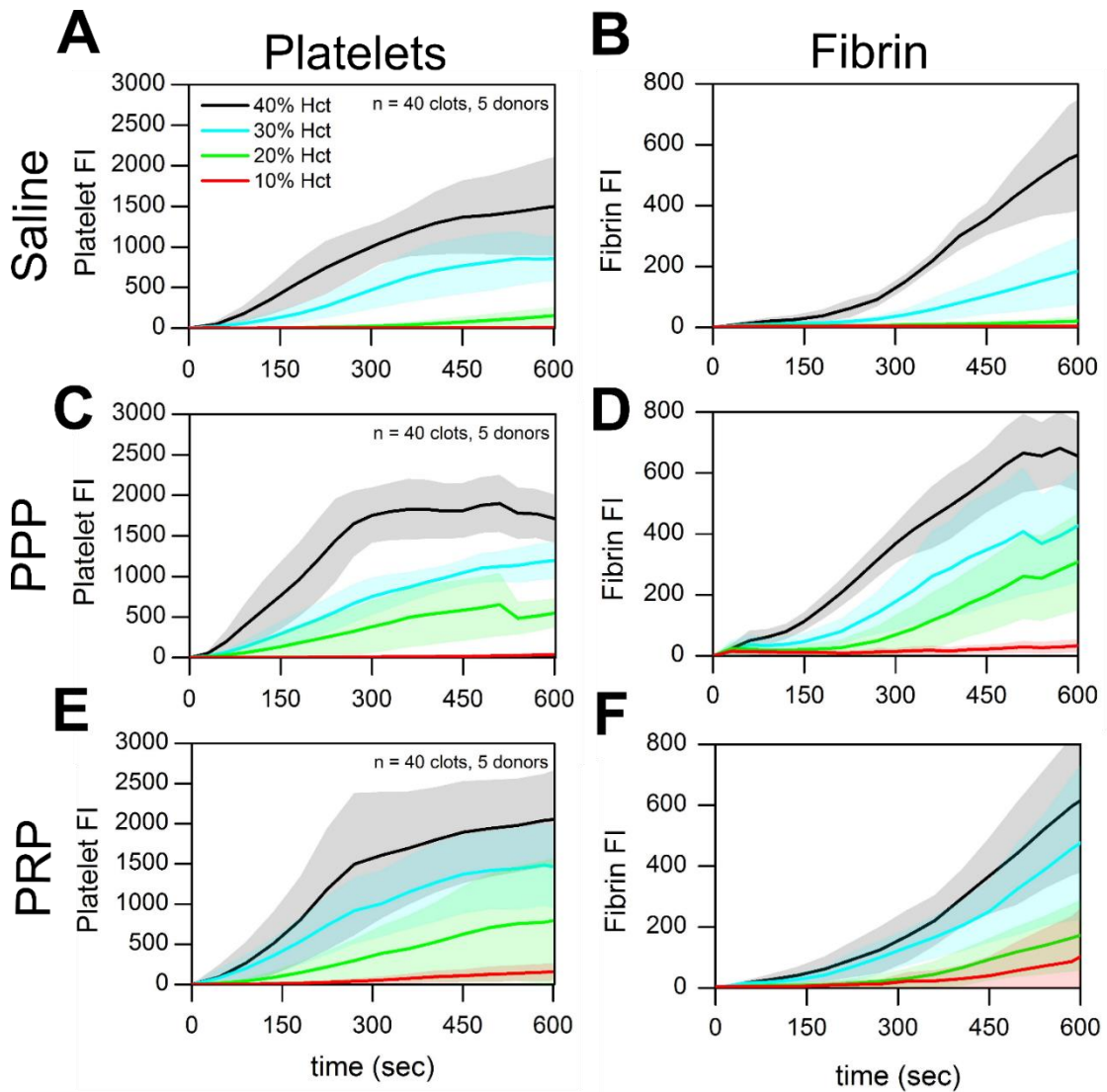
Figure 6-2 Platelet and fibrin accumulation on TF bearing collagen in healthy donors following Hct dilution

(A & B), Platelet and fibrin fluorescence intensities vs. time with saline dilution of Hct. **(C & D)**, Platelet and fibrin fluorescence intensities vs. time with PPP dilution of Hct. **(E & F)**, Platelet and fibrin fluorescence intensities vs. time with PRP dilution of Hct. Shaded traces are the mean and standard deviation of 10 clotting events from 5 donors.

6.3.2 Exogenous tPA activates the lytic state at venous and arterial shear rates and promotes hyperfibrinolysis

Following severe trauma and shock, injured endothelial cells release tPA systemically leading to hyperfibrinolysis [117]. To mimic this pathological mechanism, tPA was exogenously added to whole blood (**Figure 8-11**). At venous shear rates (200 s^{-1}), exogenous addition of tPA to whole blood had negligible effects on platelet deposition on TF bearing collagen surfaces under flow (**Figure 6-3A, B**; ns). However, the rapid production of plasmin at the surface-patterned injury site in conjunction with fibrin formation at 200 s^{-1} induced a 'lytic state' with 50 nM ex vivo tPA added. Total fibrin accumulation decreased 63.9 % by 10 min (**Figure 6-3C**; p = 0.0044). To reverse the 'lytic state' and stop fibrinolytic activity under flow, we added the lysine analogue ε-aminocaproic acid (εACA) to inhibit plasmin activity. The inhibition of plasmin by εACA restored total fibrin accumulation to levels comparable to control conditions but resulted in delayed fibrin initiation (**Figure 6-4C**). At arterial shear rates (1222s^{-1}), embolization occurred with tPA as indicated by a significant drop in the platelet signal by 12 min (**Figure 6-4**). The platelet signal continued to decrease approaching zero by the end of the 20 min assay (**Figure 6-4B**). Exogenous tPA addition minimized total fibrin accumulation while treatment with εACA non-significantly increased platelet deposition (p = 0.1024) and total fibrin accumulation (p = 0.1132) (**Figure 6-4B, C**). Interestingly, in a few channels of the microfluidic assay at either venous or arterial wall shear rates, tPA-mediated fibrinolysis was followed by destabilization of platelet deposits which then embolized downstream. This disruption of platelet rich thrombi from

the patterned injury site was followed a second round of platelet deposition and renewed

fibrin generation (**Figure 8-14**, **Figure 8-15**).
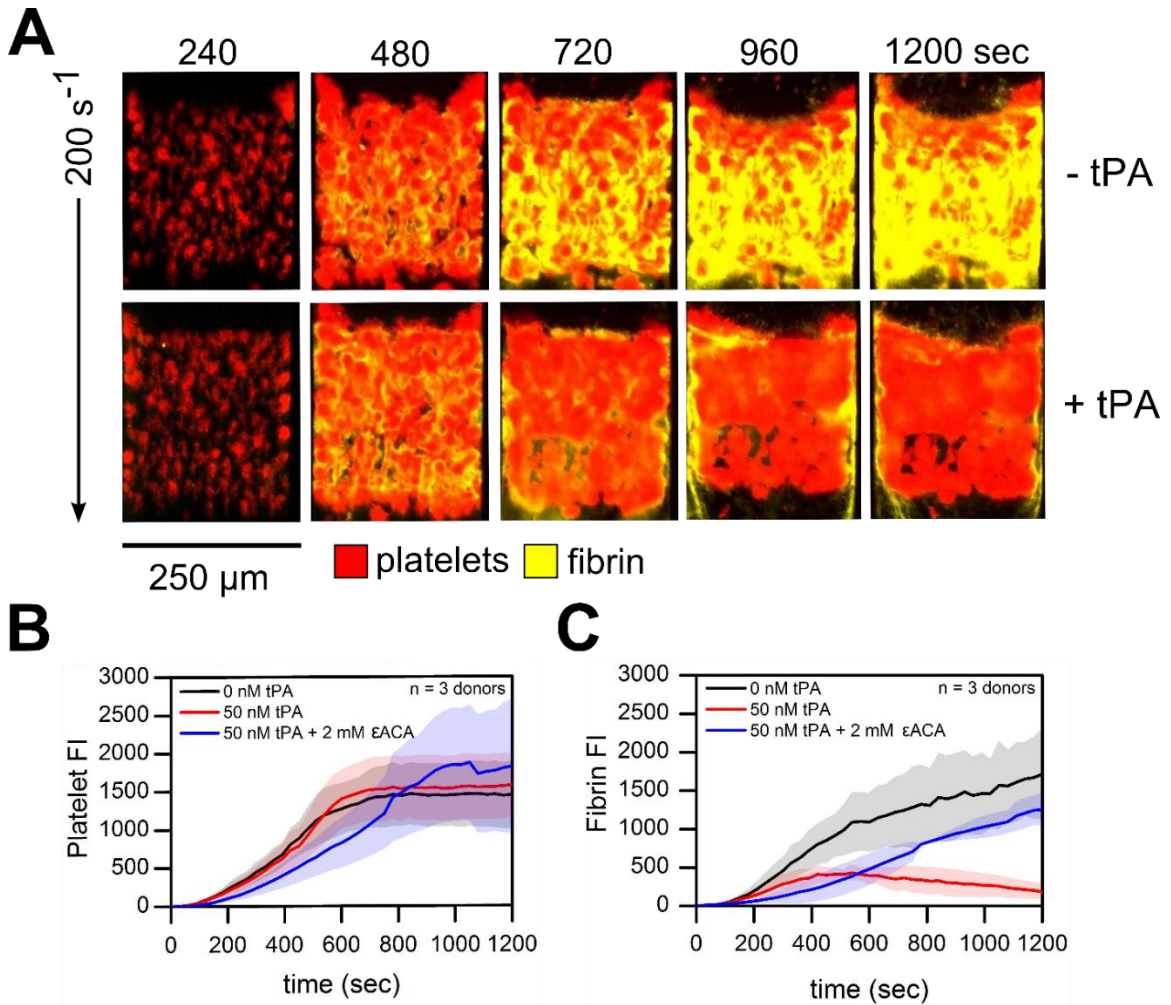
Figure 6-3 Platelet and fibrin accumulation in response to exogenous tPA $\pm$ εACA at venous shear rates

(A), Overlay of platelets (red) and fluorescent fibrinogen (yellow) deposition at 200 s^{-1} over the time course of the 20 min assay. (**B**), Platelet fluorescence intensities vs. time with exogenous tPA $\pm$ εACA. (**C**), Fibrin fluorescence intensities vs. time with exogenous tPA $\pm$ εACA. Shaded traces are the mean and standard deviation of 12 clotting events from 3 donors.
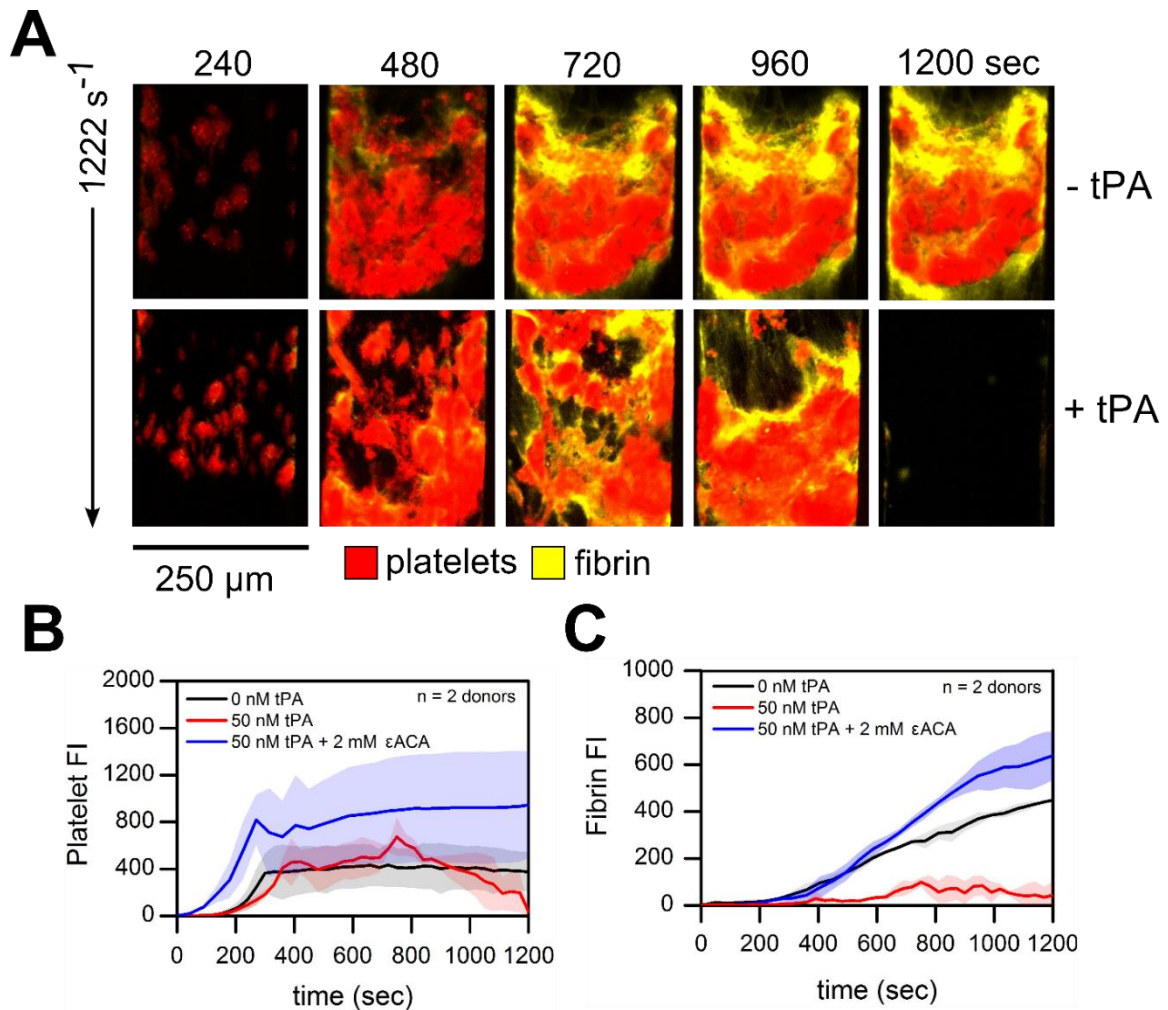
Figure 6-4 Platelet and fibrin accumulation in response to exogenous tPA ± εACA at arterial shear rates

(A), Overlay of platelets (red) and fluorescent fibrinogen (yellow) deposition at 1222 s^{-1} over the time course of the 20 min assay. (**B**), Platelet fluorescence intensities vs. time with exogenous tPA ± εACA. (**C**), Fibrin fluorescence intensities vs. time with exogenous tPA ± εACA. Shaded traces are the mean and standard deviation of 8 clotting events from 2 donors.

6.3.3 Trauma patient platelet function tests: delayed platelet recruitment to collagen and attenuated secondary aggregation

Our 20 trauma patient population had a mean age of 50.2 ± 22.84 and a median injury severity score (ISS) of 7.5 with an interquartile range of 25. There were 15% penetrating injuries and 25% brain injuries. Rapid platelet function testing of PPACK-inhibited whole blood from trauma patients (n = 20) revealed a subpopulation of patients (14/20) with reduced platelet function upon arrival to a Level 1 Trauma Center (**Figure 6-5**, **Figure 8-18**). When compared to 7 healthy donors, 14 trauma patients were found to have significantly decreased total platelet accumulation measured at 900 sec (**Figure 8-19**; $p < 0.001$). We categorized these subset of patients as 'loss of function'. Patients with statistically significant increased total platelet accumulation measured at 900 sec when compared to healthy donors were categorized as 'gain of function' (**Figure 6-5**, **Figure 8-19**) Visual inspection of platelet aggregates formed on collagen surfaces indicate two loss of function phenotypes in trauma patients. The first loss of function phenotype in trauma patients was characterized by platelets failing to adhere to the collagen surface indicative of dysfunctional platelet glycoprotein VI (GPVI) (**Figure 6-5B, C, E, K**). In a second observed loss of function phenotype, platelet aggregate growth beyond the initial monolayer of platelets was minimal or completely missing (**Figure 6-5D, F-N**). Platelet aggregates tended to form above the initial monolayer of collagen-adherent platelets but were subsequently washed downstream. Clots formed from these patients did not grow to full channel occlusion during the duration of the 900 sec assay (**Figure 6-5**, **black arrow**). This failure of secondary aggregation in these patients may be due to a lack of ADP or thromboxane A_2 mediated clot

growth. Interestingly, 3 patients exhibited hyper-responsive platelet function in this

microfluidic assay with two patients forming occlusive clots within the first 400 seconds

(**Figure 6-5R-T**).
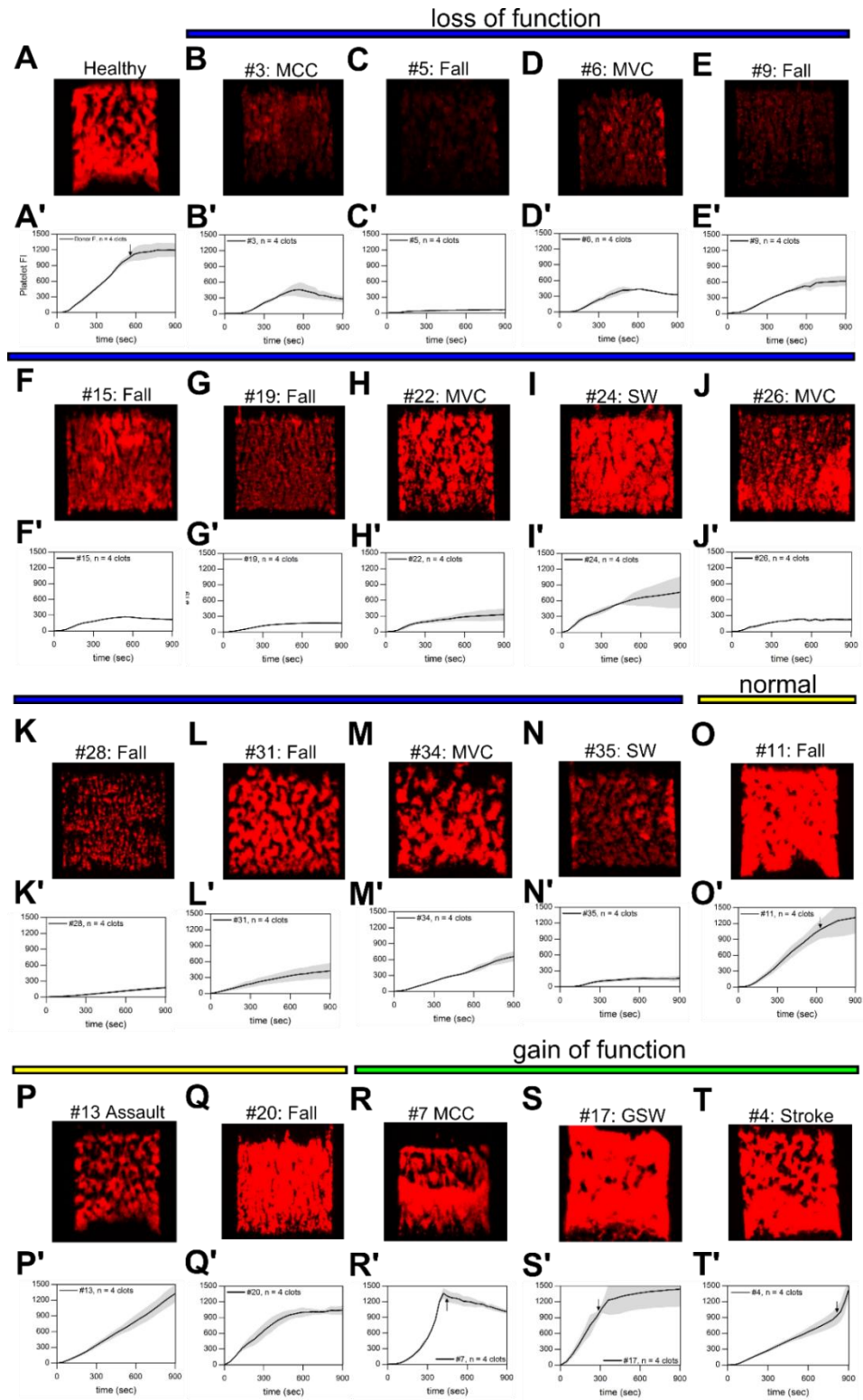
Figure 6-5 Trauma patient thrombi morphology at 900 sec and platelet deposition dynamics at venous shear rates (100 s^{-1})

(A & A'), Platelet fluorescence intensities vs. time for representative healthy donor and representative image of final platelet accumulation at 900 sec. (**B-N & B'-N', blue line),** Platelet fluorescence intensities vs. time and representative image of final platelet accumulation at 900 sec for trauma patients exhibiting loss of platelet function. **(O-Q & O'-Q', yellow line),** Platelet fluorescence intensities vs. time and representative images of final platelet accumulation at 900 sec for trauma patients exhibiting normal platelet function. **(R-T & R'-T', green line),** Platelet fluorescence intensities vs. time and representative images of final platelet accumulation at 900 sec for trauma patients exhibiting gain of platelet function. Shaded traces are the mean and standard deviation of 4 clotting evens from each patient. (MCC: Motorcycle Crash, MVC: Motor Vehicle Crash, SW: Stab wound, GSW: Gun Shot Wound)

6.3.4 Trauma patient platelets respond less to antagonism by MRS2179 and iloprost but increased sensitivity to inhibition by GSNO

To assess the various pathways that affect trauma platelet signaling under flow, we antagonized platelet function in three different manners (**Figure 8-12**). MRS 2179 was used to potently inhibit the platelet ADP receptor, P_2Y_1. The addition of GSNO was used to stimulate nitric oxide production ex vivo and iloprost was used to raise cyclic adenosine monophosphate (cAMP) levels in order to reduce platelet aggregation. On average, trauma patients with detectable baseline platelet function measured by platelet fluorescence responded to all three forms of antagonism (**Figure 8-12C**). Total platelet accumulation at 900 sec was reduced 58.8%, 43.83% and 73.80 % by MRS2179, GSNO, and iloprost respectively in trauma patients (n = 17, 68 clots, p < 0.001) as compared to 79.2%, 15.2%, and 91.81% in healthy donors (n = 6, 24 clots, p < 0.001) (**Figure 8-20**). Interestingly,

114

trauma patient platelet function responded less to the addition of MRS 2179 or iloprost but was more strongly inhibited by production of nitric oxide ex vivo (**Figure 8-20**; MRS 2179: p = 0.003, Iloprost or GSNO: p < 0.001).

6.3.5 A subpopulation of trauma patient platelets displayed decreased p-selectin expression under flow

P-selectin surface expression was also used as a marker for α-granule secretion and irreversible platelet activation in our microfluidic assay (**Figure 8-13**). A population of trauma patients (9/21) exhibited low p-selectin expression in the flow assay (data not shown) however, when normalized against the platelet fluorescence signal, a single patient displayed a severe deficit in p-selectin expression on a per platelet basis (**Figure 8-13B-D**). The lack of p-selectin expression in patient #9 may be indicative of low levels of platelet activation and potential previous degranulation of platelets prior to microfluidic testing.

6.4 Discussion

Trauma induced coagulopathy is a multi-faceted phenomenon that occurs in a setting of shock, hemodilution, hypothermia, and tissue injury. With the use of microfluidic technology we evaluated hemodilution and hyperfibrinolysis, two common mechanisms of TIC, in order to understand how derangements in platelet deposition and fibrin formation contribute to altered hemostasis. Hemodilution of healthy whole blood with saline, PPP, or PRP significantly reduced platelet adhesion to collagen in the absence of surface-triggered coagulation at all lowered Hct levels (**Figure 6-1**). Platelet deposition was also significantly decreased with this dilution scheme on TF-bearing collagen surfaces (**Figure 6-2**). RBCs

strongly influences platelet margination and enhances platelet accumulation at the collagen or collagen/TF micropatterned injury site in these assays. These results indicate a significant role for RBCs in mediating the rapid platelet response required to seal vessel injuries. Furthermore, RBCs have also been shown to release ADP thus promoting platelet aggregation and can potentially sustain thrombin generation [134]. This is could be another role in which RBCs support platelet function and coagulation in our microfluidic assays. However, ADP release from RBC is expected to be minimal under the venous flow conditions tested (**Figure 6-2**).

Furthermore, a second mechanism associated with TIC is increased fibrinolytic activity. Excessive fibrinolysis impairs clot integrity and causes bleeding. We recapitulated this mechanism and rapidly detected changes in fibrin accumulation and clot stability in microfluidic assays with exogenous addition of tPA. We promoted a 'lytic state' under flow inducing fibrin lysis at venous shear rates that was rescued with ex vivo εACA addition (**Figure 6-3**). At arterial shear rates, the 'lytic state' induced embolism as clots tore from the TF bearing collagen surfaces and washed downstream (**Figure 6-4**). In rare cases, the 'lytic state' induced a consumptive coagulopathy with complete fibrin lysis and disintegration of platelet aggregates followed by platelet re-adherence and fibrin regeneration on the TF bearing collagen surface. This observed process depletes platelets, clotting factors, and other plasma proteins in the flowing blood. The deranged hemostasis during hyperfibrinolysis we have recreated in the microfluidic assays mimics the coagulopathy of traumatic brain injuries [135]. Our results suggest that hyperfibrinolysis and excessive consumption of clotting factors work synergistically during TIC. (**Figure 8-14**, **Figure 8-15**). Finally, we were able to

detect and quantify changes in fibrin generation and clot stability during this 'lytic state' in <6 min, a time scale much faster than what is currently capable with TEG.

In clinical settings, conventional plasma-based assays are used to assess TIC instead of microfluidic-based assays. The prothrombin time (PT), partial thromboplastin time (PTT), platelet count, and fibrinogen levels are the most commonly used tests for monitoring coagulopathy following trauma. These tests, however, examine only a single component of the hemostatic process and fail to measure clot strength, fibrinolytic activity or platelet function. Furthermore, while TEG with or without platelet mapping is more indicative of global hemostasis, the use of FXII activator kaolin and citrated samples are major drawbacks with this technology. Kaolin activation of coagulation is non-physiologic as kaolin is not found in the body and citrate is known to affect platelet $\alpha_{II}\beta_{IIIa}$ integrin function. The fluid mechanics of TEG also fail to replicate the hemodynamics of the vasculature. The oscillatory movement of a cup in a closed system cannot generate the extraordinary platelet concentrations in a clot on the vessel wall. Furthermore, in TEG, the moving cup is a closed system where platelet releasates and coagulation factors can accumulate unhindered due to the lack of transport-induced washout of these components. Microfluidic assessment of trauma patient function detected platelet function defects in < 5 min while a complete TEG test may take upward to 60 min [136].

In whole blood microfluidic assays, on the other hand, platelet deposition and fibrin generation must occur under well-controlled hemodynamic conditions and in the presence of convective dilution of thrombin, soluble agonists, and plasma proteins. During these assays, the biorhelogic phenomena present can either limit or augment local enzyme

concentrations. In addition to changes in the local enzyme concentrations, platelet receptor-ligand bonds must withstand the hydrodynamic shear stress imparted by the following blood. Thus whole blood microfluidic assays provide a much more rigorous physiologic test of platelet function and fibrin generation not captured by static clotting assays and TEG [137,138].

To the best of our knowledge, our results are the first real-time platelet function testing of whole blood samples from trauma patients using microfluidic technology. One previous study by Jacoby et al. has assessed platelet function following trauma using a platelet function analyzer (PFA-100) with citrated whole blood. The PFA-100 is a cartridge-based flow system that aspirates citrated whole blood in capillaries. It measures aperture closure time following blood clotting on a membrane coated with collagen/ADP or collagen/epinephrine. Their study reported decreased closure times at initial trauma patient presentation indicating increased platelet function and hypercoagulability. Contrary to the Jacoby et al. report, we observed noticeable decreases in platelet adhesion to collagen and secondary platelet aggregation when we rapidly assessed platelet function in trauma patients (n = 20) at 100s $^{-1}$ over collagen surfaces (**Figure 6-5**). Furthermore, when comparing our microfluidic assay results to clinical patient data, we found no correlation between platelet function and injury severity score (ISS), or platelet function and the diagnosis of traumatic brain injury (TBI). All 14 patients displaying decreased platelet function had physiological Hct levels and platelet counts. With respect to the clinical static plasma clotting assays, 13 of the 14 patients with decreased platelet function were within the normal PTT reference range (20.8-34.4) [23]. These results indicate that patient hematocrit levels, platelet counts, and

plasma-based clotting tests are largely inadequate in assessing the contribution of platelet function to the acute phase of TIC.

Interestingly, of the 7 patients that did require blood products post microfluidic testing, 4 patients had decreased platelet function as initially assessed by whole blood microfluidic testing. A single patient (#31) was transfused with 14 units of blood products within 12 hrs of arrival. Microfluidic testing of this patient detected decreased platelet function upon initial presentation and continuous attenuated platelet function up to 72 hours post admission (**Figure 8-21**).

Important distinctions exist between assays that evaluate platelets under non-flow conditions and microfluidics that allow platelets to accumulate on a surface to levels >200-fold that of whole blood levels. We demonstrated that microfluidic assay of trauma patient samples is a global test of whole blood clotting function under flow with the capability of detecting platelet dysfunction. In future work, a comparison of microfluidic assay with platelet aggregometry or platelet mapping-TEG may provide further insights into platelet dysfunction during TIC. Microfluidic assay allows determination of: (1) platelet recruitment to the collagen surface, (2) total platelet accumulation, (3) platelet accumulation rate, and (4) time to full channel occlusion. These metrics could be compared to platelet mapping-TEG metrics such as maximum clot strength ($MA_{Thrombin}$), the contribution of ADP receptors (MA_{ADP}), and the contribution of the arachidonic acid pathway (MA_{AA}). For example, we previously observed a relationship between aPTT and platelet accumulation rates on collagen surfaces for hemophilic blood from patients with increase bleeding risks (10). Finally, while all trauma patient samples were collected within one hour of injury. Further validation in the

whole blood microfluidic assay is required to examine how a variation in time of sample collection within the one hour time window affects platelet function under flow as derangements in trauma patient platelet function is thought to occur rapidly prior to hospital admissions.

The high throughput nature of microfluidic whole blood testing however, will enable testing of fresh platelets, stored platelets, and other current and novel drugs used to restore platelet function during the acute phase of trauma-induced coagulopathy. In a previous study, we have shown a novel method to assess the incorporation of culture-derived platelets from human peripheral blood cells into developing human thrombi under flow (28). Using similar techniques, future studies should test whether stored platelets can incorporate into trauma patient thrombi under flow. Successful adherence and incorporation of stored platelets into patient thrombi formed ex vivo could indicate the high potential of these platelets to restore platelet function in acute traumatic coagulopathy.

The mechanisms underlying trauma platelet dysfunction have yet to be elucidated and require further investigation outside of microfluidic testing. Groups have postulated that platelet function downregulation can occur during trauma. Previous studies suggest the presence of dysfunctional circulating platelets following activation in response to tissue damage [121,123]. Platelet receptor proteolysis may be another putative pathway in which platelet function is down-regulated in trauma patients. Previous reports describe proteolysis of platelet GPVI and GPIb-IX-V receptors (29,30). Ectodomain shedding of platelet adhesion receptors is a plausible physiologic mechanism in which platelets can respond to

cases of severe endothelial injury following trauma yet prevent uncontrolled thrombus growth that leads to systemic clotting.

In this study, we have used microfluidic technology to effectively evaluate current resuscitation strategies and hyperfibrinolysis showing more rapid detection of impaired hemostasis and coagulation than what is capable with current technologies. Furthermore, we also tested trauma patient platelet function using this high throughput method. The fast identification of platelet function defects in trauma patients using whole blood microfluidic assays indicate a potential novel 15 min test to help guide coagulopathy treatments in the future.

7 FUTURE WORK

7.1 A role for FXIIIa-mediated clot stability independent of fibrin polymerization

7.1.1 Introduction

Factor XIII (FXIII) is a coagulation protein that plays an essential role in physiologic hemostasis where it can regulate fibrinolysis[141], wound healing[142], and angiogenesis[143]. Clinically, FXIII deficiency results in hemorrhage and impaired wound healing[144]. FXIII is a plasma protransglutaminase composed of 2 A (FXIII-A) and 2 B (FXIII-B) subunits that circulate as a heterotetrameric zymogen (FXIII-A_2B_2)[145]. FXIII activation occurs when thrombin cleaves an N-terminal activation peptide from FXIII-A, and calcium mediates the dissociation of the inhibitory FXIII-B subunits, producing FXIIIa[145]. FXIIIa confers clot stability by cross-linking fibrin fibers in the fibrin matrix, thus altering its rheologic properties. FXIII originates from a family of transglutaminases (TG), TG are known to catalyze the formation of covalent ε-(γ-glutamyl) lysyl bond where a lysine ε-amino group is cross-linked to the glutamine of a γ-carboxymide group[141].

FXIIIa can also cross-link inhibitors of fibrinolysis to fibrin, further enhancing fibrin's insolubility and plasmin resistance. Inhibitors cross-linked to fibrin include α_2-antiplasmin (α_2AP), thrombin activatable fibrinolysis inhibitor (TAFI), and plasminogen activator inhibitor-2. In all, there are twenty-five FXIIIa substrates that can be divided into five categories: coagulation factors, components of the fibrinolytic system, adhesive and extracellular matrix proteins, intracellular cytoskeletal proteins, and others[145]. Previous work has shown a critical role of cross-linked α_2AP in stabilizing fibrin. This was

demonstrated by either the rapid lysis of clots formed in the absence of α_2AP or when α_2AP activity is neutralized[146]. Moreover, in addition to being present in plasma, FXIII-A is also present in platelets in large quantities[147–149]. The concentration of FXIII-A is 100X greater in the platelet cytoplasm than in plasma[150]. Recently, Mitchell et al. have shown that activated platelets externalize this pool of FXIII-A onto their membranes and that this pool is functional in cross-linking α_2AP and confers lytic resistance in platelet rich thrombi under flow[151].

The (patho)physiologic roles for FXIIIa activity derived from either platelet FXIII-A (cFXIII) or plasma FXIIIa (FXIIIa) are still not well-understood. Previous research has shown that human and murine whole blood clots formed in the absence of plasma FXIII or in the presence of a small molecular inhibitor for FXIIIa have reduced red blood cell retention and are significantly smaller than control clots[9]. Further work proved that FXIIIa mediates red blood cell retention in clots by cross-linking fibrin alpha chains[152]. Using microfluidic hemostasis models and whole blood perfusion under flow we aimed to delineate the ability of cFXIII and FXIIIa to confer platelet-rich thrombus stability independent of polymerized fibrin.

7.1.2 Materials and Methods

7.1.2.1 *Materials*

The following reagents were stored according to manufacturer's instructions: Corn Trypsin Inhibitor (CTI, Haematologic Technologies, Essex Junction, VT), phycoerythrin (PE) mouse anti-human monoclonal CD61 ($\alpha_{IIb}\beta_3$) antibody (clone VI-PL2, Becton Dickson,

Franklin Lakes, NJ). Fibrinogen from human plasma, Alexa Fluor 647 conjugate (Invitrogen Life Technologies, Carlsbad, CA). Equine fibrillar collagen type I (Chronopar, Chronolog, Havertown, PA), Dade Innovin (Siemens Healthcare USA, Malvern, PA), 1,3,4,5-Tetramethyl-2-[(2-oxopropyl)thio]imidazolium chloride (T101) (Zedira, Darmstadt, Germany), Gly-Pro-Arg Pro (Billerica, Massachusetts, EMD Millipore), Sylgard 184 Silicone Elastomer Kit (Sylgard, Ellsworth Adhesives, Germantown, WI), Iodacetamide (Sigma Aldrich, St. Louis, MO).

7.1.2.2 Blood Collection and preparation

Phlebotomy was approved by the University of Pennsylvania Institutional Review Board and performed on consenting donors in accordance with the Declaration of Helsinki. Donors abstained from alcohol 48 h prior to blood donation and were free of oral medication for a minimum of 7 days prior to donation.

7.1.2.3 Microfluidic Assay

Whole blood was taken from healthy donors using standard phlebotomy techniques. Blood was drawn into 40 μg/ml CTI or FPR-chloromethylketone (PPACK, Haematologic Technologies, Essex Junction, VT, 100 μM final concentration). CTI inhibits the contact pathway for studies of surface-triggered coagulation while PPACK inhibits thrombin generation in order to examine platelet function in the absence of thrombin in vitro. Blood samples were treated with 0.125 μg/ml fluorescently conjugated anti-CD61a antibody to label platelets and fluorescently conjugated fibrinogen to label fibrin(ogen) 5 min prior to initiation of flow assays. All healthy donor microfluidic experiments were completed within 45 min of phlebotomy.

124

Microfluidic fabrication methods and device specifications were previously described [24,33,34]. Microfluidic channels ran perpendicularly over a 250 μm wide strip of patterned equine fibrillar collagen type I (Chronopar, Chronolog) or Tissue Factor (TF) bearing collagen type I surfaces (Dade Innovin, Siemens Healthcare USA, Malvern, PA). Epifluorescent microscopy and image acquisition were performed in real-time as previously described [23,24].

Blood samples were perfused at an initial venous wall shear rate of 200 s^{-1} or an initial arterial wall shear rate of 800 s^{-1} in a previously designed pressure relief mode for 20 min [37]. Platelet and fibrin accumulation were analyzed as previously described [24].

7.1.3   Results

7.1.3.1   *Nonspecific FXIIIa inhibitor confers gross platelet instability in the presence of GPRP at constant flow conditions*

To investigate the fibrin-independent role of FXIIIa activity and function, non-selective FXIIIa inhibitor iodoacetamide was used ex vivo in the presence or absence of GPRP, a short four peptide sequence that inhibits fibrin polymerization. Following incubation with iodoacetamide and GPRP, whole blood was perfused over a TF/collagen surface under venous shear rates. Decreases in platelet fluorescence intensity were observed over time in the absence of GPRP indicating a thrombin dependent role of FXIIIa (**Figure 7-1A**). The addition of exogenous iodoacetamide had not effect of fibrin initiation and accumulation over time (**Figure 7-1B**). A combination of GPRP and iodoacetamide resulted in gross platelet thrombus instability as detected by the sharp changes in platelet

125

fluorescence over time (**Figure 7-1B; red line**). Exogenous GPRP completely inhibited

fibrin generation under flow independent of iodoacetamide consistent with previous studies

under flow (**Figure 7-1B)** [37].
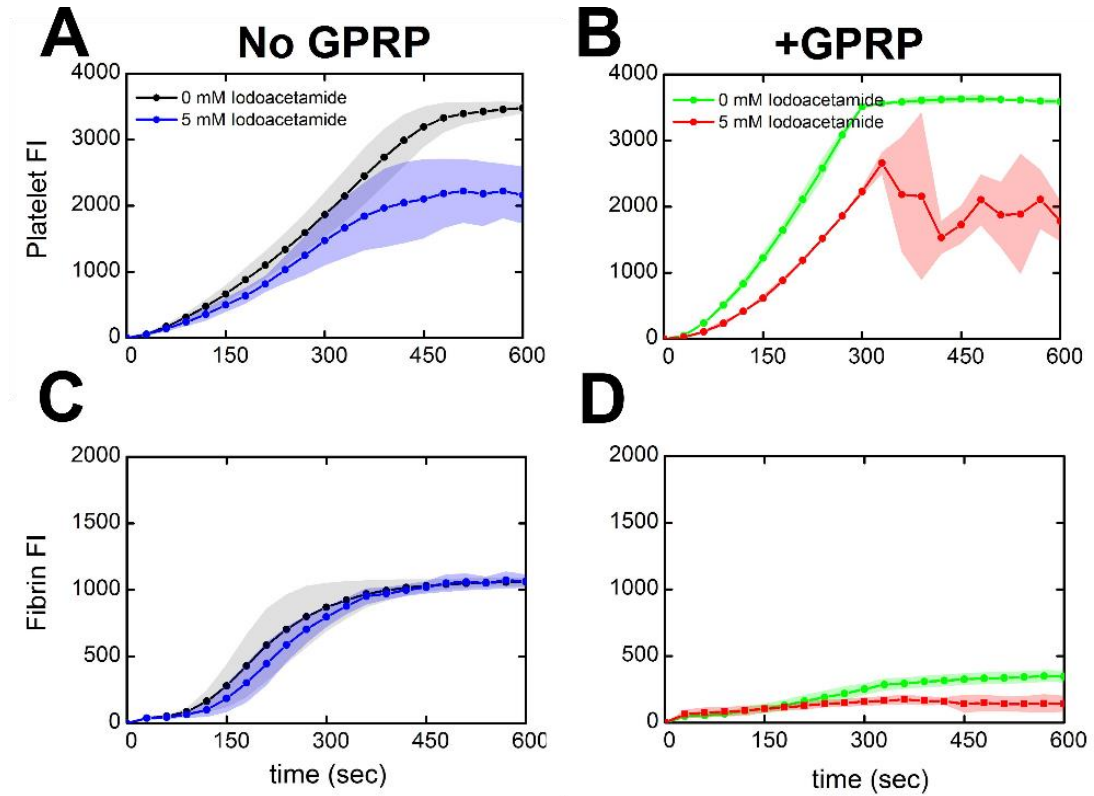
Figure 7-1 Inhibition of FXIIIa in the presence or absence of fibrin polymerization

(±GPRP) on TF/collagen surfaces at 200 s^{-1}.

(A & B), Platelet deposition dynamics measured by platelet fluorescence in the presence or absence of GPRP (5 mM). **(C & D),** Fibrin deposition dynamics measured by fibrin fluorescence in the presence or absence of GPRP (5 mM). Lines with shaded traces and points are mean and standard deviation of 4 clotting events measured in 45 sec intervals over 10 min for one healthy donor.

7.1.4 Discussion

Here we demonstrate for the first time a potential role for FXIIIa stability of platelet rich thrombi under flow in the absence of fibrin. Further work must be done to elucidate the mechanisms by which FXIIIa can stabilize platelet rich clots. It is unclear whether the weakened clot architecture and thrombus disintegration is due to the cellular form of FXIIIa (cFXIIIa) or the plasma-derived form (FXIIIa). More specific FXIIIa inhibitors with micro-molar affinity such as 1,3,4,5-Tetramethyl-2-[(2-oxopropyl)thio]imidazolium chloride (T101) should be tested ex vivo. T101 can be used exogenously in the presence or absence of thrombin inhibitors over collagen or collagen/TF surfaces. Pressure relief conditions can be used to build occlusive clots under flow for a more rigorous test of platelet/fibrin clot strength and stability. To further elucidate the role of cFXIIIa, GR145503 can be used to abate platelet aggregation under flow in order to study platelet GPVI and collagen interactions. Finally, fluorescent amine donor substrates can be used to detect transglutaminase activity under flow to delineate the contributions of FXIIIa activity emanating from platelets or platelet-bound fibrin(ogen).

8 APPENDIX

8.1 Microfluidic ASA Phenotyping Supplemental Material

8.1.1 Supplemental Discussion

8.1.1.1 *Discussion: Statistical significant inhibition*

For those subjects with < 25 % inhibition, the % inhibition was too small to be statistically significant due to the error in the measurement, but not due to the initial platelet deposition size. Statistical significance of inhibition was not correlated with initial platelet deposit size (FI_{300s}) **(Fig. S1)**. The other 12 subjects with ≤ 25 % inhibition displayed statistically significant inhibition as a group (27 % ± 15 %; p < 0.001, n = 12). Eleven of 28 subjects with less than 25 % inhibition following ASA ingestion did not reach statistical significance because of the percent error in the smaller signal, not because their original platelet deposition at t = 0 was low. With more sampling at the 0 μM ex vivo ASA condition (eg. 4 lanes per device), we anticipate that donors with < 25 % inhibition of FI_{300s} following ASA ingestion would be detected with statistical significance. In fact, the microfluidic approach detected only 1 out of 28 donors (donor # 253) that failed to display any decrease at all in platelet deposition after ASA ingestion (Fig. 3A).

8.1.1.2 *Discussion: Timing of primary versus secondary phase of platelet accumulation*

The starting time for the secondary aggregation phase (150 sec) is a phase in which a significant platelet monolayer has already deposited on the collagen surface, thus the majority of the collagen surface has been covered with adherent platelets **(Fig. S2)**. The effect of COX-1 inhibitors added ex vivo to whole blood after 150 sec of platelet deposition on collagen in this microfluidic device is a time-scale consistent with previous findings in Ref. 19 (Flamm et

al., Blood. 2012). Thus, growth in platelet coverage in two dimensions is significant between 60 -150 sec while after 150 sec, thrombus growth in the third dimension becomes significant under flow mediated by soluble agonists such as thromboxane A_2 and ADP in this device.

8.1.1.3 Discussion: R value and future studies

The R-value in Fig. 4 helps to internally normalize each donor (since we cannot normalize to a pooled plasma result, for example). The R-value also has the property of scoring the effect of ASA on platelet deposition with R = 1 representing the cut-off between native blood (R > 1 for almost all donors) and ASA ingestion (R < 1 for most but not all donors). The results in Fig. 4F set the stage to identify individuals (blue points) worthy of future study who derive no functional response to aspirin (possibly due to higher ADP release or ADP sensitivity), despite the expectation of their COX-1 being fully acetylated and thromboxane synthesis being strongly inhibited. Ideally, such a future study would involve both healthy donors and patients with cardiovascular risk.

8.1.1.4 Discussion: Receiver-Operator Curve Analysis

A rigorous approach to assay validation was completed using an objective receiver-operator curve (ROC) approach. Two cases were tested in this approach and are presented as follows.

CASE I: 0 μM ASA (Period 1 and 2) vs. 26-hr ASA ingestion

The R-value is a metric of secondary aggregation that normalizes the late stage platelet deposition rate to early stage deposition rate for each blood sample. Receiver Operator Curve (ROC) analysis was conducted with *JLABROC4v1.0.1* (Dr. J. Eng, Johns Hopkins Univ., available   through   public   domain   software   at

www.rad.jhmi.edu/jeng/javarad/roc/JROCFITi.html based on *LABROC4*, Dr. C. Metz, Univ. Chicago). In comparing 56 measurement of the R-value for subjects not taking ASA (at t = 0 during Period 1 and 2) [true full COX-1 activity] to 28 individual measurements of R-value for subjects taking 325 mg ASA [true full COX-1 inhibition], the receiver-operator curve had an area under curve (ROC AUC) = 0.741, indicative of an adequate, but not outstanding diagnostic discrimination between the two populations **(Fig. S3)**. Interestingly, the assay had high discrimination (high true positive rate with low false positive rate) at an R-value ~ 1 where the true positive fraction TPF was 71 % (sensitivity) and the false positive fraction FPF was 36 % (specificity = 1 – FPF = 64 %).

INPUT DATA

Scores from the 28 actually negative cases:

(True INHIBITION of ASA: t = 26 hr following ASA ingestion)

1.1233	0.6034	0.7836	0.9767	0.7722
0.8585	0.8080	0.7077	1.6151	0.8603
0.9088	0.8099	1.2039	1.3272	0.8068
1.5131	0.7501	0.9849	0.8680	0.7233
0.9317	0.4908	0.8485	0.4195	0.6296
0.8973	0.9438	1.7459		

Scores from the 56 actually positive cases:

(True Full COX1 activity: Period 1 and 2 at t=0; 0 ASA)

0.7416	0.8656	1.1536	1.2645	1.2050
1.1738	0.8545	0.9592	1.3055	1.1071
1.1600	1.2014	1.4020	1.3010	1.5024
0.8560	1.6547	1.0767	1.3708	1.4339
1.4688	0.8096	1.2178	1.0163	1.0863

1.0642   1.1327   1.1241   0.9999   1.0100

1.9264   1.2613   0.3817   1.1537   0.6803

1.0146   1.4208   1.3810   0.9649   1.4063

1.8150   1.2511   1.4529   0.4988   1.1964

1.1595   1.5706   1.2382   1.3985   1.1455

1.4131   1.2984   1.0613   1.3313   0.9103

1.5890

OPERATING POINTS CORRESPONDING TO THE INPUT DATA

FPF:	0.0000	0.0000	0.0357	0.0357	0.0714
TPF:	0.0000	0.0357	0.0357	0.0536	0.0536
FPF:	0.0714	0.1071	0.1071	0.1429	0.1429
TPF:	0.0893	0.0893	0.3036	0.3036	0.4643
FPF:	0.1786	0.1786	0.2143	0.2143	0.2857
TPF:	0.4643	0.6429	0.6429	0.8036	0.8036
FPF:	0.2857	0.3571	0.3571	0.4643	0.4643
TPF:	0.8393	0.8393	0.8571	0.8571	0.8750
FPF:	0.5357	0.5357	0.6071	0.6071	0.7857
TPF:	0.8750	0.9107	0.9107	0.9286	0.9286
FPF:	0.7857	0.8571	0.8571	0.9286	0.9286
TPF:	0.9464	0.9464	0.9643	0.9643	0.9821
PF:	1.0000	1.0000			
TPF:	0.9821	1.0000			

FINAL ESTIMATES OF BINORMAL ROC PARAMETERS A AND B:

A = 0.9531   Std. Error (A) = 0.2659

B = 1.0831   Std. Error (B) = 0.2050

Correlation (A, B) = 0.2561

AREA UNDER ROC CURVE:

Area under fitted curve (Az) = 0.7410

Estimated std. error = 0.0568

Trapezoidal (Wilcoxon) area = 0.7659

Estimated std. error = 0.0514

ESTIMATED BINORMAL ROC CURVE, WITH LOWER AND UPPER BOUNDS

OF THE ASYMMETRIC 95% CONFIDENCE INTERVAL FOR TRUE-POSITIVE

FRACTION AT A VARIETY OF FALSE-POSITIVE FRACTIONS:

FPF	TPF	95% Conf. Interv.
0.005	0.0331	(0.0021, 0.2107)
0.010	0.0586	(0.0060, 0.2676)
0.020	0.1017	(0.0167, 0.3388)
0.030	0.1391	(0.0297, 0.3884)
0.040	0.1727	(0.0442, 0.4276)
0.050	0.2036	(0.0596, 0.4605)
0.060	0.2323	(0.0756, 0.4891)
0.070	0.2593	(0.0921, 0.5145)
0.080	0.2847	(0.1089, 0.5375)
0.090	0.3088	(0.1259, 0.5586)
0.100	0.3317	(0.1429, 0.5781)
0.110	0.3537	(0.1600, 0.5962)
0.120	0.3746	(0.1770, 0.6131)
0.130	0.3948	(0.1940, 0.6291)
0.140	0.4141	(0.2108, 0.6442)
0.150	0.4327	(0.2274, 0.6585)
0.200	0.5166	(0.3078, 0.7209)

0.250 0.5882 (0.3823, 0.7719)

0.300 0.6501 (0.4506, 0.8147)

0.400 0.7515 (0.5692, 0.8818)

0.500 0.8297 (0.6671, 0.9298)

0.600 0.8901 (0.7489, 0.9627)

0.700 0.9358 (0.8187, 0.9834)

0.800 0.9689 (0.8799, 0.9947)

0.900 0.9904 (0.9357, 0.9992)

0.950 0.9969 (0.9636, 0.9999)

ESTIMATED RELATIONSHIP BETWEEN THE CRITICAL TEST RESULT VALUE (WHICH SEPARATES "POSITIVE" RESULTS FROM "NEGATIVE" RESULTS) AND ITS CORRESPONDING OPERATING POINT PROJECTED ONTO THE FITTED BINORMAL ROC CURVE:

CASE (+ = Full COX1, 0 ASA; - = No COX1, 325 ASA)

	Critical test	
CASE	R-VALUE	(FPF, TPF)
+	1.9264	(0.0008, 0.0069)
+	1.8150	(0.0038, 0.0265)
-	1.7459	(0.0071, 0.0443)
+	1.6547	(0.0105, 0.0608)
-	1.6151	(0.0140, 0.0768)
+	1.5890	(0.0176, 0.0922)
+	1.5706	(0.0214, 0.1073)
-	1.5131	(0.0254, 0.1224)
+	1.5024	(0.0294, 0.1370)
+	1.4688	(0.0335, 0.1515)

+	1.4529	(0.0379, 0.1660)
+	1.4339	(0.0424, 0.1804)
+	1.4208	(0.0471, 0.1949)
+	1.4131	(0.0519, 0.2094)
+	1.4063	(0.0570, 0.2239)
+	1.4020	(0.0622, 0.2384)
+	1.3985	(0.0675, 0.2529)
+	1.3810	(0.0731, 0.2673)
+	1.3708	(0.0788, 0.2818)
+	1.3313	(0.0847, 0.2962)
-	1.3272	(0.0907, 0.3106)
+	1.3055	(0.0969, 0.3248)
+	1.3010	(0.1032, 0.3389)
+	1.2984	(0.1096, 0.3529)
+	1.2645	(0.1163, 0.3670)
+	1.2613	(0.1231, 0.3810)
+	1.2511	(0.1301, 0.3951)
+	1.2382	(0.1374, 0.4091)
+	1.2178	(0.1448, 0.4231)
+	1.2050	(0.1524, 0.4371)
-	1.2039	(0.1602, 0.4510)
+	1.2014	(0.1681, 0.4647)
+	1.1964	(0.1762, 0.4784)
+	1.1738	(0.1845, 0.4920)
+	1.1600	(0.1930, 0.5057)
+	1.1595	(0.2018, 0.5193)
+	1.1537	(0.2108, 0.5329)

+	1.1536	(0.2201, 0.5465)
+	1.1455	(0.2296, 0.5602)
+	1.1327	(0.2394, 0.5738)
+	1.1241	(0.2496, 0.5876)
-	1.1233	(0.2601, 0.6012)
+	1.1071	(0.2705, 0.6145)
+	1.0863	(0.2812, 0.6276)
+	1.0767	(0.2923, 0.6409)
+	1.0642	(0.3037, 0.6541)
+	1.0613	(0.3155, 0.6674)
+	1.0163	(0.3277, 0.6807)
+	1.0146	(0.3402, 0.6939)
+	1.0100	(0.3533, 0.7072) ← Optimal Discrimination by R value = 1
+	0.9999	(0.3668, 0.7205) ← (Sensitivity ~ 71 %, Specificity ~ 64 %)
-	0.9849	(0.3808, 0.7339)
-	0.9767	(0.3948, 0.7466)
+	0.9649	(0.4087, 0.7590)
+	0.9592	(0.4231, 0.7713)
-	0.9438	(0.4382, 0.7836)
-	0.9317	(0.4532, 0.7955)
+	0.9103	(0.4683, 0.8070)
-	0.9088	(0.4838, 0.8183)
-	0.8973	(0.4994, 0.8293)
-	0.8680	(0.5150, 0.8399)
+	0.8656	(0.5308, 0.8501)
-	0.8603	(0.5469, 0.8601)
-	0.8585	(0.5632, 0.8698)

+	0.8560	(0.5797, 0.8792)
+	0.8545	(0.5967, 0.8884)
-	0.8485	(0.6144, 0.8976)
-	0.8099	(0.6323, 0.9064)
+	0.8096	(0.6504, 0.9149)
-	0.8080	(0.6691, 0.9232)
-	0.8068	(0.6879, 0.9311)
-	0.7836	(0.7068, 0.9385)
-	0.7722	(0.7258, 0.9455)
-	0.7501	(0.7447, 0.9521)
+	0.7416	(0.7639, 0.9583)
-	0.7233	(0.7840, 0.9644)
-	0.7077	(0.8043, 0.9700)
+	0.6803	(0.8251, 0.9753)
-	0.6296	(0.8472, 0.9804)
-	0.6034	(0.8696, 0.9850)
+	0.4988	(0.8927, 0.9892)
-	0.4908	(0.9186, 0.9931)
-	0.4195	(0.9452, 0.9964)
+	0.3817	(0.9773, 0.9991)

Fitted ROC Area: 0.741

Fitted points

FPF	TPF	Lower	Upper
0.0000	0.0000	0.0000	0.0000
0.0050	0.0331	0.0021	0.2107
0.0100	0.0586	0.0060	0.2676

0.0200	0.1017	0.0167	0.3388
0.0300	0.1391	0.0297	0.3884
0.0400	0.1727	0.0442	0.4276
0.0500	0.2036	0.0596	0.4605
0.0600	0.2323	0.0756	0.4891
0.0700	0.2593	0.0921	0.5145
0.0800	0.2847	0.1089	0.5375
0.0900	0.3088	0.1259	0.5586
0.1000	0.3317	0.1429	0.5781
0.1100	0.3537	0.1600	0.5962
0.1200	0.3746	0.1770	0.6131
0.1300	0.3948	0.1940	0.6291
0.1400	0.4141	0.2108	0.6442
0.1500	0.4327	0.2274	0.6585
0.2000	0.5166	0.3078	0.7209
0.2500	0.5882	0.3823	0.7719
0.3000	0.6501	0.4506	0.8147
0.4000	0.7515	0.5692	0.8818
0.5000	0.8297	0.6671	0.9298
0.6000	0.8901	0.7489	0.9627
0.7000	0.9358	0.8187	0.9834
0.8000	0.9689	0.8799	0.9947
0.9000	0.9904	0.9357	0.9992
0.9500	0.9969	0.9636	0.9999
1.0000	1.0000	1.0000	1.0000

CASE II: 0 µM ASA (Period 1 and 2) VS. 500 µM ASA Ex Vivo

In comparing 56 measurement of the R-value for subjects not taking ASA (at t = 0 during Period 1 and 2) [true full COX-1 activity] to 56 individual measurements of R-value for ex vivo 500 µM ASA addition [true full COX-1 inhibition], the receiver-operator curve had an area under curve (ROC AUC) = 0.783, indicative of a good, but not outstanding diagnostic discrimination between the two populations **(Fig. S3)**. Interestingly, the assay had optimal discrimination (best true positive rate and minimum false positive rate) at an R-value ~ 1 where the true positive fraction TPF was 75 % (sensitivity) and the false positive fraction FPF was 33 % (specificity = 1 – FPF = 67 %).

INPUT DATA

Scores from the 56 actually negative cases:

True Inhibition of COX1 with 500 uM ASA

0.5468	0.7292	0.6258	0.8920	0.8226
0.9299	0.7806	0.7691	1.1218	0.7727
1.1059	0.8476	1.0033	1.0534	0.8654
0.8333	0.8730	0.9148	0.8196	1.2122
1.3131	0.6908	1.1451	0.2065	0.9521
0.8769	1.0290	0.8648	0.9114	1.4386
1.0893	0.8516	0.1217	0.8566	0.6950
0.6501	0.9521	0.8055	1.2264	0.8961
1.6720	0.5441	0.8210	0.4755	0.8776
1.1593	0.7903	0.5619	1.1969	1.1594
0.8804	0.6476	0.8153	0.8193	0.7628
1.3335				

Scores from the 56 actually positive cases:

True Full COX1 activity: Period 1 and 2 at t = 0; 0 ASA

0.7416	0.8656	1.1536	1.2645	1.2050
1.1738	0.8545	0.9592	1.3055	1.1071
1.1600	1.2014	1.4020	1.3010	1.5024
0.8560	1.6547	1.0767	1.3708	1.4339
1.4688	0.8096	1.2178	1.0163	1.0863
1.0642	1.1327	1.1241	0.9999	1.0100
1.9264	1.2613	0.3817	1.1537	0.6803
1.0146	1.4208	1.3810	0.9649	1.4063
1.8150	1.2511	1.4529	0.4988	1.1964
1.1595	1.5706	1.2382	1.3985	1.1455
1.4131	1.2984	1.0613	1.3313	0.9103
1.5890				

OPERATING POINTS CORRESPONDING TO THE INPUT DATA

FPF: 0.0000   0.0000   0.0179   0.0179   0.0357

TPF: 0.0000   0.0357   0.0357   0.1429   0.1429

FPF: 0.0357 0.0536 0.0536 0.0714 0.0714

TPF: 0.2857 0.2857 0.3036 0.3036 0.4286

FPF: 0.0893 0.0893 0.1071 0.1071 0.1250

TPF: 0.4286 0.4464   0.4464   0.4821   0.4821

FPF: 0.1250   0.1607   0.1607   0.1786   0.1786

TPF: 0.5536   0.5536   0.6071   0.6071   0.6429

FPF: 0.1964   0.1964   0.2321   0.2321   0.2679

TPF: 0.6429   0.6607   0.6607   0.7321   0.7321

FPF: 0.2679   0.2857   0.2857   0.3750   0.3750

TPF: 0.7857   0.7857   0.8393   0.8393   0.8571

```
FPF:   0.4821  0.4821  0.5357  0.5357  0.6786

TPF:   0.8571  0.8750  0.8750  0.9107  0.9107

FPF:   0.6786  0.7857  0.7857  0.8393  0.8393

TPF:   0.9286  0.9286  0.9464  0.9464  0.9643

FPF:   0.9464  0.9464  0.9643  0.9643  1.0000

TPF:   0.9643  0.9821  0.9821  1.0000  1.0000
```

FINAL ESTIMATES OF BINORMAL ROC PARAMETERS A AND B:

A = 1.0714   Std. Error (A) = 0.2145

B = 0.9357   Std. Error (B) = 0.1519

Correlation (A, B) = 0.3923

AREA UNDER ROC CURVE:

Area under fitted curve (Az) = 0.7830

Estimated std. error = 0.0423

Trapezoidal (Wilcoxon) area = 0.7943

Estimated std. error = 0.0425

ESTIMATED BINORMAL ROC CURVE, WITH LOWER AND UPPER BOUNDS
OF THE ASYMMETRIC 95% CONFIDENCE INTERVAL FOR TRUE-POSITIVE
FRACTION AT A VARIETY OF FALSE-POSITIVE FRACTIONS:

FPF	TPF	95% Conf. Interv.
0.005	0.0903	(0.0199, 0.2666)
0.010	0.1344	(0.0392, 0.3259)
0.020	0.1975	(0.0747, 0.3976)
0.030	0.2455	(0.1072, 0.4460)

0.040 0.2854 (0.1372, 0.4837)

0.050 0.3199 (0.1653, 0.5148)

0.060 0.3506 (0.1916, 0.5417)

0.070 0.3784 (0.2165, 0.5654)

0.080 0.4038 (0.2401, 0.5867)

0.090 0.4273 (0.2626, 0.6060)

0.100 0.4491 (0.2840, 0.6238)

0.110 0.4696 (0.3044, 0.6403)

0.120 0.4888 (0.3239, 0.6556)

0.130 0.5070 (0.3427, 0.6701)

0.140 0.5242 (0.3607, 0.6836)

0.150 0.5405 (0.3780, 0.6964)

0.200 0.6118 (0.4555, 0.7518)

0.250 0.6703 (0.5209, 0.7964)

0.300 0.7194 (0.5771, 0.8335)

0.400 0.7981 (0.6693, 0.8910)

0.500 0.8580 (0.7425, 0.9321)

0.600 0.9046 (0.8031, 0.9611)

0.700 0.9408 (0.8553, 0.9805)

0.800 0.9685 (0.9017, 0.9924)

0.900 0.9884 (0.9453, 0.9984)

0.950 0.9955 (0.9679, 0.9996)

ESTIMATED RELATIONSHIP BETWEEN THE **CRITICAL TEST RESULT**
VALUE (WHICH SEPARATES "POSITIVE" RESULTS FROM "NEGATIVE"
RESULTS) AND ITS CORRESPONDING OPERATING POINT PROJECTED
ONTO THE FITTED BINORMAL ROC CURVE:

Truth	Critical test result value	(FPF, TPF)
+	1.9264	(0.0001, 0.0077)
+	1.8150	(0.0008, 0.0293)
-	1.6720	(0.0018, 0.0486)
+	1.6547	(0.0028, 0.0647)
+	1.5890	(0.0041, 0.0801)
+	1.5706	(0.0055, 0.0955)
+	1.5024	(0.0071, 0.1110)
+	1.4688	(0.0090, 0.1264)
+	1.4529	(0.0110, 0.1419)
-	1.4386	(0.0132, 0.1571)
+	1.4339	(0.0154, 0.1715)
+	1.4208	(0.0178, 0.1856)
+	1.4131	(0.0204, 0.1998)
+	1.4063	(0.0232, 0.2140)
+	1.4020	(0.0261, 0.2282)
+	1.3985	(0.0293, 0.2424)
+	1.3810	(0.0326, 0.2566)
+	1.3708	(0.0361, 0.2707)
-	1.3335	(0.0398, 0.2847)
+	1.3313	(0.0436, 0.2983)
-	1.3131	(0.0474, 0.3116)

+	1.3055	(0.0514, 0.3246)
+	1.3010	(0.0556, 0.3375)
+	1.2984	(0.0599, 0.3503)
+	1.2645	(0.0643, 0.3631)
+	1.2613	(0.0690, 0.3759)
+	1.2511	(0.0739, 0.3888)
+	1.2382	(0.0790, 0.4015)
-	1.2264	(0.0843, 0.4141)
+	1.2178	(0.0896, 0.4265)
-	1.2122	(0.0951, 0.4387)
+	1.2050	(0.1007, 0.4507)
+	1.2014	(0.1065, 0.4626)
-	1.1969	(0.1124, 0.4743)
+	1.1964	(0.1184, 0.4858)
+	1.1738	(0.1245, 0.4972)
+	1.1600	(0.1309, 0.5086)
+	1.1595	(0.1375, 0.5200)
-	1.1594	(0.1444, 0.5314)
-	1.1593	(0.1512, 0.5424)
+	1.1537	(0.1581, 0.5531)
+	1.1536	(0.1651, 0.5637)
+	1.1455	(0.1725, 0.5745)
-	1.1451	(0.1800, 0.5852)
+	1.1327	(0.1876, 0.5955)
+	1.1241	(0.1954, 0.6058)
-	1.1218	(0.2035, 0.6162)
+	1.1071	(0.2116, 0.6263)

-	1.1059	(0.2199, 0.6363)
-	1.0893	(0.2282, 0.6460)
+	1.0863	(0.2364, 0.6554)
+	1.0767	(0.2449, 0.6647)
+	1.0642	(0.2538, 0.6741)
+	1.0613	(0.2629, 0.6837)
-	1.0534	(0.2724, 0.6932)
-	1.0290	(0.2818, 0.7023)
+	1.0163	(0.2911, 0.7111)
+	1.0146	(0.3007, 0.7199)
+	1.0100	(0.3107, 0.7289)
-	1.0033	(0.3210, 0.7378)
+	0.9999	(0.3313, 0.7464)
+	0.9649	(0.3418, 0.7549)
+	0.9592	(0.3528, 0.7636)
+	0.9521	(0.3697, 0.7765)
-	0.9299	(0.3867, 0.7888)
-	0.9148	(0.3980, 0.7966)
-	0.9114	(0.4092, 0.8042)
+	0.9103	(0.4204, 0.8115)
-	0.8961	(0.4320, 0.8189)
-	0.8920	(0.4437, 0.8261)
-	0.8804	(0.4553, 0.8331)
-	0.8776	(0.4669, 0.8398)
-	0.8769	(0.4785, 0.8464)
-	0.8730	(0.4900, 0.8527)
+	0.8656	(0.5017, 0.8589)

Optimal Discrimination by R value = 1
(Sensitivity ~ 75 %, Specificity ~ 67 %)

-	0.8654	(0.5136, 0.8650)
-	0.8648	(0.5255, 0.8710)
-	0.8566	(0.5375, 0.8769)
+	0.8560	(0.5495, 0.8826)
+	0.8545	(0.5619, 0.8882)
-	0.8516	(0.5744, 0.8938)
-	0.8476	(0.5871, 0.8993)
-	0.8333	(0.5998, 0.9046)
-	0.8226	(0.6125, 0.9097)
-	0.8210	(0.6252, 0.9147)
-	0.8196	(0.6379, 0.9195)
-	0.8193	(0.6506, 0.9242)
-	0.8153	(0.6634, 0.9287)
+	0.8096	(0.6763, 0.9331)
-	0.8055	(0.6893, 0.9374)
-	0.7903	(0.7024, 0.9416)
-	0.7806	(0.7156, 0.9457)
-	0.7727	(0.7288, 0.9496)
-	0.7691	(0.7419, 0.9534)
-	0.7628	(0.7551, 0.9571)
+	0.7416	(0.7684, 0.9606)
-	0.7292	(0.7820, 0.9641)
-	0.6950	(0.7957, 0.9675)
-	0.6908	(0.8094, 0.9707)
+	0.6803	(0.8232, 0.9738)
-	0.6501	(0.8375, 0.9768)
-	0.6476	(0.8519, 0.9798)

-	0.6258	(0.8663, 0.9825)
-	0.5619	(0.8806, 0.9851)
-	0.5468	(0.8950, 0.9876)
-	0.5441	(0.9094, 0.9899)
+	0.4988	(0.9240, 0.9921)
-	0.4755	(0.9394, 0.9942)
+	0.3817	(0.9555, 0.9961)
-	0.2065	(0.9734, 0.9980)
-	0.1217	(0.9930, 0.9996)

FPF	TPF	Lower	Upper
0.0000	0.0000	0.0000	0.0000
0.0050	0.0903	0.0199	0.2666
0.0100	0.1344	0.0392	0.3259
0.0200	0.1975	0.0747	0.3976
0.0300	0.2455	0.1072	0.4460
0.0400	0.2854	0.1372	0.4837
0.0500	0.3199	0.1653	0.5148
0.0600	0.3506	0.1916	0.5417
0.0700	0.3784	0.2165	0.5654
0.0800	0.4038	0.2401	0.5867
0.0900	0.4273	0.2626	0.6060
0.1000	0.4491	0.2840	0.6238
0.1100	0.4696	0.3044	0.6403
0.1200	0.4888	0.3239	0.6556
0.1300	0.5070	0.3427	0.6701
0.1400	0.5242	0.3607	0.6836

0.1500	0.5405	0.3780	0.6964
0.2000	0.6118	0.4555	0.7518
0.2500	0.6703	0.5209	0.7964
0.3000	0.7194	0.5771	0.8335
0.4000	0.7981	0.6693	0.8910
0.5000	0.8580	0.7425	0.9321
0.6000	0.9046	0.8031	0.9611
0.7000	0.9408	0.8553	0.9805
0.8000	0.9685	0.9017	0.9924
0.9000	0.9884	0.9453	0.9984
0.9500	0.9955	0.9679	0.9996
1.0000	1.0000	1.0000	1.0000

8.1.2 Final Platelet Fluorescence (FI$_{300s}$), Platelet Deposition Rates, R-values

Subject ID	FI$_{300s}$ (0 µM ASA) Period 1 0 hr	FI$_{300s}$ (0 µM ASA) Period 2 0 hr	F'$_{(300-150s)}$ (0 µM ASA) Period 1 0 hr	F'$_{(300-150s)}$ (0 µM ASA) Period 2 0 hr	R (0 µM ASA) Period 1 0 hr	R (0 µM ASA) Period 2 0 hr	R (500 µM ASA) Period 1 0 hr	R (500 µM ASA) Period 2 0 hr	R (0 µM ASA) Period 1 26 hr
217	3078	5937	10.00	21.60	0.7416	0.9999	0.5468	0.9114	1.1233
246	4495	4363	13.72	17.79	0.8656	1.0100	0.7292	1.4386	0.6034
272	11079	9864	44.07	47.81	1.1536	1.9264	0.6258	1.0893	0.7836
259	6336	9246	26.72	37.94	1.2645	1.2613	0.8920	0.8516	0.9767
262	8436	12890	35.38	55.55	1.2050	0.3817	0.8226	0.1217	0.7722
225	7541	2648	30.12	24.02	1.1738	1.1537	0.9299	0.8566	0.8585
250	5413	5949	18.30	7.94	0.8545	0.6803	0.7806	0.6950	0.8080
241	10253	2471	36.37	9.58	0.9592	1.0146	0.7691	0.6501	0.7077
283	10178	6100	44.50	27.75	1.3055	1.4208	1.1218	0.9521	1.6151
268	4225	7404	16.40	32.43	1.1071	1.3810	0.7727	0.8055	0.8603
203	2058	1312	8.46	5.06	1.1600	0.9649	1.1059	1.2264	0.9088
248	4111	5946	16.76	26.76	1.2014	1.4063	0.8476	0.8961	0.8099
239	8521	6571	36.17	36.43	1.4020	1.8150	1.0033	1.6720	1.2039

216	3862	4308	16.76	17.80	1.3010	1.2511	1.0534	0.5441	1.3272
226	4686	1977	20.91	8.92	1.5024	1.4529	0.8654	0.8210	0.8068
235	4627	3430	17.27	7.49	0.8560	0.4988	0.8333	0.4755	1.5131
238	3438	3268	17.31	40.92	1.6547	1.1964	0.8730	0.8776	0.7501
240	5172	3616	20.74	14.85	1.0767	1.1595	0.9148	1.1593	0.9849
255	6294	2484	27.70	20.29	1.3708	1.5706	0.8196	0.7903	0.8680
212	3177	6139	14.75	23.87	1.4339	1.2382	1.2122	0.5619	0.7233
231	6148	3207	17.55	14.60	1.4688	1.3985	1.3131	1.1969	0.9317
243	4194	5141	14.43	19.58	0.8096	1.1455	0.6908	1.1594	0.4908
278	2028	5208	8.85	24.08	1.2178	1.4131	1.1451	0.8804	0.8485
293	5477	4994	19.70	20.97	1.0163	1.2984	0.2065	0.6476	0.4195
253	3243	1441	12.87	12.02	1.0863	1.0613	0.9521	0.8153	0.6296
256	12716	16498	47.96	67.36	1.0642	1.3313	0.8769	0.8193	0.8973
277	7539	7548	26.62	25.54	1.1327	0.9103	1.0290	0.7628	0.9438
282	10221	6506	42.15	29.99	1.1241	1.5890	0.8648	1.3335	1.7459
Average	6020	5588	24	25	1.16	1.21	0.88	0.89	0.93
Stdev	2888	5576	24	25	0.22	0.34	0.22	0.32	0.31

Table 6. Microfluidic ASA Phenotyping Quantification Metrics

8.1.3 Total platelet accumulation with no in vitro ASA addition at 0 hr vs. % inhibition

148
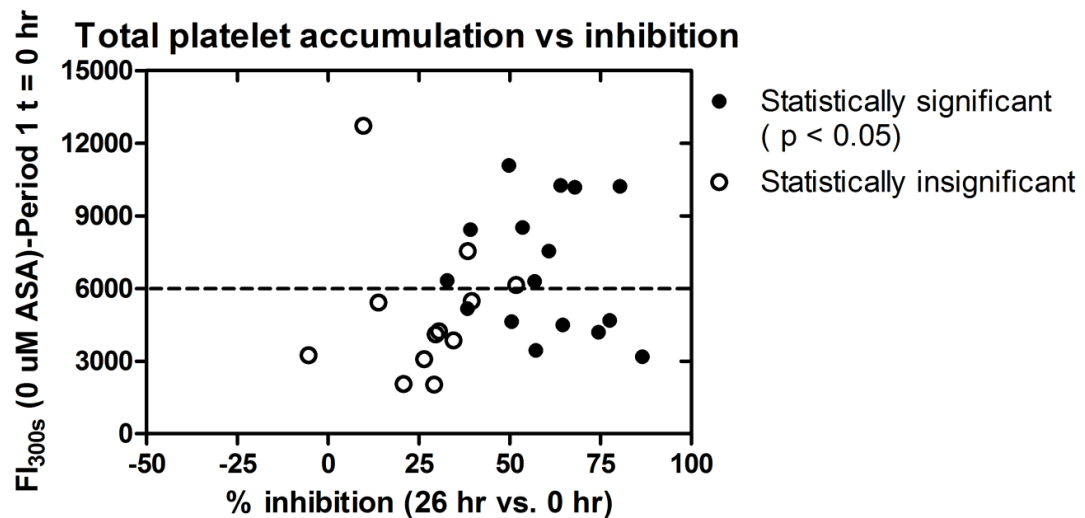
Figure 8-1 Total platelet accumulation with no ex vivo ASA addition at 0 hr vs. % inhibition.

8.1.4   Collagen % surface coverage by platelet with no in vitro addition of agonists in PPACK inhibited whole blood

Platelet Surface Coverage on Collagen
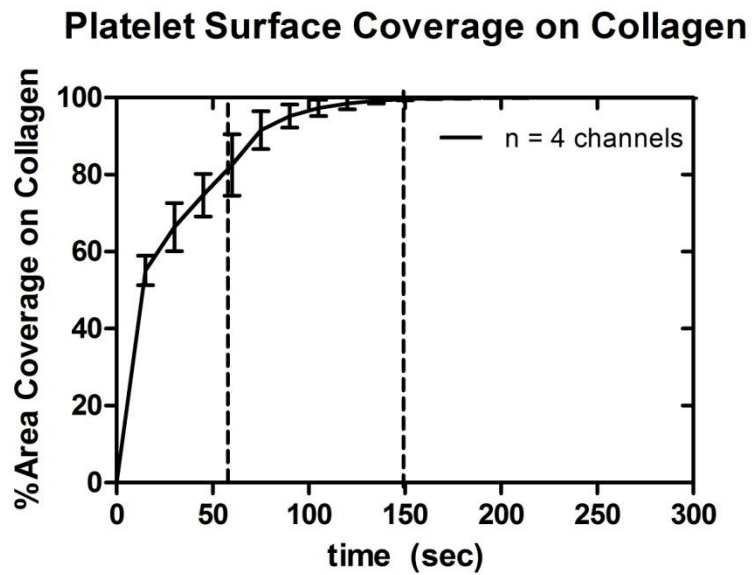
Figure 8-2 % surface coverage by platelets on collagen with no in vitro addition of agonists in PPACK treated whole blood in the 8-channel microfluidic device.

8.1.5   ROC Curve Case I: 0 μM ASA (Period 1 & 2) vs. 26 h ASA ingestion
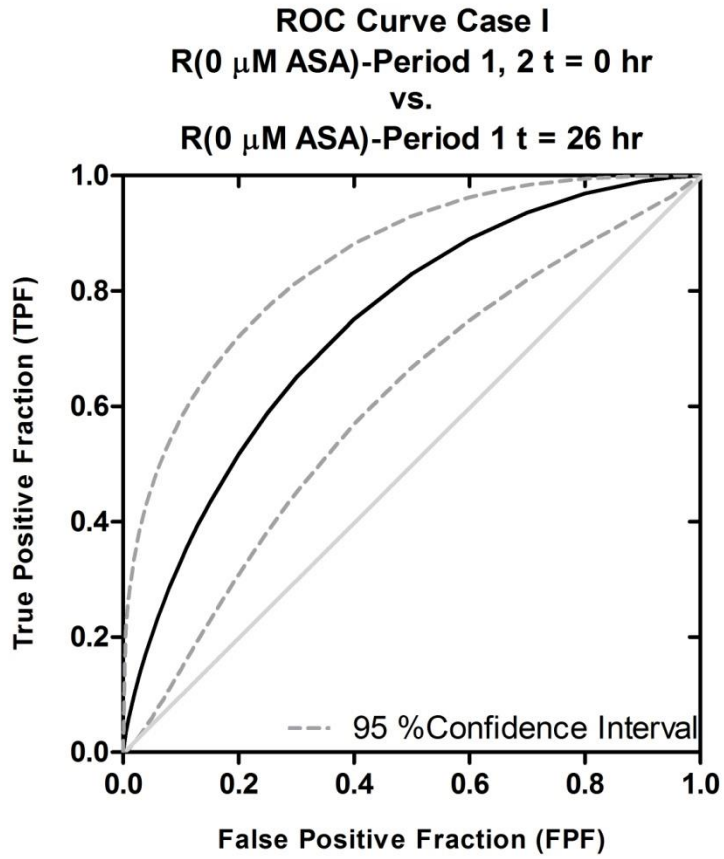
Figure 8-3 ROC Curve Case I: 0 μM *in vitro* ASA (Period 1 and 2) vs. 26 h ASA ingestion
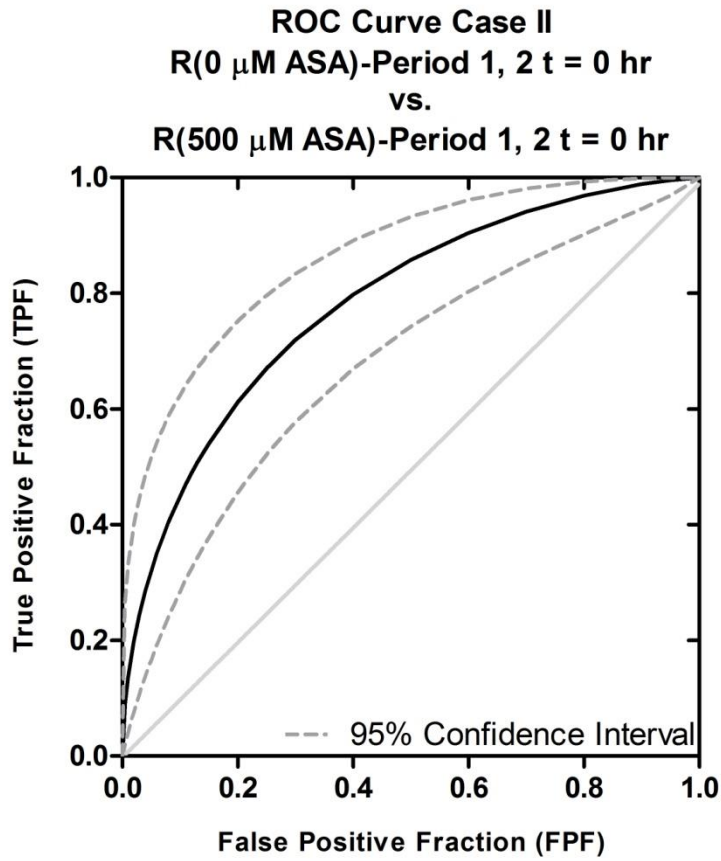
Figure 8-4 ROC Curve Case II: 0 μM in vitro ASA (Period 1 and 2) vs. 500 μM in vitro ASA

8.2 Detection of platelet sensitivity to inhibitors of COX-1, P_2Y_1, and P_2Y_{12} using a whole blood microfluidic assay: Supplemental Material

8.2.1 Supplemental Materials and Methods

8.2.1.1 *Response to ex vivo 2MeSAMP and MRS2179 dosing at venous and arterial shear rates*

For combined venous ($200s^{-1}$) and arterial wall shear rate ($1000s^{-1}$) studies, blood was collected from 5 healthy donors; one donor of the 5 tested was not examined in the primary study of this work. Blood collection, labeling, addition of antagonists, and exclusion criteria for donors for these assays were identical as the main protocol. PPACK treated whole blood was perfused through the device within 40 min of phlebotomy. For dose-response testing of $P2Y_{12}$ and $P2Y_1$ antagonists, 8 distinct concentrations of either antagonist previously incubated with whole blood is perfused through a single 8 channel device with 3 devices tested simultaneously at the same wall shear rate. A custom stage insert holds 3 microfluidic devices, allowing 24 simultaneous platelet aggregation events under flow to be imaged in 15 s intervals. The protocol is repeated with the second wall shear rate. The order of which wall shear rate was tested first was randomized. Final ex vivo concentrations of 2 MeSAMP and MRS 2179 used are as indicated [2 MeSAMP: 0, 0.1, 0.5, 1, 5, 10, 50, 100 μM; MRS 2179: 0, 0.01, 0.05, 0.1, 0.5, 1, 5, 10 μM]. The respective arterial wall shear rate of $1000s^{-1}$ was established in other assays with the same microfluidic device[34,37,64].

8.2.2 Healthy donor phenotyping of platelet function response to P_2Y_1 or P_2Y_{12} antagonists under flow, baseline final platelet fluorescence values

Intradonor variability of $FI_{300s}(0)$: Different Devices									
Donor	Device 1	Device 1	Device 2	Device 2	Device 3	Device 3	Average	SD	CV%
1	1545.77	1311.61	1454.20	1465.33	1462.44	1427.59	1444.49	76.23	5.3%
2	1640.33	2082.70	1452.06	1724.67	1705.70	2142.69	1791.36	267.59	14.9%
3	2014.25	2308.29	2428.46	2477.85	2942.26	2311.79	2413.82	304.88	12.6%
4	5037.89	4563.72	3806.69	4905.00	5745.34	5360.22	4902.77	671.39	13.7%
5	4386.49	4335.76	3090.64	4468.44	5418.45	5067.75	4461.28	798.04	17.9%
6	3711.38	4644.85	2933.58	3587.71	2991.93	3083.38	3261.60	650.42	19.9%
7	5733.93	6521.59	4891.77	3956.05	4928.05	3210.83	4862.83	1188.78	24.4%
8	5733.93	6521.59	4891.77	3956.05	4928.05	3210.83	4873.70	1188.78	24.4%
9	3441.47	2539.59	2246.24	2417.76	2426.44	2420.57	2614.30	431.38	16.5%
10	2357.16	2053.67	2276.70	2366.31	1664.21	2792.64	2251.78	374.66	16.6%
11	13832.1	12883.99	11644.54	10971.13	15391.014	14979.67	13283.74	1778.34	13.4%
Avg	4494.06	4524.30	3737.88	3845.12	4509.46	4182.54	4196.52	702.77	16.3%

Intradonor variability of $FI_{300s}(0)$: Same Device									
Donor	Avg D1	SD D1	CV% D1	Avg D2	SD D2	CV% D2	Avg D3	SD D3	CV% D3
1	1428.69	165.58	11.6%	1459.76	7.87	0.5%	1445.01	24.64	1.7%
2	1861.51	312.81	16.8%	1588.37	192.77	12.1%	1924.20	309.00	16.1%
3	2161.27	207.92	9.6%	2453.15	34.92	1.4%	2627.03	445.81	17.0%
4	4800.80	335.29	7.0%	3806.69	776.62	20.4%	5552.78	272.32	4.9%
5	4361.12	35.88	0.8%	3779.54	974.25	25.8%	5243.18	248.10	4.7%
6	4178.12	660.07	15.8%	3260.65	462.54	14.2%	3037.66	64.66	2.1%
7	6127.76	556.96	9.1%	4423.91	661.65	15.0%	4069.44	1214.26	29.8%
8	6127.76	556.96	9.1%	4423.91	661.65	15.0%	4069.44	1214.26	29.8%
9	2990.53	637.72	21.3%	2332.00	121.28	5.2%	2426.44	4.15	0.2%
10	2205.41	214.60	9.7%	2321.50	63.36	2.7%	2228.43	797.92	35.8%
11	13358.04	670.42	5.0%	11307.84	476.17	4.2%	15185.34	290.87	1.9%
Avg	4509.18	395.84	11.0%	3741.57	403.01	11.0%	4346.27	444.18	13.1%

Table 7. Intradonor variability of platelet fluorescence intensity on collagen [$FI_{300s}(0)$]: same 8-channel device or cross-device coefficient of variability (CV)

153

8.2.3 Healthy donor phenotyping of platelet function response to P_2Y_1 or P_2Y_{12} antagonists under flow: Intradonor R(0) variability

Intradonor variability of R(0): Different Devices								
Donor	Device 1	Device 1	Device 2	Device 2	Device 3	Device 3	Average	SD	CV%
1	0.682	0.814	0.867	0.752	0.725	0.609	0.741	0.092	12.4%
2	1.096	1.269	1.040	1.091	0.983	0.816	1.049	0.149	14.2%
3	1.657	1.522	1.772	1.713	1.800	2.067	1.755	0.182	10.4%
4	2.210	2.540	1.170	1.830	1.805	1.469	1.839	0.493	26.8%
5	1.200	1.141	1.014	1.165	1.396	1.143	1.176	0.125	10.6%
6	1.219	1.335	1.075	0.942	1.086	1.153	1.095	0.135	12.3%
7	1.174	1.153	0.803	0.930	0.802	0.949	1.002	0.163	16.3%
8	1.232	1.127	0.733	0.948	1.193	0.974	1.035	0.187	18.0%
9	0.914	0.911	0.978	1.169	1.167	1.206	1.028	0.138	13.4%
10	0.917	0.882	0.948	0.861	0.745	1.447	0.967	0.245	25.3%
11	1.249	1.074	1.373	1.272	1.083	1.182	1.206	0.116	9.6%
Avg	1.232	1.252	1.070	1.152	1.162	1.183	1.172	0.184	15.4%

Intradonor variability of R(0): Same Device								
Donor	Avg D1	SD D1	CV% D1	Avg D2	SD D2	CV% D2	Avg D3	SD D3	CV% D3
1	0.748	0.094	12.6%	0.809	0.081	10.1%	0.667	0.082	12.2%
2	1.182	0.122	10.3%	1.066	0.036	3.3%	0.900	0.118	13.2%
3	1.590	0.095	6.0%	1.742	0.042	2.4%	1.934	0.189	9.8%
4	2.375	0.233	9.8%	1.170	0.466	39.8%	1.637	0.238	14.5%
5	1.170	0.042	3.6%	1.089	0.107	9.8%	1.270	0.179	14.1%
6	1.277	0.082	6.4%	1.008	0.094	9.3%	1.119	0.047	4.2%
7	1.163	0.015	1.3%	0.866	0.089	10.3%	0.876	0.104	11.9%
8	1.179	0.074	6.3%	0.841	0.152	18.1%	1.084	0.155	14.3%
9	0.912	0.002	0.2%	1.074	0.135	12.6%	1.167	0.027	2.3%
10	0.900	0.025	2.8%	0.905	0.061	6.8%	1.096	0.496	45.2%
11	1.162	0.124	10.7%	1.323	0.071	5.4%	1.133	0.070	6.2%
Avg	1.242	0.083	0.064	1.081	0.121	0.116	1.171	0.155	13.2%

Table 8. Intradonor variability of R(0): same 8-channel device or cross-device coefficient of variability (CV)

8.2.4   Concentration-dependent response of platelet function under flow to ex vivo 2MeSAMP or MRS2179 at initial venous and arterial wall shear rates
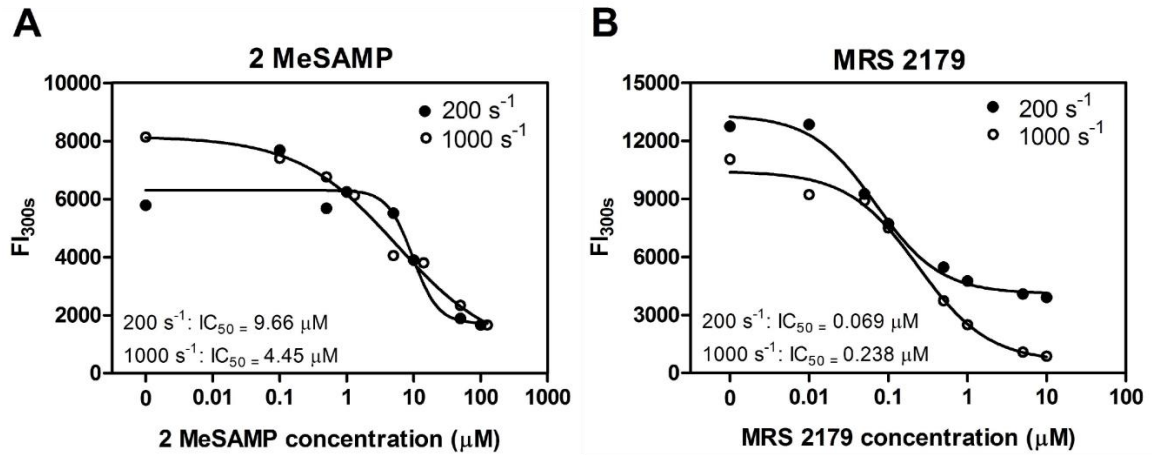
Figure 8-5 Response to ex vivo P2Y12 or P2Y1 inhibition by incubation with 2MeSAMP or MRS2179 respectively at 200 s^{-1} and 1000 s^{-1} initial wall shear rates.

(A, B), Average IC$_{50}$ curves for 2MeSAMP and MRS 2179 at venous and arterial shear rates. Nine microfluidic assays were run at each initial wall shear rate for a total of 3 donors. Each point on the dose response curve is an average of 9 clotting events under flow. 95% CI for ex vivo 2MeSAMP addition were 6.62-14.11 μM and 1.02-30.20 μM at 200 s^{-1} and 1000s^{-1} respectively and 0.029-0.164 μM, 0.03-1.87 μM for MRS 2179 at 200 s^{-1} and 1000s^{-1} respectively.

8.3 Recombinant factor VIIa enhances platelet deposition from flowing hemophilic blood but requires the contact way to promote fibrin deposition: Supplemental Material

8.3.1 Supplemental Material and Methods

8.3.1.1 Validation of the dependency of fibrin generation on the contact pathway in the microfluidic hemostasis model and the role of rFVIIa in a cell free system

To isolate platelet poor plasma (PPP), WB was collected from healthy donors in 1 part sodium citrate from Sigma (St. Louis, MO) to 9 parts blood and 4 μg/ml CTI. Samples were subsequently centrifuged at 1000 g for 10 min. FXI, FIX, and FVIII-deficient plasma samples were purchased from Haematologic Technologies (Essex Junction, VT). Factor-deficient plasma samples were inhibited with 4 μg/ml CTI. Five minutes prior to experimentation, normal pooled plasma (n = 3 donors) or factor-deficient plasma were treated with fluorescently conjugated anti-fibrin antibody, recalcified with 10 mM $CaCl_2$, and indicated concentrations of rFVIIa were added. Two microfluidic devices were tested allowing 16 simultaneous collagen strips to be imaged in 30 sec intervals. Healthy pooled plasma, FXI, FIX, or FVIII-deficient plasma samples were tested in replicate on each 8-channel device. Plasma samples were perfused at an initial local wall shear rate of $100s^{-1}$ for a total perfusion time of 20 minutes.

8.3.1.2 FVIIa Fluorogenic Substrate detection

The fluorogenic FVIIa substrate D-Phe-Pro-Arg-6-amino-1-naphthalenesulfonamide (D-FPR-ANSNH $C_4H_9 \cdot$ 2 HCl) was obtained from Haematologic Technologies (Essex Junction, VT). Prior to experimentation, D-FPR-ANSNH C_4H_9 2*HCl (50 μM) was added

to each well in a 384 well plate (Nunc, Thermo Scientific, Waltham, MA). A fluoroskan

(Fluoroskan Ascent, Thermo Scientific, Waltham, MA) detected the fluorescence of the

released ANSN reporter group. Addition of low or high CTI occurred at 1 min followed by

addition of rFVIIa at 5 min. Each well was read twice per minute for 90 minutes. Fractional

conversion of the fluorogenic substrate was determined according to:

(Equation 8-1)

$$C = \frac{F - F_{min}}{F_{max} - F_{min}}$$

where C is the fractional conversion, F is the instantaneous fluorescence at any time, F_{min} or

F_{max} is the respective minimum or maximum fluorescence for an individual well.

8.3.1.3   *Thrombin Fluorogenic Substrate detection*

The fluorogenic thrombin substrate t-Butyloxycarbonyl-β-benzyl-L-aspartyl-L-prolyl-

L-arginine-4 methylcoumaryl-7-amide [Boc-Asp(OBzl)-Pro-Arg-AMC] was obtained from

Peptide International (Louisville, KY). Lipids, L-α-phosphatidylcholine (PC), L-α-

phosphatidyserine (PS) were purchased from Avanti Polar Lipids (Alabaster, AL). WB was

collected in two syringes containing 1 part sodium citrate to 9 parts blood and either 4

μg/ml or 40 μg/ml CTI. To isolate platelet poor plasma (PPP), WB was centrifuged at 1000

g for 10 min. Citrated and high or low CTI-inhibited PPP was diluted 1:10 in HBS and

recalcified to 10 mM final calcium concentration in all wells. Prior to experimentation all

wells were pre-loaded with indicated concentrations of rFVIIa and 5 μM PC:PS vesicles. To

ensure simultaneous detection of thrombin activity, Boc-Asp(OBzl)-Pro-Arg-AMC (10 μM)

was added simultaneously to all wells with distinct conditions in a 384 well plate and the

157

fluorescence of the released aminomethylcoumarin (AMC) was measured. Each well was read twice per minute for 90 minutes and fractional conversion of the substrate was determined as previously described.

8.3.1.4   Assessment of platelet-rFVIIa function in the microfluidic hemostasis model in the complete absence of thrombin

WB was drawn into 4 μg/ml CTI and either 1 μM FXa inhibitor apixaban (Selleckchem. Houston, TX) or 100 μM H-D-Phe-Pro-Arg-chloromethylketone (Haematologic Technologies. Essex Junction, VT), or a combination of both with low CTI. Blood samples were treated with fluorescently conjugated anti-CD41a antibody and fluorescently conjugated anti-fibrin antibody to label platelets and fibrin respectively as previously mentioned. Blood samples were also treated with vehicle HBS buffer or 4 nM rFVIIa. Two microfluidic devices were tested allowing 16 simultaneous thrombi to be imaged in 60 sec intervals. Conditions were tested at minimum in replicate with 2 different forms of anti-coagulation (ie. Low CTI vs. Low CTI + Apixaban + PPACK) tested on each device. Blood samples were perfused at a local wall shear rate of $100s^{-1}$. The total perfusion time was 15 min for all flow assays. Platelet and fibrin accumulation were analyzed in the same manner as previously mentioned.

8.3.2   Supplemental Discussion

Though potent thrombin inhibitors have been used in study of rFVIIa, the effect of the contact pathway with in vitro flow assays is not often considered[153,154]. Enhancement of fibrin formation under flow conditions by rFVIIa have been shown previously[76,154,155]. However, these studies used heparin or citrate as anticoagulants, not considering contact

pathway-associated thrombin generation as FXII activation is known to occur independently of heparin or plasma calcium. In these prior studies, thrombin was most likely already present prior to perfusion through activation of the contact pathway. Thus rFVIIa mediated fibrin generation could be due to FXIIa in these cases. Interestingly, only a triple cocktail of anticoagulants blocking thrombin with a potent thrombin inhibitor (PPACK), FXa inhibitor (Apixaban), and FXIIa inhibitor (CTI) completely abolished the platelet effects from rFVIIa (**Supplemental Figure S4**). This establishes a requirement for thrombin in order to observe substantial effects from rFVIIa.

In platelet poor plasma (PPP) under static conditions, contact pathway engagement and rFVIIa initiated thrombin faster when compared to strong contact pathway inhibition with high CTI (**Supplemental Figure S5**). Under flow conditions, ex vivo rFVIIa had no effect on fibrin generation from healthy PPP or factor-deficient plasma (**Supplemental Figure S1**). We anticipate that potentiation of rFVIIa function by the contact pathway requires the platelet surface or platelet-derived products. Future studies would involve carefully titrating varying levels of FVIII, FIX, or FXI into hemophillic WB to examine the role of the contact pathway in rFVIIa function.

8.3.3 Fibrin fluorescence at t = 10 min for low CTI-inhibited recalcified healthy pooled plasma, FXI, FIX, or FVIII-deficient plasma ± rFVIIa
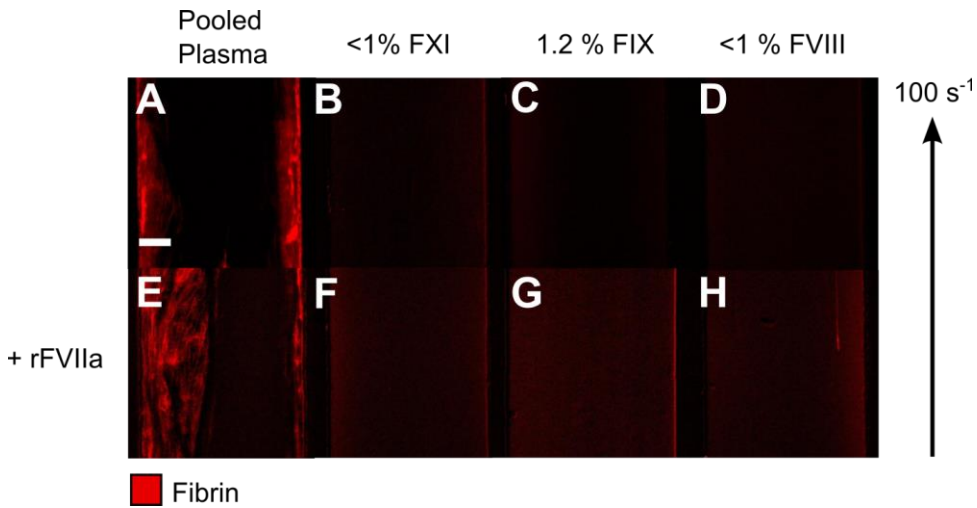
Figure 8-6. Representative images at 10 min of fibrin fluorescence intensity for low CTI-inhibited recalcified healthy pooled plasma, FXI, FIX, or FVIII-deficient plasma ± rFVIIa.

Fibrin initiation and accumulation was observed in the corners of the microfluidic channels in areas of low flow where coagulation factors accumulate for healthy pooled plasma **(A&E)**. In healthy pooled plasma, accumulation of fibrin fibers was independent of rFVIIa. No fibrin fluorescence signal was detected in all factor-deficient plasma samples **(B-D, F-H)** with or without rFVIIa. The scale bar indicates 50 μm.

8.3.4 Detection of CTI interaction with rFVIIa with fluorogenic FVIIa substrate

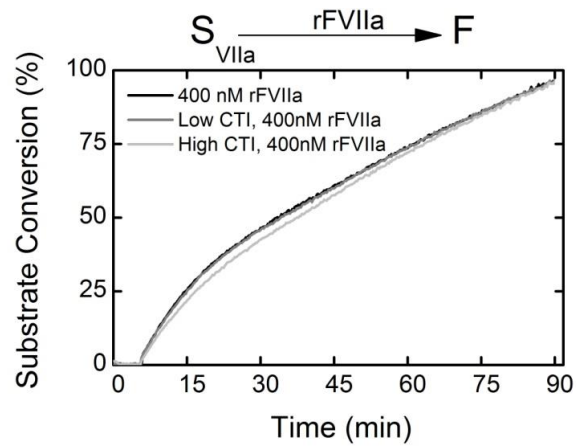**Figure 8-7 Conversion of fluorogenic FVIIa substrate in the absence or presence of low or high CTI with 400 nM rFVIIa**

8.3.5 Effect of exogenous rFVIIa in two additional severely FVIII-deficient patients #57 and #56
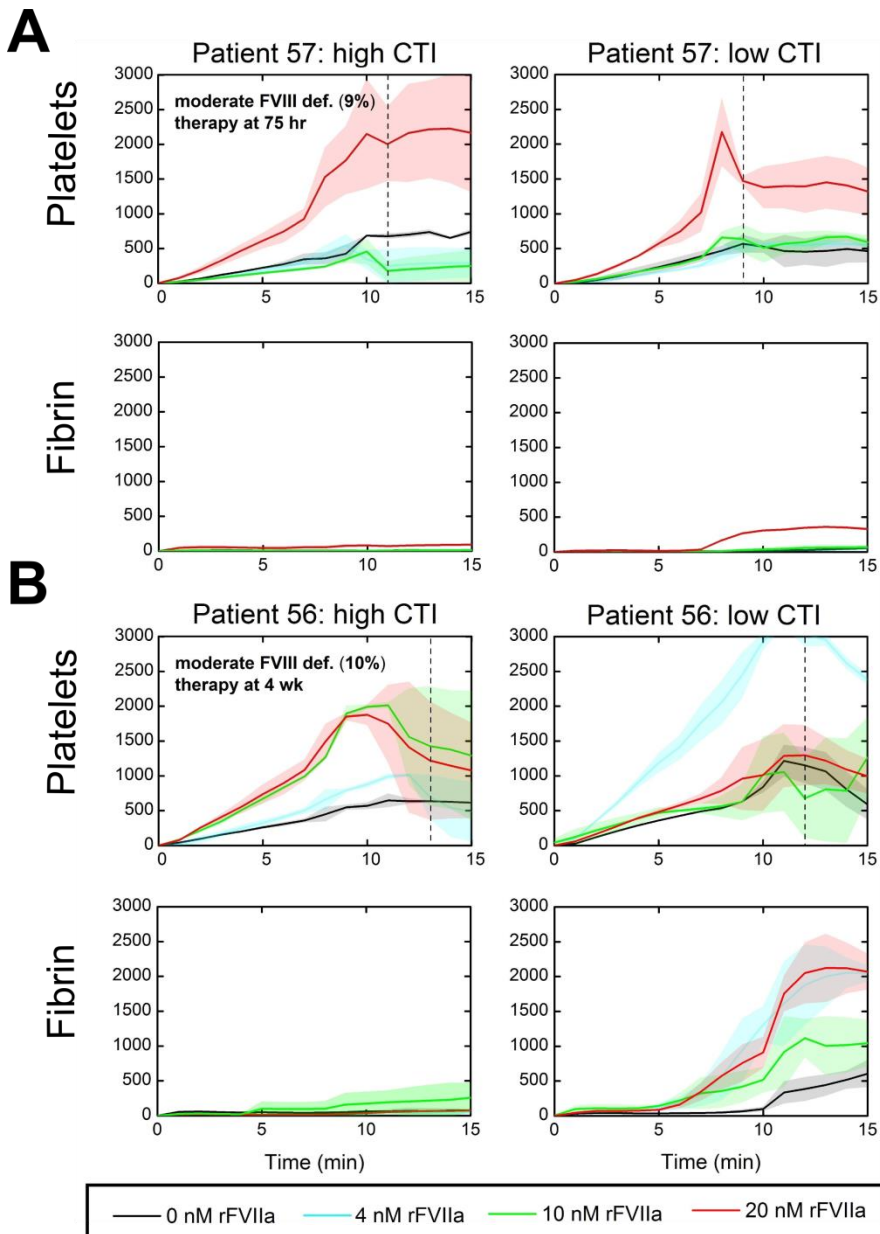
Figure 8-8 Effect of exogenous rFVIIa in severely FVIII-deficient patient #57 and 56 after recovery of critical factor levels to 9 and 10% respectively due to therapy.

(A), Platelet and fibrin fluorescence over time in high or low CTI-inhibited WB for patient #57. **(B)**, Platelet and fibrin fluorescence in high or low CTI-inhibited WB for patient #56. Timing of recent hemostatic therapy is as indicated. Shaded traces are the standard deviation of two clotting events measured in 60 sec intervals over 15 min. Dashed lines indicate full channel occlusion.

8.3.6   Effect of ex vivo rFVIIa to WB under flow with inhibition of the contact pathway, thrombin, and FXa
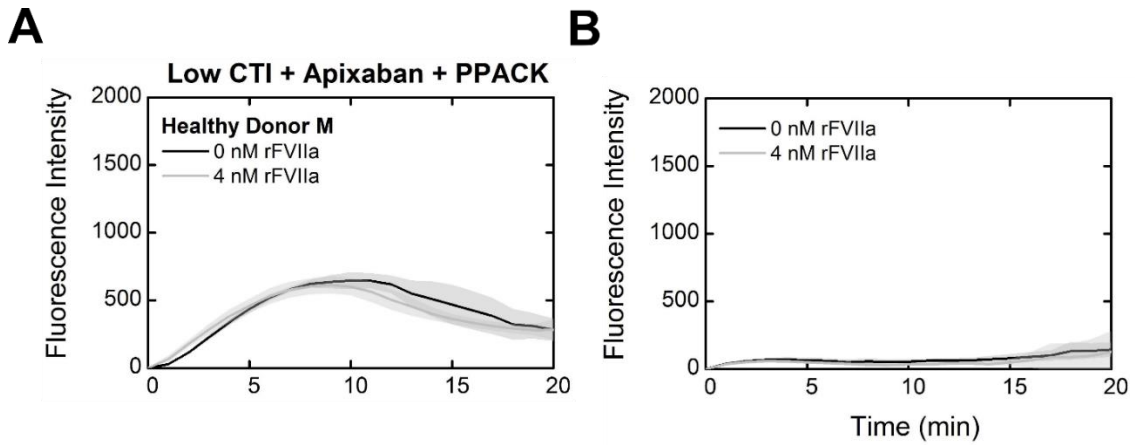
Figure 8-9 Exogenous rFVIIa addition to WB anti-coagulated with low CTI, PPACK and direct FXa inhibitor Apixaban

(A), Platelet fluorescence dynamics with exogenous rFVIIa addition in thrombin-inhibited flow environment.

(B), Fibrin fluorescence dynamics with exogenous rFVIIa addition in thrombin-inhibited flow environment.

Shaded traces are standard deviation of 4 clotting events measured in 30 sec intervals

8.3.7   Detection of contact pathway mediated rFVIIa efficacy using fluorogenic thrombin substrate
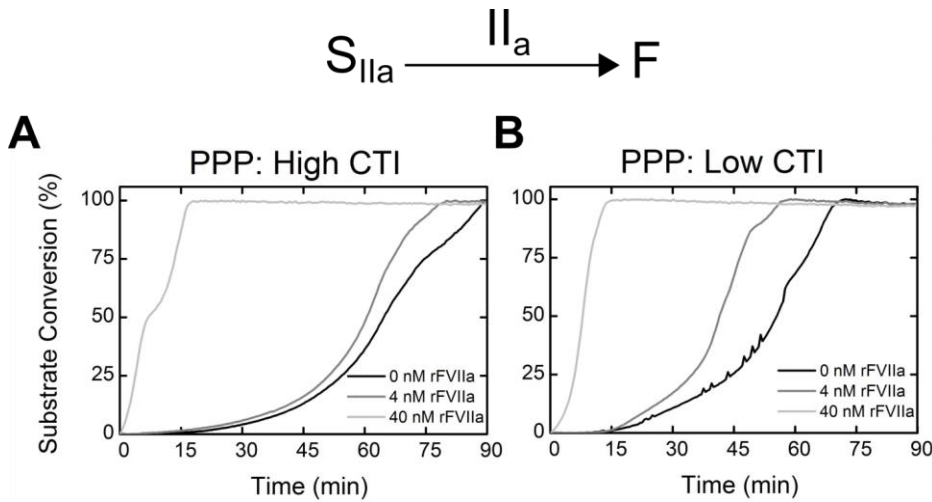
Figure 8-10 Conversion of fluorogenic thrombin substrate in low or high CTI inhibited PPP upon addition of indicated concentrations of rFVIIa

(A), Detection of thrombin activity in recalcified high CTI-inhibited PPP supplemented with rFVIIa and PS:PC vesicles. **(B),** Detection of thrombin activity in recalcified low CTI-inhibited PPP supplemented with rFVIIa and PS:PC vesicles. Traces are average of 4 repeats per condition.

8.4   Ex vivo recapitulation of trauma-induced coagulopathy and preliminary assessment of trauma patient platelet function under flow using microfluidic technology

8.4.1   Supplementary Materials and Methods

8.4.1.1   Blood collection

Whole blood was collected from healthy donors either into 100 μM PPACK or into an empty BD syringe. 1 mL of whole blood from the empty syringe was then aliquoted into

four separate tubes containing 10 µL PPACK at 1, 2, 3, and 4 min after the initial blood draw to mimic phlebotomy blood collection methods in the HUP trauma and resuscitation bay.

8.4.1.2 *Validation by flow cytometry that minor delays in anticoagulation do not affect platelet activation*

All fluorescent antibodies were purchased from BD Biosciences. Each well of a flat-bottom 96 well plate (Corning, Corning, NY, USA) was loaded with 72 µL HBS, 2 µL of Cy5 annexin V, 2 µL PE anti-CD62P, and 4 µL FITC PAC-1. Each row received 10 µL of 1:10 diluted whole blood inhibited at 0, 1, 2, 3, 4 min post-phlebotomy. ADP and collagen (final concentration 50 µM and 100 nM respectively) were selected as agonists to stimulate platelet activation. Ten minutes prior to flow cytometry analysis, 10 µL of a 10X stock of the appropriate agonist or HBS was added, giving a final volume of 100 µL. Accuri C6 flow cytometer with CSampler was used for plate handling. The sample flow rate was set to slow, and samples were analyzed for 1 min following the 10 minute incubation with agonist(s).

8.4.1.3 *Validation of thrombin inhibition by 100 uM PPACK in whole blood anticoagulated up to 4 min after initial phlebotomy*

Fluorogenic thrombin substrate Boc-Val-Pro-Arg-methylcoumarinamide (Boc-VPR-MCA) was obtained from Bachem (King of Prussia, PA). Boc-VPR-MCA diluted in HBS was added to each well in a 384 well plate (Corning). Whole blood anticoagulated with 100 µM PPACK at 0, 1, 2, 3, 4 min post-phlebotomy was diluted in HBS. Diluted whole blood was added simultaneously to each row of substrate to ensure a simultaneous detection of thrombin activity yielding a final concentration of 9 µM Boc-VPR-MCA and 20% whole

blood. A fluoroskan (Fluoroskan Ascent, Thermo Scientific, Waltham, MA) detected the fluorescence of the released aminomethylcoumarin (AMC) reporter group. Each well was read twice per minute for 45 min. Fractional conversion of the fluorogenic substrate was determined according to (Equation 8-1).

8.4.2 Ex vivo protocol to mimic modules of trauma-induced coagulopathy in the 8-channel device under pressure relief flow regimes
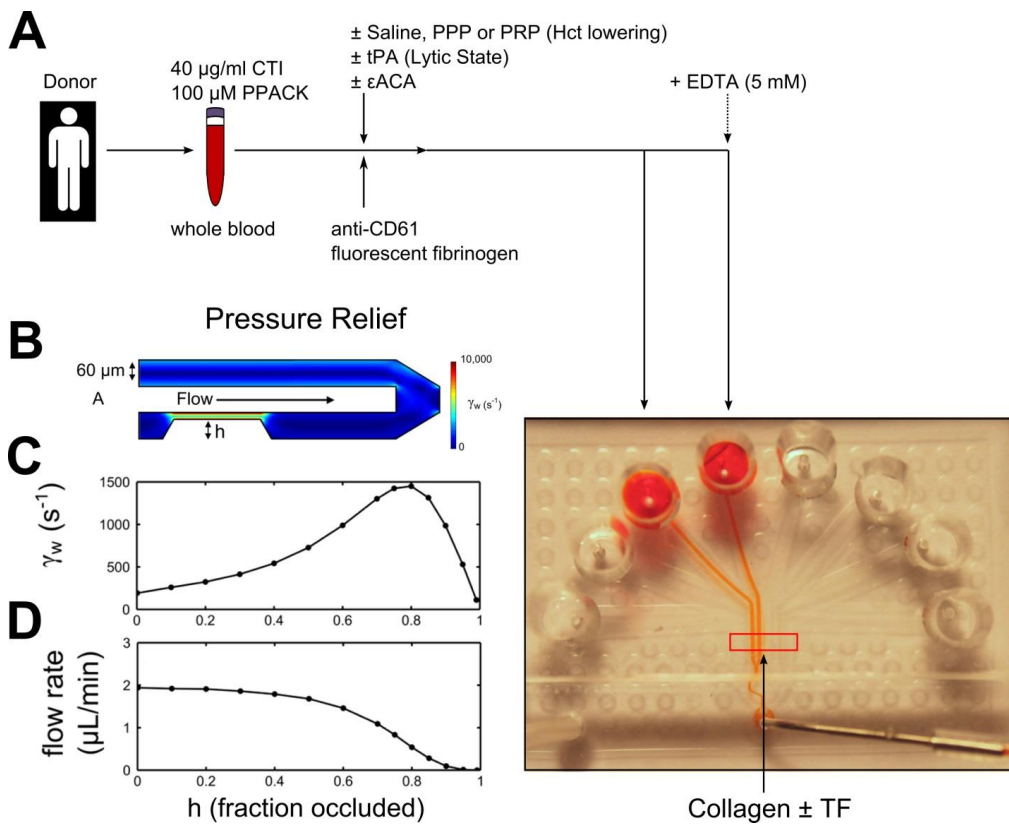
Figure 8-11 Ex vivo protocol to mimic resuscitation-induced hemodilution and hyperfibrinolysis in the 8-channel microfluidic device under pressure relief mode

(A), WB is inhibited with 40 μg/ml CTI or 100 μM PPACK and diluted with saline, PPP or PRP to mimic Hct lowering. To promote a 'lytic state' exogenous tPA (0-50 nM) was added to whole blood. **(B),** Flow through a cross section of a pair of microfluidic channels was previously modeled using COMSOL. The growing clot with variable height was represented by a trapezoidal shape in a single channel[37]. Pressure relief mode was recreated by setting the flow rate at the outlet to 4 μl/min. **(C),** Shear rate calculated at the wall in the center of the model clot[37]. **(D),** Flow rate calculated at the wall in center of the model clot[37].

8.4.3 Platelet accumulation fluorescence dynamics and total platelet accumulation at 900 sec (Healthy subject vs Trauma patient #24: Response to ex vivo MRS2179, GSNO, iloprost)
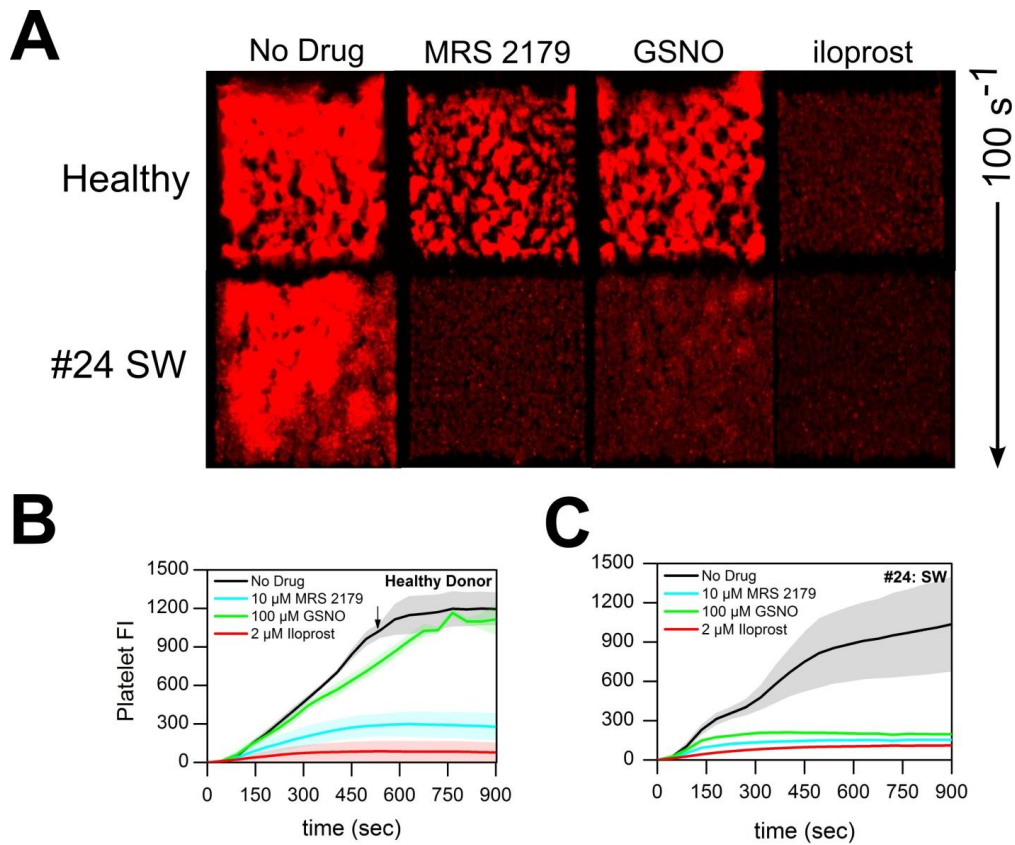
Figure 8-12 Platelet accumulation dynamics measured by platelet fluorescence and total platelet accumulation morphology at 900 sec in representative healthy donor and trauma patient (#24) in response to ex vivo MRS2179, GSNO, or iloprost.

(A), Total platelet accumulation at 900 sec following ex vivo treatment with antagonists MRS2179, GSNO, or iloprost. **(B)**, Platelet fluorescence dynamics in representative healthy donor in the presence of indicated concentrations of ex vivo MRS 2179, GSNO, or iloprost. **(C)**, Platelet fluorescence dynamics in trauma patient (#24) in the presence of indicated concentrations of ex vivo MRS 2179, GSNO, or iloprost. Shaded traces are the mean and standard deviation of 4 clotting events from each healthy donor or patient.

8.4.4 P-selectin expression measured by p-selectin antibody staining and platelet accumulation in representative healthy donor and trauma patient #9.
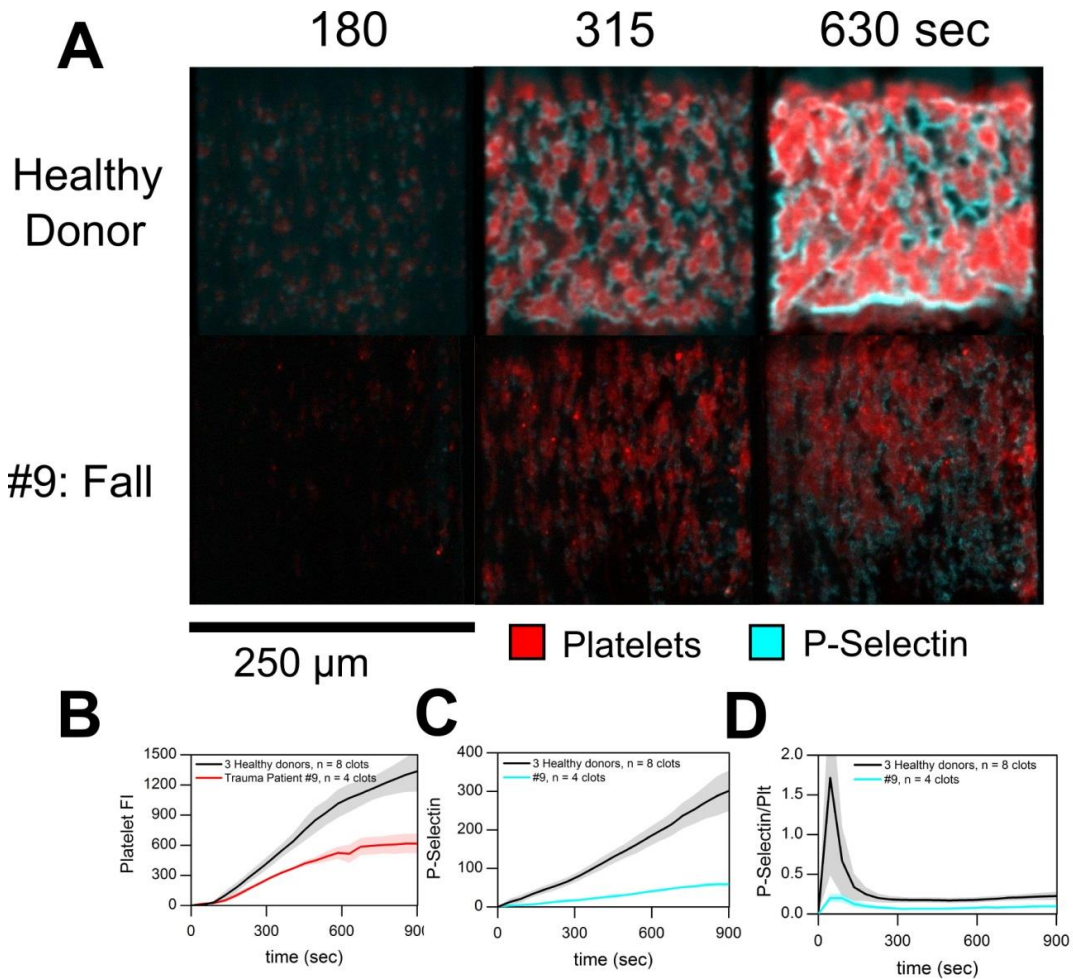
Figure 8-13 Dynamic p-selectin expression and platelet accumulation in representative healthy donor and trauma patient (9).

(A), Overlay of platelet deposition (red) and p-selectin expression (aqua) over the time course of the flow assay. **(B),** Platelet fluorescence and p-selectin expression dynamics over time in three healthy donors in comparison to a trauma patient (#9). Shaded traces are the mean and standard deviation of a minimum of 4 clotting evens from each donor or patient.

8.4.5   Gross thrombus instability due to the lytic state at venous shear rates
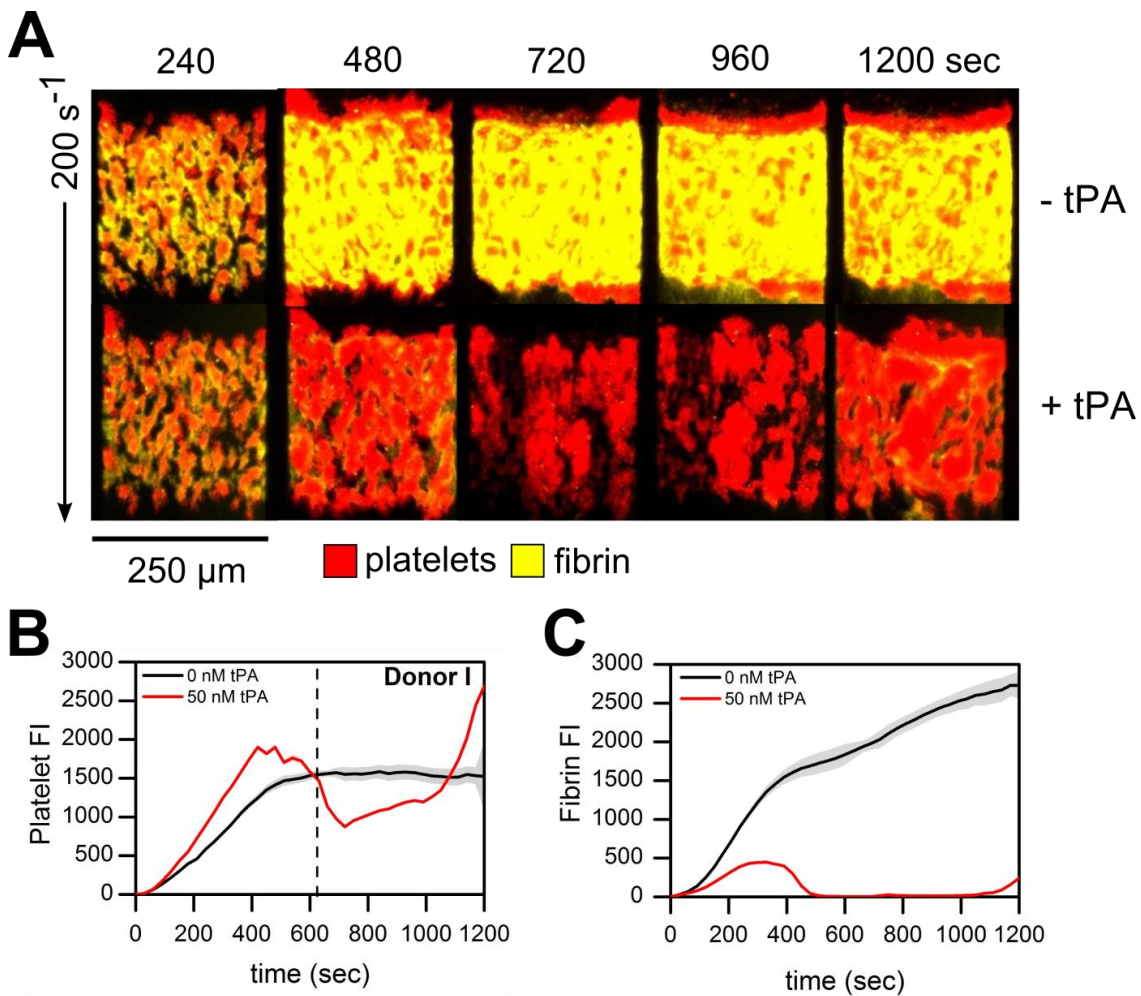
Figure 8-14 Disintegration of platelet aggregates and fibrin accumulation in response to exogenous tPA ± εACA at venous shear rates.

(A), Overlay of platelets (red) and fluorescent fibrinogen (yellow) deposition at 200s^{-1}. (B), Platelet fluorescence intensities vs. time with exogenous tPA ± εACA added. (C), Fibrin fluorescence intensities vs. time with exogenous tPA ± εACA added. Shaded traces are the average and standard deviation of two clotting events.

8.4.6 Gross thrombus instability due to the lytic state at arterial shear rates
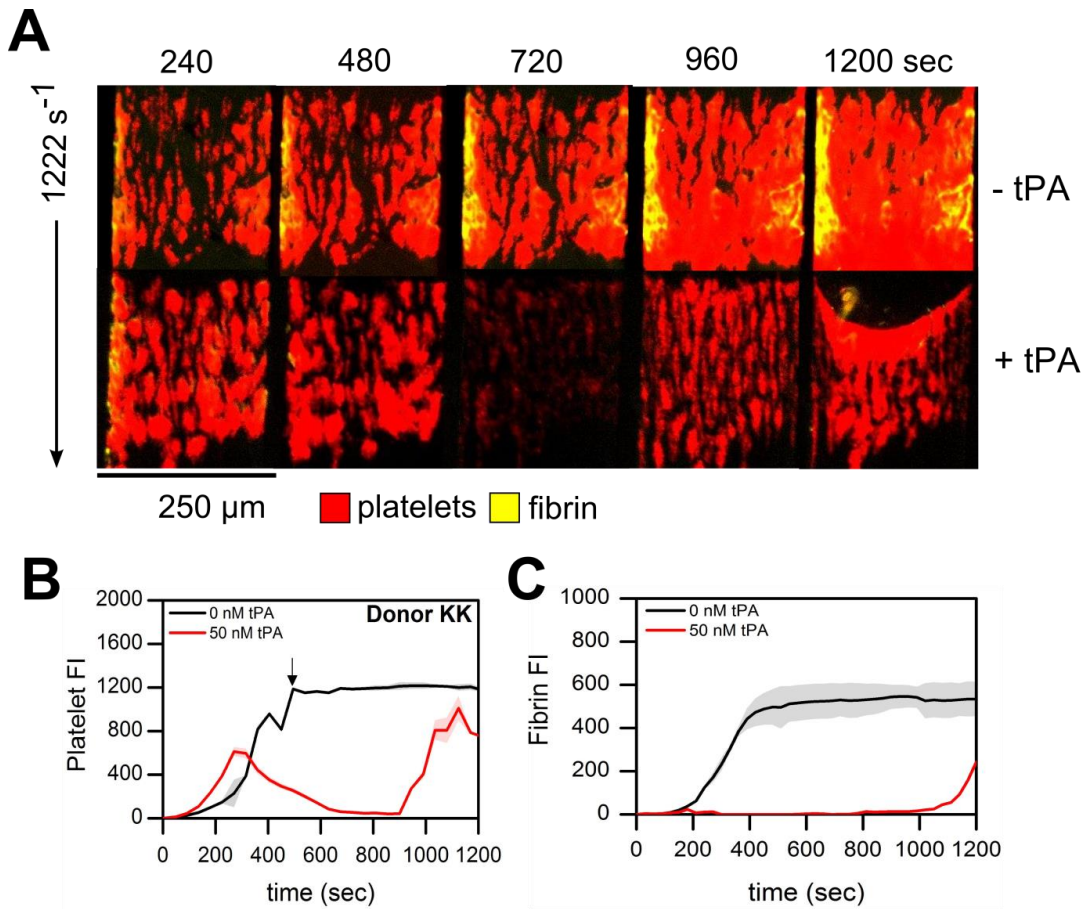
Figure 8-15 Disintegration of platelet aggregates and fibrin accumulation in response to exogenous tPA ± εACA at arterial shear rates

(A), Overlay of platelets (red) and fluorescent fibrinogen (yellow) deposition at 1222 s^{-1} over the time course of the 20 min assay. (**B**), Platelet fluorescence intensities vs. time with exogenous tPA ± εACA added. (**C**), Fibrin fluorescence intensities vs. time with exogenous tPA ± εACA added. Shaded traces are the average and standard deviation of two clotting events.

8.4.7 Detection of platelet desensitization from stimulation of WB anticoagulated with PPACK up to 4 min post phlebotomy with ADP or collagen in flow cytometry
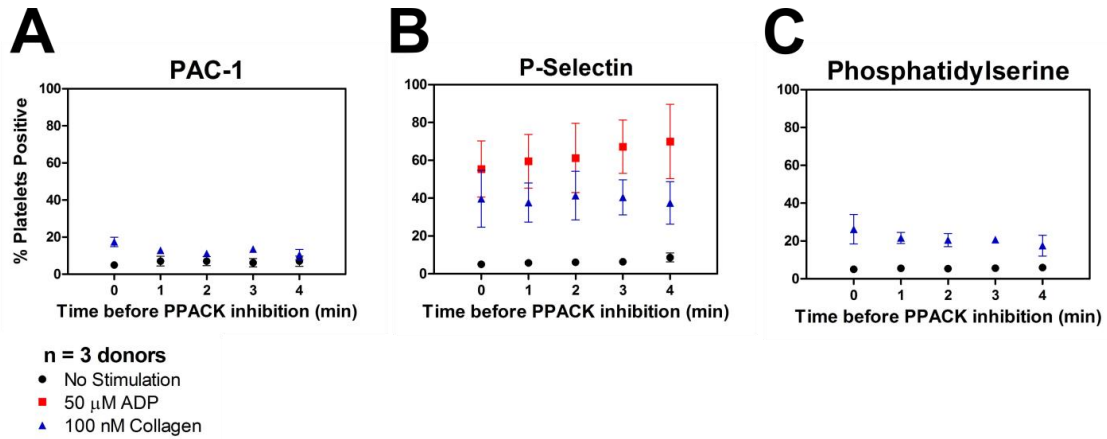
Figure 8-16 Stimulation of whole blood anticoagulated with 100 μM PPACK up to 4 min post-phlebotomy with ADP or collagen in flow cytometry

The percentage of platelets staining positive for PAC-1 expression **(A)**, P-Selectin expression **(B)**, and PS exposure **(C)** upon stimulation with indicated agonists in 1% whole blood samples anticoagulated with 100 μM PPACK at 0, 1, 2, 3, 4 min following initial blood draw. These results indicate that platelets were not significantly activated for up to 3 minutes in the syringe prior to anticoagulation. Markers are the average and standard deviation of 3 measurements from 3 donors.

8.4.8 Detection of thrombin using a fluorogenic thrombin-sensitive substrate in WB anticoagulated with PPACK up to 4 min post phlebotomy
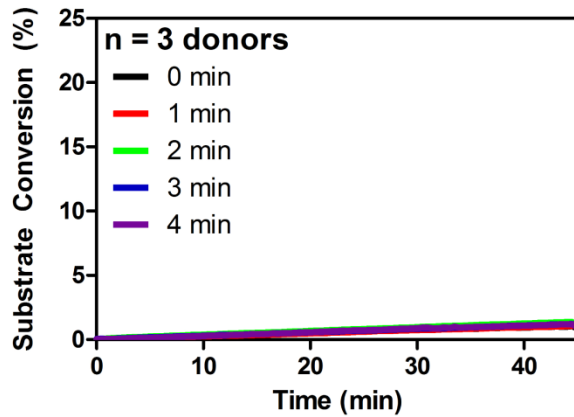
Figure 8-17 Conversion of fluorogenic thrombin-sensitive substrate in whole blood anticoagulated with 100 μM PPACK up to 4 min post-phlembotomy

To evaluate whether 100 μM PPACK fully inhibits thrombin generation post-phlebotomy, the conversion of the thrombin sensitive flurogenic substrate was measured for 45 min. A delay of up to 4 min prior to anticoagulation with PPACK does not illicit thrombin generation. Shaded traces are the average and standard deviation of 12 measurements from 3 donors.

8.4.9   Trauma Patient #36 platelet function under flow at venous shear rates

loss of function

A   #36 Pedestrian Struck

B
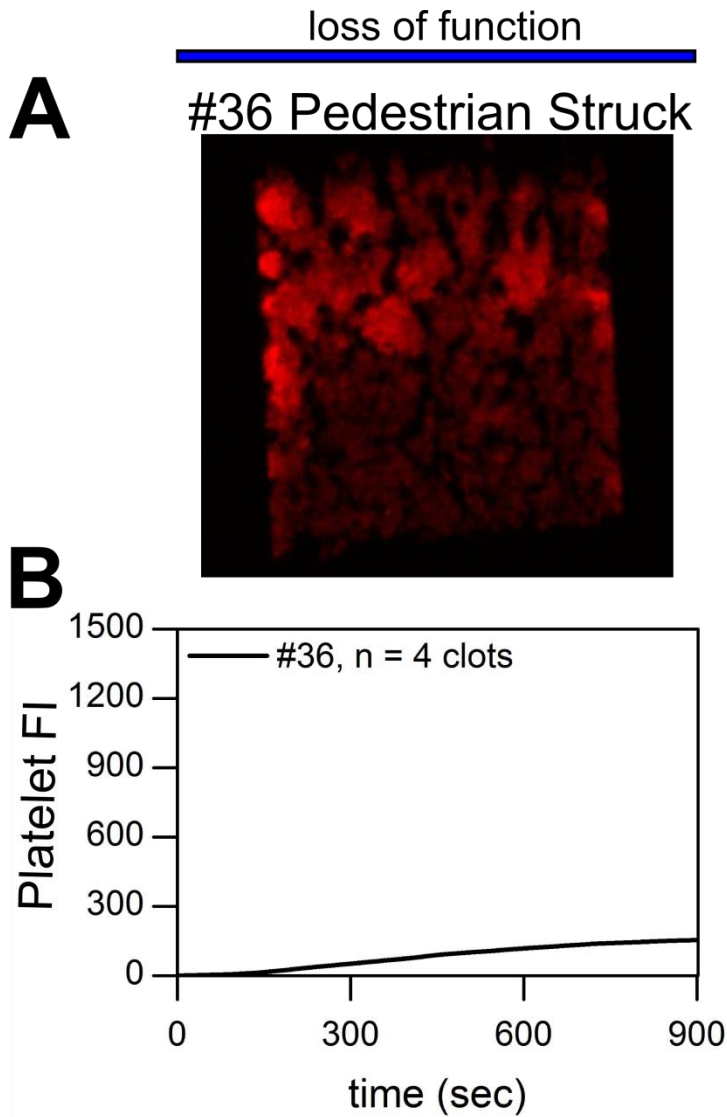
Figure 8-18 Trauma patient #36

(**A**) Total platelet accumulation at 900 sec. (**B**) Platelet deposition dynamics at venous shear rates ($100s^{-1}$).

Shaded trace is the mean and standard deviation of 4 clotting events from patient #36.

8.4.10 Comparison of baseline platelet accumulation on collagen (healthy subjects vs. trauma patients)
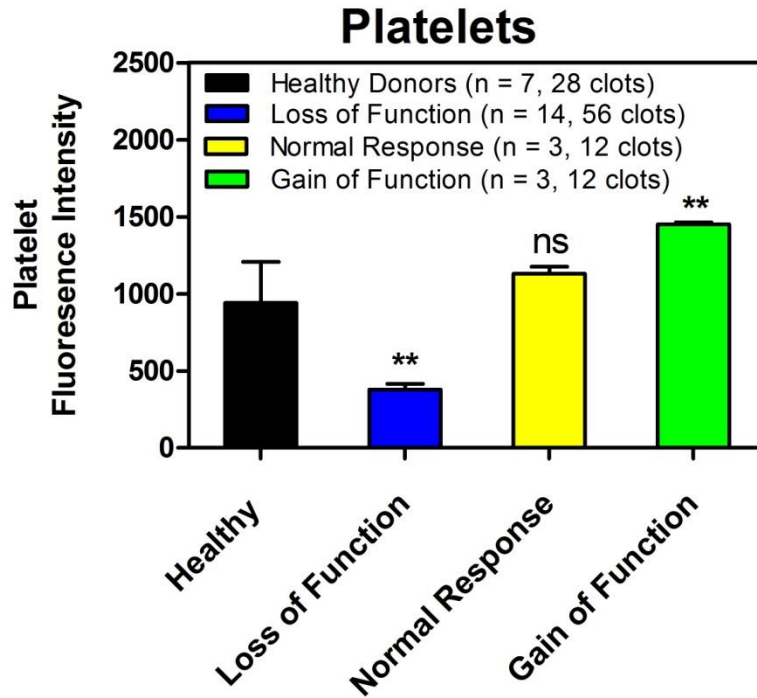
Figure 8-19 Comparison of healthy and trauma patient total platelet accumulation at 900 sec

Bars are average and standard deviation from the indictated number of donors or patients tested (n) at 4 clotting events per donor or patient. **p<0.001

8.4.11 Comparison of response to ex vivo addition of MRS2179, GSNO, or iloprost (healthy subjects vs trauma patients)
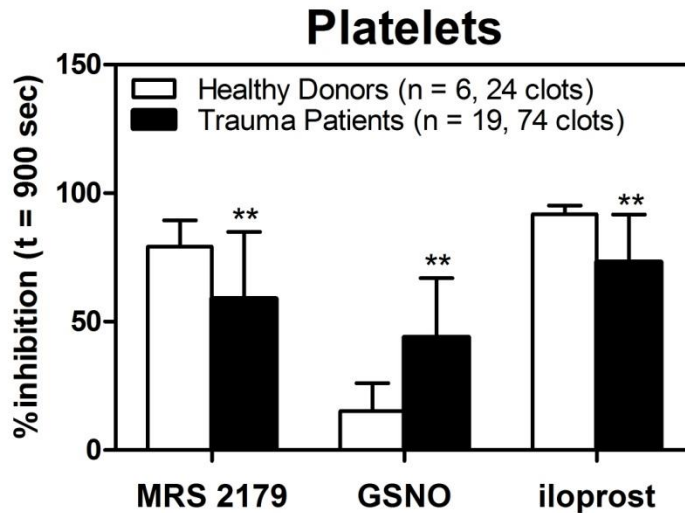
Figure 8-20 Ex vivo addition of GSNO reduced total platelet accumulation more significantly in trauma patients then healthy donors

Trauma patients responded less to ex vivo antagonism with MRS 2179 or iloprost. Bars are average and standard deviation from the indictated number of donors or patients tested (n) at 4 clotting events per donor or patient. **MRS 2179: $p = 0.003$, GSNO: $p < 0.001$, Iloprost: $p < 0.001$

8.4.12 Platelet function measured by platelet fluorescence over time post-admissions for massively transfused patient #31
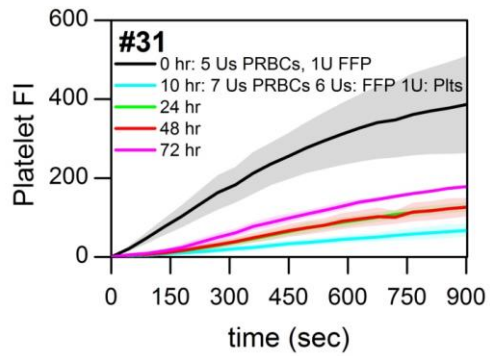
Figure 8-21 Platelet fluorescence vs. time for massively transfused patient #31

Shaded traces are the average and standard deviation of 4 clotting events.

REFERENCES

1   Gaydos L, J Freireich E, Mantel N. The Quantitative Relation Between Platelet Count and Hemorrhage in Patients with Acute Leukemia. *N Engl J Med* **1991;** 266.

2   Brass LF. Thrombin and Platelet Activation. *Chest* **2003;** 124: 18S – 25S.

3   Weisel JW, Litvinov RI. Mechanisms of fibrin polymerization and clinical implications. *Blood* **2013;** 121: 1712–9.

4   Bhatt DL, Topol EJ. Scientific and therapeutic advances in antiplatelet therapy. *Nat Rev Drug Discov* **2003;** 2: 15–28.

5   Chatterjee MS, Purvis JE, Brass LF, Diamond SL. Pairwise agonist scanning predicts cellular signaling responses to combinatorial stimuli. *Nat Biotechnol* Nature Publishing Group; **2010;** 28: 727–32.

6   Geddis AE. Megakaryopoiesis. *Semin Hematol* **2011;** 47: 212–9.

7   Kyrle PA, Eichinger S. Deep vein thrombosis. *Lancet* **2005;** 365: 1163–74.

8   Lippi G, Franchini M, Targher G. Arterial thrombus formation in cardiovascular disease. *Nat Rev Cardiol* Nature Publishing Group; **2011;** 8: 502–12.

9   Aleman MM, Byrnes JR, Wang JG, Tran R, Lam W a., Paola J Di, Mackman N, Degen JL, Flick MJ, Wolberg AS. Factor XIII activity mediates red blood cell retention in venous thrombi. *J Clin Invest* **2014;** 124: 3590–600.

10   Savage B, Almus-Jacobs F, Ruggeri ZM. Specific Synergy of Multiple Substrate–Receptor Interactions in Platelet Thrombus Formation under Flow. *Cell* **1998;** 94: 657–66.

11   Brass LF, Stalker TJ. Platelets. 3rd ed. New York: Cambridge University Press; **2007.**

12   Shattil SJ, Newman PJ. Integrins: dynamic scaffolds for adhesion and signaling in platelets. *Blood* **2004;** 104: 1606–15.

13   Muthard RW, Diamond SL. Blood clots are rapidly assembled hemodynamic sensors: flow arrest triggers intraluminal thrombus contraction. *Arterioscler Thromb Vasc Biol* **2012;** 32: 2938–45.

14   Lam WA, Chaudhuri O, Crow A, Webster KD, Li T-D, Kita A, Huang J, Fletcher DA. Mechanics and contraction dynamics of single platelets and implications for clot stiffening. *Nat Mater* Nature Publishing Group; **2011;** 10: 61–6.

15   Clark SR, Thomas CP, Hammond VJ, Aldrovandi M, Wilkinson GW, Hart KW, Murphy RC, Collins PW, O'Donnell VB. Characterization of platelet aminophospholipid externalization reveals fatty acids as molecular determinants that regulate coagulation. *Proc Natl Acad Sci U S A* **2013;** 110: 5875–80.

16   Lentz BR. Exposure of platelet membrane phosphatidylserine regulates blood coagulation. *Prog Lipid Res* **2003;** 42: 423–38.

17   Denny WS. Simulated and experimental coagulation of human blood. *Univeristy Pennsylvania ProQuest Diss* **2007;** : 1–149.

18   Mann KG, Nesheim ME, Church WR, Haley P KS. Surface-dependent reactions of the vitamin K-dependent enzyme complexes. *Blood* **1990;** 76: 1–16.

19   Bach J, Endler G, Winkelmann BR, Boehm BO, Maerz W, Mannhalter C, Hellstern P. Coagulation factor XII (FXII) activity, activated FXII, distribution of FXII C46T gene

polymorphism and coronary risk. *J Thromb Haemost* **2008;** 6: 291–6.

20   Renné T, Pozgajová M, Grüner S, Schuh K, Pauer H-U, Burfeind P, Gailani D, Nieswandt B. Defective thrombus formation in mice lacking coagulation factor XII. *J Exp Med* **2005;** 202: 271–81.

21   Litvinov RI, Gorkun O V, Owen SF, Shuman H, Weisel JW. Polymerization of fibrin: specificity, strength, and stability of knob-hole interactions studied at the single-molecule level. *Blood* **2005;** 106: 2944–51.

22   Kalb ML, Potura L, Scharbert G, Kozek-Langenecker SA. The effect of ex vivo anticoagulants on whole blood platelet aggregation. *Platelets* **2009;** 20: 7–11.

23   Colace T, Fogarty PF, Panckeri KA, Li R, Diamond SL. Microfluidic assay of hemophilic blood clotting: Distinct deficits in platelet and fibrin deposition at low factor levels. *J Thromb Haemost* **2014;** 12: 147–58.

24   Li R, Panckeri K, Fogarty P, Diamond S. Recombinant factor VIIa enhances platelet deposition from flowing haemophilic blood but requires the contact pathway to promote fibrin deposition. *Haemophilia* **2015;** 21: 266–74.

25   White-Adams T, Berny M, Patel I, Tucker E, Gailani D, Gruber A, McCarty O. Laminin promotes coagulation and thrombus formation in a factor XII-dependent manner. *J Thromb Haemost* **2010;** 8: 1295–301.

26   Campos I, Guimarães BG, Medrano F, Tanaka A, Barbosa J. Crystallization, data collection and phasing of infestin 4, a factor XIIa inhibitor. *Acta Crystallogr D Biol Crystallogr* **2004;** 60: 2051–3.

27   Campos I, Tanaka-Azevedo A, Tanaka A. Identification and characterization of a novel factor XIIa inhibitor in the hematophagous insect, Triatoma infestans (Hemiptera: Reduviidae). *FEBS Lett* **2004;** 577: 512–6.

28   Navaneetham D, Sinha D, Walsh PN. Mechanisms and specificity of factor XIa and trypsin inhibition by protease nexin 2 and basic pancreatic trypsin inhibitor. *J Biochem* **2010;** 148: 467–79.

29   Lee MY, Diamond SL. A Human Platelet Calcium Calculator Trained by Pairwise Agonist Scanning. *PLOS Comput Biol* **2015;** 11: e1004118.

30   Barr JD, Chauhan AK, Schaeffer G V, Hansen JK, Motto DG. Red blood cells mediate the onset of thrombosis in the ferric chloride murine model. *Blood* **2013;** 121: 3733–41.

31   Ciciliano JC, Sakurai Y, Myers DR, Fay ME, Hechler B, Meeks S, Li R, Dixon JB, Lyon LA, Gachet C, Lam WA. Resolving the multifaceted mechanisms of the ferric chloride thrombosis model using an interdisciplinary microfluidic approach. **2015;** 126: 817–25.

32   Duffy DC, McDonald JC, Schueller OJ, Whitesides GM. Rapid Prototyping of Microfluidic Systems in Poly(dimethylsiloxane). *Anal Chem* **1998;** 70: 4974–84.

33   Neeves KB, Maloney SF, Fong KP, Schmaier A, Kahn ML, Brass LF, Diamond SL. Microfluidic focal thrombosis model for measuring murine platelet deposition and stability: PAR4 signaling enhances shear-resistance of platelet aggregates. *J Thromb Haemost* **2008;** 6: 2193–201.

34   Maloney SF, Brass LF, Diamond SL. P2Y12 or P2Y1 inhibitors reduce platelet deposition in a microfluidic model of thrombosis while apyrase lacks efficacy under flow conditions. *Integr*

Biol (Camb) **2010;** 2: 183–92.

35   Colace TV, Jobson J, Diamond SL. Relipidated tissue factor linked to collagen surfaces potentiates platelet adhesion and fibrin formation in a microfluidic model of vessel injury. *Bioconjug Chem* **2011;** 22: 2104–9.

36   Smith S, Morrissey JH. Rapid and efficient incorporation of tissue factor into liposomes. *J Thromb Haemost* **2004;** 2: 1155–62.

37   Colace TV, Muthard RW, Diamond SL. Thrombus growth and embolism on tissue factor-bearing collagen surfaces under flow: role of thrombin with and without fibrin. *Arterioscler Thromb Vasc Biol* **2012;** 32: 1466–76.

38   Patrono C, Coller B, FitzGerald GA, Hirsh J, Roth G. Platelet-active drugs: The relationships among dose, effectiveness, and side effects. *Chest* **2004;** 126: 243S – 264S.

39   Vane J, Botting R. The mechanism of action of aspirin. *Thromb Res* **2003;** 110: 255–8.

40   Campbell CL, Smyth S, Montalescot G, Steinhubl S. Aspirin Dose for the Prevention of Cardiovascular Disease: A Systematic Review. *JAMA* **2007;** 297: 2018–24.

41   Michelson AD, Frelinger A, Furman M. Resistance to antiplatelet drugs. *Eur Hear J Suppl* **2006;** 8: G53–8.

42   Fries S, Grosser T. The cardiovascular pharmacology of COX-2 inhibition. *Hematology Am Soc Hematol Educ Program* **2005;** : 445–51.

43   Grosser T, Yu Y, Fitzgerald GA. Emotion recollected in tranquility: lessons learned from the COX-2 saga. *Annu Rev Med* **2010;** 61: 17–33.

44   Michelson AD. Platelet function testing in cardiovascular diseases. *Circulation* **2004;** 110: e489–93.

45   Michelson A, Cattaneo M, Eikelboom J, Gurbel P. Aspirin resistance: position paper of the Working Group on Aspirin Resistance. *Haemostasis* **2005;** 3: 1309–11.

46   Bhatt DL. Aspirin resistance: more than just a laboratory curiosity. *J Am Coll Cardiol* **2004;** 43: 1127–9.

47   Cattaneo M. Aspirin and clopidogrel: efficacy, safety, and the issue of drug resistance. *Arterioscler Thromb Vasc Biol* **2004;** 24: 1980–7.

48   Cuisset T, Frere C, Quilici J, Gaborit B, Bali L, Poyet R, Faille D, Morange PE, Alessi M-C, Bonnet J-L. Aspirin noncompliance is the major cause of "aspirin resistance" in patients undergoing coronary stenting. *Am Heart J* **2009;** 157: 889–93.

49   Hirata T, Kakizuka A, Ushikubi F, Fuse I, Okuma M, Narumiya S. Arg 60 to leu mutation of the human thromboxane A2 receptor in a dominantly inherited bleeding disorder. *J Clin Invest* **1994;** 94: 1662–7.

50   Reny J-L, Berdagué P, Poncet A, Barazer I, Nolli S, Fabbro-Peray P, Schved J-F, Bounameaux H, Mach F, de Moerloose P, Fontana P. Antiplatelet drug response status does not predict recurrent ischemic events in stable cardiovascular patients: results of the Antiplatelet Drug Resistances and Ischemic Events study. *Circulation* **2012;** 125: 3201–10.

51   Frelinger AL, Li Y, Linden MD, Barnard MR, Fox ML, Christie DJ, Furman MI, Michelson AD. Association of cyclooxygenase-1-dependent and -independent platelet function assays with adverse clinical outcomes in aspirin-treated patients presenting for cardiac catheterization. *Circulation* **2009;** 120: 2586–96.

52   Flamm MH, Colace TV, Chatterjee MS, Jing H, Zhou S, Jaeger D, Brass LF, Sinno T, Diamond SL. Multiscale prediction of patient-specific platelet function under flow. *Blood* **2012;** 120: 190–8.

53   Neeves KB, Onasoga AA, Wufsus AR. The use of microfluidics in hemostasis: clinical diagnostics and biomimetic models of vascular injury. *Curr Opin Hematol* **2013;** 20: 417–23.

54   Cryer B, M F. Cyclooxygenase-1 and cyclooxygenase-2 selectivity of widely used anti-inflammatory drugs. *Am J Med* **1998;** 9343: 413–21.

55   Rinder CS, Student LA, Bonan JL, Rinder HM, Smith BR. Aspirin does not inhibit adenosine diphosphate-induced platelet alpha- granule release. *Blood* **1993;** 82: 505–12.

56   Lordkipanidzé M, Pharand C, Schampaert E, Turgeon J, Palisaitis D a, Diodati JG. A comparison of six major platelet function tests to determine the prevalence of aspirin resistance in patients with stable coronary artery disease. *Eur Heart J* **2007;** 28: 1702–8.

57   Hankey GJ, Eikelboom JW. Aspirin resistance. *Lancet* **2006;** 367: 606–17.

58   Stephens G, He M, Wong C, Jurek M, Luedemann H-C, Shapurian G, Munnelly K, Muir C, Conley PB, Phillips DR, Andre P. Development of a perfusion chamber assay to study in real time the kinetics of thrombosis and the antithrombotic characteristics of antiplatelet drugs. *Thromb J* Thrombosis Journal; **2012;** 10: 11.

59   Vane JR, Bakhle YS, Botting RM. Cyclooxygenases 1 and 2. *Annu Rev Pharmacol Toxicol* **1998;** 38: 97–120.

60   Michelson AD. Antiplatelet therapies for the treatment of cardiovascular disease. Nature Publishing Group; **2010;** 9.

61   Bhatt DL, Stone GW, Mahaffey KW, Gibson CM, Steg PG, Hamm CW, Price MJ, Leonardi S, Gallup D, Bramucci E, Radke PW, Widimský P, Tousek F, Tauth J, Spriggs D, McLaurin BT, Angiolillo DJ, Généreux P, Liu T, Prats J, et al. Effect of Platelet Inhibition with Cangrelor during PCI on Ischemic Events. *N Engl J Med* **2013;** 368: 1303–13.

62   Chang H, Yanachkov IB, Dix EJ, Li YF, Barnard MR, Wright GE, Michelson AD, Frelinger AL. Modified diadenosine tetraphosphates with dual specificity for P2Y1 and P2Y12 are potent antagonists of ADP-induced platelet activation. *J Thromb Haemost* **2012;** 10: 2573–80.

63   Muthard RW, Diamond SL. Side view thrombosis microfluidic device with controllable wall shear rate and transthrombus pressure gradient. *Lab Chip* **2013;** 13: 1883–91.

64   Li R, Fries S, Li X, Grosser T, Diamond SL. Microfluidic assay of platelet deposition on collagen by perfusion of whole blood from healthy individuals taking aspirin. *Clin Chem* **2013;** 59: 1195–204.

65   Eng J. Receiver Operating Characteristic Analysis. *Am J Roentgenol* **2011;** 197: W784–W784.

66   Gurbel PA, Bliden KP, DiChiara J, Newcomer J, Weng W, Neerchal NK, Gesheff T, Chaganti SK, Etherington A, Tantry US. Evaluation of dose-related effects of aspirin on platelet function: results from the Aspirin-Induced Platelet Effect (ASPECT) study. *Circulation* **2007;** 115: 3156–64.

67   Lucitt MB, O'Brien S, Cowman J, Meade G, Basabe-Desmonts L, Somers M, Kent N, Ricco AJ, Kenny D. Assaying the efficacy of dual-antiplatelet therapy: use of a controlled-shear-rate microfluidic device with a well-defined collagen surface to track dynamic platelet adhesion. *Anal Bioanal Chem* **2013;** 405: 4823–34.

68   Mendolicchio GL, Zavalloni D, Bacci M, Corrada E, Marconi M, Lodigiani C, Presbitero P, Rota L, Ruggeri ZM. Variable effect of P2Y12 inhibition on platelet thrombus volume in flowing blood. *J Thromb Haemost* **2011;** 9: 373–82.

69   Jeong YH, Bliden KP, Antonino MJ, Park KS, Tantry US, Gurbel P a. Usefulness of the VerifyNow P2Y12 assay to evaluate the antiplatelet effects of ticagrelor and clopidogrel therapies. *Am Heart J* Mosby, Inc.; **2012;** 164: 35–42.

70   Neeves KB, Onasoga AA, Hansen RR, Lilly JJ, Venckunaite D, Sumner MB, Irish AT, Brodsky G, Manco-Johnson MJ, Di Paola J a. Sources of variability in platelet accumulation on type 1 fibrillar collagen in microfluidic flow assays. *PLoS One* **2013;** 8: e54680.

71   Hosokawa K, Ohnishi T, Kondo T, Fukasawa M, Koide T, Maruyama I, Tanaka K a. A novel automated microchip flow-chamber system to quantitatively evaluate thrombus formation and antithrombotic agents under blood flow conditions. *J Thromb Haemost* **2011;** 9: 2029–37.

72   Mannucci P, Tuddenham E. The Hemophilias-From Royal Genes to Gene Therapy. *N Engl J Med* **2011;** 344: 1773–9.

73   Gomez K, Bolton-Maggs P. Factor XI deficiency. *Haemophilia* **2008;** 14: 1183–9.

74   Astermark J, Donfield SM, DiMichele DM, Gringeri A, Gilbert SA, Waters J, Berntorp E. A randomized comparison of bypassing agents in hemophilia complicated by an inhibitor: The FEIBA NovoSeven Comparative (FENOC) study. *Blood* **2007;** 109: 546–51.

75   Sørensen B, Ingerslev J. Whole blood clot formation phenotypes in hemophilia A and rare coagulation disorders. Patterns of response to recombinant factor VIIa. *J Thromb Haemost* **2004;** 2: 102–10.

76   Lisman T, Moschatsis S, Adelmeijer J, Karel Nieuwenhuis H, De Groot PG. Recombinant factor VIIa enhances deposition of platelets with congenital or acquired ??IIb??3 deficiency to endothelial cell matrix and collagen under conditions of flow via tissue factor-independent thrombin generation. *Blood* **2003;** 101: 1864–70.

77   Onasoga-Jarvis AA, Leiderman K, Fogelson AL, Wang M, Manco-Johnson MJ, Di Paola J a, Neeves KB. The Effect of Factor VIII Deficiencies and Replacement and Bypass Therapies on Thrombus Formation under Venous Flow Conditions in Microfluidic and Computational Models. *PLoS One* **2013;** 8: e78732.

78   Li R, Diamond SL. Detection of platelet sensitivity to inhibitors of COX-1, P2Y1, and P2Y12 using a whole blood microfluidic flow assay. *Thromb Res* **2014;** 133: 203–10.

79   Hojima Y, Pierce J, JJ P. Hageman Factor Fragment Inhibitor in Corn Seeds: Purification and Characterization. *Thromb Res* **1980;** : 160.

80   Chatterjee MS, Denney WS, Jing H, Diamond SL. Systems biology of coagulation initiation: kinetics of thrombin generation in resting and activated human blood. *PLoS Comput Biol* **2010;** 6: 1–24.

81   Monroe DM, Hoffman M, Oliver J a, Roberts HR. Platelet activity of high-dose factor VIIa is independent of tissue factor. *Br J Haematol* **1997;** 99: 542–7.

82   Konkle B. Clinical challenges within the aging hemophilia population. *Thromb Res* Elsevier Ltd; **2011;** 127: S10–3.

83   Biere-Rafi S, Baarslag MA, Peters M, Kruip MJHA, Kraaijenhagen RA, den Heijer M, Büller HR, Kamphuisen PW. Cardiovascular risk assessment in haemophilia patients. *Thromb*

Haemost **2010;** 105: 274–8.

84   Mackman N. Role of Tissue Factor in Hemostasis, Thrombosis, and Vascular Development. *Arterioscler Thromb Vasc Biol* **2004;** 24: 1015–22.

85   Cheng Q, Tucker EI, Pine MS, Sisler I, Matafonov A, Sun M-F, White-Adams TC, Smith SA, Hanson SR, McCarty OJT, Renné T, Gruber A, Gailani D. A role for factor XIIa-mediated factor XI activation in thrombus formation in vivo. *Blood* **2010;** 116: 3981–9.

86   Meijden PEJ Van Der, Munnix ICA, Auger JM, Govers-riemslag JWP, Cosemans JMEM, Kuijpers MJE, Spronk HM, Watson SP, Renné T, Heemskerk JWM, Dc W. Dual role of collagen in factor XII − dependent thrombus formation Dual role of collagen in factor XII – dependent thrombus formation. **2013;** : 881–90.

87   Walsh P, Griffin J. Contributions of human platelets to the proteolytic activation of blood coagulation factors XII and XI. *Blood* **1981;** 57: 106–19.

88   Fuchs T a, Brill A, Duerschmied D, Schatzberg D, Monestier M, Myers DD, Wrobleski SK, Wakefield TW, Hartwig JH, Wagner DD. Extracellular DNA traps promote thrombosis. *Proc Natl Acad Sci U S A* **2010;** 107: 15880–5.

89   Puy C, Tucker EI, Matafonov A, Cheng Q, Zientek KD, Gailani D. Activated factor XI increases the procoagulant activity of the extrinsic pathway by inactivating tissue factor pathway inhibitor. **2015;** 125: 1488–97.

90   Girolami A, Scandellari R, Zanon E, Sartori R, Girolami B. Non-catheter associated venous thrombosis in hemophilia A and B. A critical review of all reported cases. *J Thromb Thrombolysis* **2006;** 21: 279–84.

91   Carcao MD, van den Berg HM, Ljung R, Mancuso ME, PedNet. Correlation between phenotype and genotype in a large unselected cohort of children with severe hemophilia A. *Blood* **2013;** 121: 3946–53.

92   Santagostino E, Mancuso ME, Tripodi A, Chantarangkul V, Clerici M, Garagiola I, Mannucci PM. Severe hemophilia with mild bleeding phenotype: molecular characterization and global coagulation profile. *J Thromb Haemost* **2010;** 8: 737–43.

93   van den Berg HM, De Groot PHG, Fischer K. Phenotypic heterogeneity in severe hemophilia. *J Thromb Haemost* **2007;** 5: 151–6.

94   Lisman T, de Groot PG. The role of cell surfaces and cellular receptors in the mode of action of recombinant factor VIIa. *Blood Rev* **2015;** 29: 223–9.

95   van 't Veer C, Golden N, Mann K. Inhibition of thrombin generation by the zymogen factor VII: implications for the treatment of hemophilia A by factor VIIa. *Blood* **2000;** 95: 1330–5.

96   Francisco S, Butenas S, Brummel KE, Branda RF, Paradis SG, Mann KG. Mechanism of factor VIIa − dependent coagulation in hemophilia blood : Presented in part at the 42nd Annual Meeting of the American Society of. *Vascular* **2012;** 99: 923–30.

97   Butenas S, Brummel KE, Paradis SG, Mann KG. Influence of factor VIIa and phospholipids on coagulation in "acquired" hemophilia. *Arterioscler Thromb Vasc Biol* **2003;** 23: 123–9.

98   Shibeko AM, Woodle SA, Lee TK, Ovanesov M V. Unifying the mechanism of recombinant FVIIa action: Dose dependence is regulated differently by tissue factor and phospholipids. *Blood* **2012;** 120: 891–9.

99   Augustsson C, Persson E. In vitro evidence of a tissue factor-independent mode of action of

recombinant factor VIIa in hemophilia. *Blood* **2014;** 124: 3172–4.

100   Aljamali MN, Kjalke M, Hedner U, Ezban M, Tranholm M. Thrombin generation and platelet activation induced by rFVIIa (NovoSeven) and NN1731 in a reconstituted cell-based model mimicking haemophilia conditions. *Haemophilia* **2009;** 15: 1318–26.

101   Brummel-Ziedins KE, Branda RF, Butenas S, Mann KG. Discordant fibrin formation in hemophilia. *J Thromb Haemost* **2009;** 7: 825–32.

102   Wolberg AS, Allen GA, Monroe DM, Hedner U, Roberts HR, Hoffman M. High dose factor VIIa improves clot structure and stability in a model of haemophilia B. *Br J Haematol* **2005;** 131: 645–55.

103   Fressinaud E, Sakariassen KS, Rothschild C, Baumgartner HR, Meyer D. Shear rate-dependent impairment of thrombus growth on collagen in nonanticoagulated blood from patients with von Willebrand disease and hemophilia A. *Blood* **1992;** 80: 988–94.

104   Weiss HJ, Turitto VT, Vicic WJ, Baumgartner HR. Fibrin formation, fibrinopeptide A release, and platelet thrombus dimensions on subendothelium exposed to flowing native blood: greater in factor XII and XI than in factor VIII and IX deficiency. *Blood* **1984;** 63: 1004–14.

105   Ogawa S, Szlam F, Dunn A, Bolliger D, Ohnishi T, Hosokawa K, Tanaka K. Evaluation of a novel flow chamber system to assess clot formation in factor VIII-deficient mouse and anti-factor IXa-treated human blood. *Haemophilia* **2012;** 18: 926–32.

106   Bi L, Lawler A, Antonarakis SE, High K, Gearhart JD, Kazazian HH. Targeted disruption of the mouse factor VIII gene produces a model of haemophilia A. *Nat Genet* **1995;** 10: 119–21.

107   Chauhan AK, Kisucka J, Lamb CB, Bergmeier W, Wagner DD. von Willebrand factor and factor VIII are independently required to form stable occlusive thrombi in injured veins. *Blood* **2007;** 109: 2424–9.

108   Neyman M, Gewirtz J, Poncz M. Analysis of the spatial and temporal characteristics of platelet-delivered factor VIII-based clots. *Blood* **2008;** 112: 1101–8.

109   Drake TA, Morrissey JH, Edgington TS. Selective cellular expression of tissue factor in human tissues. Implications for disorders of hemostasis and thrombosis. *Am J Pathol* **1989;** 134: 1087–97.

110   Fleck A, Rao LVM, Rapaport SI. Localization of human tissue factor antigen by immunostaining with monospecific, polyclonal anti-human tissue factor antibody. *Thromb Res* **1990;** 59: 421–37.

111   Swieringa F, Kuijpers MJE, Lamers MME, van der Meijden PEJ, Heemskerk JWM. Rate-limiting roles of the tenase complex of factors VIII and IX in platelet procoagulant activity and formation of platelet-fibrin thrombi under flow. *Haematologica* **2015;** 100: 748–56.

112   Kitchens CS. To bleed or not to bleed? Is that the question for the PTT? *J Thromb Haemost* **2005;** 3: 2607–11.

113   Zhu S, Travers RJ, Morrissey JH, Diamond SL. FXIa and platelet polyphosphate as therapeutic targets during human blood clotting on collagen/tissue factor surfaces under flow. *Blood* **2015;** 126: 1494–502.

114   Welsh JD, Stalker TJ, Voronov R, Muthard RW, Tomaiuolo M, Diamond SL, Brass LF. A systems approach to hemostasis: 1. The interdependence of thrombus architecture and agonist movements in the gaps between platelets. *Blood* **2014;** 124: 1808–16.

115   Stalker TJ, Traxler EA, Wu J, Wannemacher KM, Samantha L, Voronov R, Diamond SL, Brass LF, Dc W, Cermignano SL. Hierarchical organization in the hemostatic response and its relationship to the platelet-signaling network. *Blood* **2013;** 121: 1875–85.

116   Stalker TJ, Welsh JD, Tomaiuolo M, Wu J, Colace T V, Diamond SL, Brass LF. A systems approach to hemostasis: 3. Thrombus consolidation regulates intrathrombus solute transport and local thrombin activity. *Blood* **2014;** 124: 1824–32.

117   Hess JR, Brohi K, Dutton RP, Hauser CJ, Holcomb JB, Kluger Y, Mackway-Jones K, Parr MJ, Rizoli SB, Yukioka T, Hoyt DB, Bouillon B. The coagulopathy of trauma: a review of mechanisms. *J Trauma* **2008;** 65: 748–54.

118   Brohi K, Cohen MJ, Ganter MT, Matthay MA, Mackersie RC, Pittet J-F. Acute traumatic coagulopathy: initiated by hypoperfusion: modulated through the protein C pathway? *Ann Surg* **2007;** 245: 812–8.

119   Rugeri L, Levrat a., David JS, Delecroix E, Floccard B, Gros a., Allaouchiche B, Negrier C. Diagnosis of early coagulation abnormalities in trauma patients by rotation thrombelastography. *J Thromb Haemost* **2007;** 5: 289–95.

120   Rourke C, Curry N, Khan S, Taylor R, Raza I, Davenport R, Stanworth S, Brohi K. Fibrinogen levels during trauma hemorrhage, response to replacement therapy, and association with patient outcomes. *J Thromb Haemost* **2012;** 10: 1342–51.

121   Kutcher ME, Redick BJ, McCreery RC, Crane IM, Greenberg MD, Cachola LM, Nelson MF, Cohen MJ. Characterization of platelet dysfunction after trauma. *J Trauma Acute Care Surg* **2012;** 73: 13–9.

122   Solomon C, Traintinger S, Ziegler B, Hanke A, Rahe-Meyer N, Voelckel W, Schöchl H. Platelet function following trauma; A multiple electrode aggregometry study. *Thromb Haemost* **2011;** 106: 322–30.

123   Jacoby RC, Owings JT, Holmes J, Battistella FD, Gosselin RC, Paglieroni TG. Platelet activation and function after trauma. *J Trauma* **2001;** 51: 639–47.

124   Wohlauer M V., Moore EE, Thomas S, Sauaia A, Evans E, Harr J, Silliman CC, Ploplis V, Castellino FJ, Walsh M. Early platelet dysfunction: An unrecognized role in the acute coagulopathy of trauma. *J Am Coll Surg* Elsevier Inc.; **2012;** 214: 739–46.

125   Davis PK, Musunuru H, Walsh M, Cassady R, Yount R, Losiniecki A, Moore EE, Wohlauer M V., Howard J, Ploplis V a., Castellino FJ, Thomas SG. Platelet dysfunction is an early marker for traumatic brain injury-induced coagulopathy. *Neurocrit Care* **2013;** 18: 201–8.

126   Rana K, Timmer BJ, Neeves KB. A combined microfluidic-microstencil method for patterning biomolecules and cells. *Biomicrofluidics* **2014;** 8: 056502.

127   de Witt SM, Swieringa F, Cavill R, Lamers MME, van Kruchten R, Mastenbroek T, Baaten C, Coort S, Pugh N, Schulz A, Scharrer I, Jurk K, Zieger B, Clemetson KJ, Farndale RW, Heemskerk JWM, Cosemans JMEM. Identification of platelet function defects by multi-parameter assessment of thrombus formation. *Nat Commun* Nature Publishing Group; **2014;** 5: 4257.

128   Kuijpers MJE, Van Der Meijden PEJ, Feijge M a H, Mattheij NJ a, May F, Govers-Riemslag J, Meijers JCM, Heemskerk JWM, Renné T, Cosemans JMEM. Factor XII regulates the pathological process of thrombus formation on ruptured plaques. *Arterioscler Thromb Vasc Biol* **2014;** 34: 1674–80.

129   Li X, Fries S, Li R, Lawson JA, Propert KJ, Diamond SL, Blair IA, FitzGerald GA, Grosser T. Differential impairment of aspirin-dependent platelet cyclooxygenase acetylation by nonsteroidal antiinflammatory drugs. *Proc Natl Acad Sci* **2014;** 111: 16830–5.

130   Johansson PI, Stensballe J, Oliveri R, Wade CE, Ostrowski SR, Holcomb JB. How I treat patients with massive hemorrhage. *Blood* **2014;** 124: 3052–8.

131   Bolliger D, Görlinger K, Tanaka K a. Pathophysiology and treatment of coagulopathy in massive hemorrhage and hemodilution. *Anesthesiology* **2010;** 113: 1205–19.

132   Sperry JL, Ochoa JB, Gunn SR, Alarcon LH, Minei JP, Cuschieri J, Rosengart MR, Maier R V, Billiar TR, Peitzman AB, Moore EE. An FFP:PRBC transfusion ratio >/=1:1.5 is associated with a lower risk of mortality after massive transfusion. *J Trauma* **2008;** 65: 986–93.

133   Sihler KC, Napolitano LM. Massive transfusion: New insights. *Chest* **2009;** 136: 1654–67.

134   Whelihan MF, Mann KG. The role of the red cell membrane in thrombin generation. *Thromb Res* Elsevier Ltd; **2013;** 131: 377–82.

135   Stein SC, Smith DH. Coagulopathy in traumatic brain injury. *Neurocrit Care* **2004;** 1: 479–88.

136   Teodoro L, Nascimento B, Rizoli S. Thrombelastography (TEG W): practical considerations on its clinical use in trauma resuscitation. **2013;** : 1–8.

137   Neeves KB, Illing D a R, Diamond SL. Thrombin flux and wall shear rate regulate fibrin fiber deposition state during polymerization under flow. *Biophys J* Biophysical Society; **2010;** 98: 1344–52.

138   Haynes LM, Dubief YC, Orfeo T, Mann KG. Dilutional control of prothrombin activation at physiologically relevant shear rates. *Biophys J* Biophysical Society; **2011;** 100: 765–73.

139   Bender M, Hofmann S, Stegner D, Chalaris A, Bösl M, Braun A, Scheller J, Rose-john S, Nieswandt B, Bo M. Differentially regulated GPVI ectodomain shedding by multiple plateletexpressed proteinases Differentially regulated GPVI ectodomain shedding by multiple platelet – expressed proteinases. **2010;** 116: 3347–55.

140   Bergmeier W, Piffath CL, Cheng G, Dole VS, Zhang Y, Von Andrian UH, Wagner DD. Tumor necrosis factor-α-converting enzyme (ADAM17) mediates GPIbα shedding from platelets in vitro and in vivo. *Circ Res* **2004;** 95: 677–83.

141   Ariëns R a S, Lai T, Weisel JW, Greenberg CS, Grant PJ, Arie R a S. Role of factor XIII in fibrin clot formation and effects of genetic polymorphisms Review article Role of factor XIII in fibrin clot formation and effects of genetic polymorphisms. **2011;** 100: 743–54.

142   Barry EL, Mosher DF. Factor XIIIa-mediated cross-linking of fibronectin in fibroblast cell layers. Cross-linking of cellular and plasma fibronectin and of amino-terminal fibronectin fragments. *J Biol Chem* **1989;** 264: 4179–85.

143   Dardik R, Solomon A, Loscalzo J, Eskaraev R, Bialik A, Goldberg I, Schiby G, Inbal A. Novel proangiogenic effect of factor XIII associated with suppression of thrombospondin 1 expression. *Arterioscler Thromb Vasc Biol* **2003;** 23: 1472–7.

144   Aziz M, Azizur S. Congenital Deficiency of Fibrin-stabilizing factor (Factor XIII): A Report of Four Cases (Two Families) and Family Members. *Blood* **1972;** 40: 11–5.

145   Muszbek L, Bereczky Z, Bagoly Z, Komáromi I, Katona É. Factor XIII: a coagulation factor with multiple plasmatic and cellular functions. *Physiol Rev* **2011;** 91: 931–72.

146   Fraser SR, Booth N a., Mutch NJ. The antifibrinolytic function of factor XIII is exclusively expressed through 2-antiplasmin cross-linking. *Blood* **2011;** 117: 6371–4.

147   Lopaciuk S, Lovette K, McDonagh J, Chuang H, McDonagh R. Subcellular Distribution of Fibrinogen and Factor XIII in Human Blood Platelets. *Thromb Res* **1976;** 8: 433–63.

148   Nurden A, Kunicki T, Dupuis D, Soria C, Caen J. Specific protein and glycoprotein deficiencies in platelets isolated from two patients with gray platelet syndrome. *BloodBlood* **1982;** 59: 709–19.

149   Zhu Y, Tassi L, Lane W, Mendelsohn ME. Specific binding of the transglutaminase, platelet factor XIII, to HSP27. *JBiol Chem* **1994;** 269: 22379–84.

150   Muszbek L, Yee VC, Hevessy Z. Blood Coagulation Factor XIII: Structure and Function. *Thromb Res* **1999;** 94: 271–305.

151   Mitchell JL, Lionikiene AS, Fraser SR, Whyte CS, Booth N a, Mutch NJ. Functional factor XIII-A is exposed on the stimulated platelet surface. **2015;** 124: 3982–91.

152   Byrnes JR, Wang Y, Hansen CE, Ahn B, Mooberry MJ, Clark M a, Johnsen JM, Lord ST, Lam W a, Meijers JCM, Ni H, Ari R a S, Wolberg AS. Factor XIIIa-dependent retention of red blood cells in clots is mediated by fibrin a-chain crosslinking. **2015;** 126: 1940–9.

153   Tonda R, Galán AM, Pino M, Cirera I, Bosch J, Hernández MR, Ordinas A, Escolar G. Hemostatic effect of activated recombinant factor VII (rFVIIa) in liver disease: Studies in an in vitro model. *J Hepatol* **2003;** 39: 954–9.

154   Galán A, Tonda R, Pino M, Reverter JC, Ordinas A. recombinant FVIIa in PLT disorders. *Transfusion* **2003;** 43: 885–92.

155   Lisman T, Adelmeijer J, Cauwenberghs S, Van Pampus ECM, Heemskerk JWM, De Groot PG. Recombinant factor VIIa enhances platelet adhesion and activation under flow conditions at normal and reduced platelet count. *J Thromb Haemost* **2005;** 3: 742–51.